Effect of Mechanical Stress
On Stem Cells to Improve Better Bone Regeneration
Die Auswirkung von mechanischer Belastung auf
Stammzellen zur Verbesserung der Knochenregeneration

Doctoral thesis for a doctoral degree
at the Graduate School of Life Sciences,
Julius-Maximilians-Universität Würzburg,
Section Biomedicine
Submitted by

Ramkumar Ramani Mohan

from

From Madurai, India

Würzburg 2021

Submitted on: ……..……..

Office stamp

Members of the Promotionskomitee:

Chairperson: Prof. Thomas Dandekar

Primary Supervisor: Prof. Heike Walles

Supervisor (Second): Prof. Franz Jakob

Supervisor (Third): Prof. Jan Hansmann

Date of Public Defence: ……..……

Date of Receipt of Certificates: …….

Affidavit

I hereby confirm that my thesis entitled “Effect of Mechanical Stress on Stem Cells to Improve Better Bone Regeneration” is the result of my own work. I did not receive any help or support from commercial consultants. All sources and / or materials applied are listed and specified in the thesis. Furthermore, I confirm that this thesis has not yet been submitted as part of another examination process neither in identical nor in similar form.

Würzburg, 2.06.2021

Place, Date Signature

Eidesstattliche Erklärung

Hiermit erkläre ich an Eides statt, die Dissertation “ Auswirkung der mechanischen Belastung von Stammzellen für eine bessere Knochenregeneration “ eigenständig, d.h. insbesondere selbständig und ohne Hilfe eines kommerziellen Promotionsberaters, angefertigt und keine anderen als die von mir angegebenen Quellen und Hilfsmittel verwendet zu haben. Ich erkläre außerdem, dass die Dissertation weder in gleicher noch in ähnlicher Form bereits in einem anderen Prüfungsverfahren vorgelegen hat.

Würzburg, 2.06.2021

Ort, Datum Unterschrift

Acknowledgment

I would first like to express my sincere gratitude to my advisor, Prof. Jan Hansmann, who recognized me and gave me the opportunity to pursue a PhD. I am grateful to him for his continuous support during my study, his patience and motivation, and the immense knowledge he shared with me. His guidance helped me throughout my research and the writing process for this thesis. I could not have asked for a better advisor or mentor.

I also express my sincere gratitude to Prof. Heike Walles, who welcomed me with open arms when I joined the Department of Tissue Engineering and Regenerative Medicine as a PhD student. I am thankful to her for letting me explore my research questions, facilitating my research, and constantly offering encouragement. I would also like to thank Prof. Dr. med. Franz Jakob, who guided my PhD research and provided insight into the field of bone regeneration that was pivotal for my research. I appreciate his support and encouragement.

I am thankful to all my collaborators for facilitating my research by sharing materials, including Assoc. Prof. Anna Finne Wistrand of KTH Royal Institute of Technology, Dr. Swaraj Paul of PP Polymer AB, and Dr. Gloria Ramirez Rodriguez of the Institute of Science and Technology for Ceramics.

I am indebted to the German Academic Exchange Service (DAAD) for giving me a fellowship that provided three years of financial support during my PhD research. I also thank the Graduate School of Life Sciences at the Julius–Maximilian–University of Würzburg for organizing many workshops which not only bolstered scientific knowledge but also focused on careers beyond a PhD.

Besides my advisors, I would like to thank the rest of my colleagues who helped me during experiments: Gabriele Vaacun, Claudia Klinhans, Ivo Schwedhelm, and Tobias Weigel. I also thank my friends, Anna Schliermann, Richard Schmid and Carolin Krziminski, who supported and encouraged me during my PhD thesis time. I am grateful to all my fellow lab mates for the stimulating discussions, sleepless nights we were working together before deadlines, and all the fun we have had over the past four years.

I must also thank Prama Pallavi for all the assistance I received while writing my thesis, for enduring rigorous corrections, and for her moral support in general.

Last but not least, I dedicate this thesis to my parents and my sister, who stood with me during challenging times, offering constant encouragement and motivation and supporting me spiritually both during the thesis process and throughout my life.

Dedicated to my mother, father and sister

When it's all over, it's not who you were … it's whether you made a difference.

—Bob Dole

Table of contents

Summary

Critical size bone defects and nonunion fractures remain difficult to treat. Although cell-loaded bone substitutes have improved bone ingrowth and formation, the lack of methods for achieving viability and the uniform distribution of cells in the scaffold limits their use as bone grafts. In addition, the predominant mechanical stimulus that drives early osteogenic cell maturation has not been clearly identified. Further, it is challenging to evaluate mechanical stimuli (*i.e.*, deformation and fluid–flow-induced shear stress) because they are interdependent. This thesis compares different mechanical stimuli applied to cell-seeded scaffolds to develop bone grafts efficiently for the treatment of critical size bone defects. It also seeks to understand how deformation strain and interstitial fluid–flow-induced shear stress promote osteogenic lineage commitment.

In this thesis, different scaffolds were seeded with primary human bone marrow mesenchymal stem cells (BM-MSCs) from different donors and subjected to static and dynamic culture conditions. In contrast with the static culture conditions, homogenous cell distributions were accomplished under dynamic culture conditions. Additionally, the induction of osteogenic lineage commitment without the addition of soluble factors was observed in the bioreactor system after one week of cell culture.

To determine the role of mechanical stimuli, a bioreactor was developed to apply mechanical deformation force to a mesenchymal stem sell (MSC) line (telomerase reverse transcriptase (TERT)) expressing a strain-responsive AP-1 luciferase reporter construct on porous scaffolds. Increased luciferase expression was observed in the deformation strain compared with the shear stress strain. Furthermore, the expression of osteogenic lineage commitment markers such as osteonectin, osteocalcin (OC), osteopontin, runt-related transcription factor 2 (RUNX2), alkaline phosphate (AP), and collagen type 1 was significantly downregulated in the shear stress strain compared with the deformation strain. These findings establish that the deformation strain was the predominant stimulus causing skeletal precursors to undergo osteogenesis in earlier stages of osteogenic cell maturation.

Finally, these findings were used to develop a bioreactor *in vitro* test system in which the effect of medication on osteoporosis could be tested. Primary human BM-MSCs from

osteoporotic donors were subjected to strontium ranelate (an osteoporotic drug marketed as Protelos®). Increased expression of collagen type 1 and calcification was seen in the drug-treated osteoporotic stem cells compared with the nondrug-treated osteoporotic stem cells. Thus, this bioreactor technology can easily be adapted into an *in vitro* osteoporotic drug testing system.

Zusammenfassung

Knochendefekte kritischer Größe und Frakturen mit Pseudoarthrose bleiben schwierig zu behandeln. Obwohl zellbeladene Knochenersatzprodukte das Einwachsen und die Bildung von Knochen verbessert haben, schränken fehlende Methoden zur Erreichung der Lebensfähigkeit und der gleichmäßigen Verteilung der Zellen im Gerüst die Verwendung von Knochenersatzprodukten als Knochentransplantate ein. Ebenfalls konnte der vorherrschende mechanische Reiz, der die frühe osteogene Zellreifung antreibt nicht eindeutig identifiziert werden. Ferner ist es schwierig, mechanische Reize (d. H. Verformung und durch Flüssigkeitsströmung induzierte Scherbeanspruchung) zu bewerten, da diese Größen sie voneinander abhängig sind. Diese Arbeit vergleicht die Auswirkung verschiedener mechanischer Reize auf mit Zellen besiedelte Gerüste, um herauszufinden, ob Knochentransplantate effizient entwickelt werden können damit sie für die Behandlung von Knochendefekten einsetzbar sind. Des Weiteren wird versucht zu verstehen, wie Verformungsdehnung und durch interstitielle Flüssigkeitsströmung induzierte Scherbeanspruchung die Bindung osteogener Linien fördern.

In dieser Arbeit wurden verschiedene Gerüste mit primären mesenchymalen Knochenmarkstammzellen (BM-MSCs) von verschiedenen Spendern ausgesät und statischen und dynamischen Kulturbedingungen ausgesetzt. Im Gegensatz zu den statischen Kulturbedingungen wurde unter dynamischen Kulturbedingungen eine homogene Zellverteilungen erreicht. Zusätzlich wurde im Bioreaktorsystem nach einer Woche Zellkultur eine Formung einer osteogenen Linienbindung auch ohne Zusätze von löslichen Faktoren beobachtet.

Um die Rolle mechanischer Stimuli zu bestimmen, wurde ein Bioreaktor entwickelt, um auf porösen Scaffolds eine mechanische Verformungskraft auf eine mesenchymale Stammzelllinie (MSC) (Telomerase Reverse Transkriptase (TERT)) auszuüben. Diese exprimiert ein auf Dehnung ansprechendes AP-1-Luciferase-Reporterkonstrukt. Eine erhöhte Luciferase-Expression wurde in der Verformungsdehnung im Vergleich zur Scherspannungsdehnung beobachtet. Darüber hinaus war die Expression von osteogenen Linien Marker wie Osteonektin, Osteocalcin (OC), Osteopontin, Runt-verwandtem Transkriptionsfaktor 2 (RUNX2), alkalischem Phosphat (AP) und Kollagen Typ 1 in der Scherbeanspruchungsbelastung

im Vergleich zur Verformungsdehnung signifikant herabreguliert. Diese Befunde belegen, dass die Verformungsdehnung der vorherrschende Stimulus war, der dazu führte, dass Skelettvorläufer in früheren Stadien der osteogenen Zellreifung eine Osteogenese durchliefen.

Schließlich wurden diese Ergebnisse verwendet, um ein Bioreaktor-In-vitro-Testsystem zu entwickeln, in dem die Wirkung von Medikamenten auf Osteoporose getestet werden konnte. Primäre humane BM-MSCs von osteoporotischen Spendern wurden Strontiumranelat (einem als Protelos® vertriebenen Arzneimittel zur Therapie der Osteoporose) ausgesetzt. Eine erhöhte Expression von Kollagen Typ 1 und Verkalkung wurde in den mit Arzneimitteln behandelten osteoporotischen Stammzellen im Vergleich zu den nicht mit Arzneimitteln behandelten osteoporotischen Stammzellen beobachtet. Somit kann diese Bioreaktortechnologie leicht in ein *in vitro* Arzneimitteltestsystem angepasst werden.

List of Abbreviations and Units

2D	Two-dimensional
3D	Three-dimensional
AT	Annealing temperature
ALPL	Alkaline phosphatase
BGLAP	Bone Gamma-Carboxyglutamate Protein (Osteocalcin)
BMP-2	Bone morphogenic protein-2
β-TCP	Beta-tricalcium phosphate
cDNA	CopyRNA
CAD	Computer-aided design
Col1A1	Collagen type 1 alpha 1
DMEM	Dulbecco's Modified Eagle Medium
DNase	Desoxyribonuclease
ECM	Extracellular matrix
EDTA	Ethylenediaminetetraacetic acid
ELISA	Enzyme linked immunosorbent assay
FACS	Fluorescence-activated cell sorting
FCS	Fetal calf serum
g0	Standard acceleration due to gravity
hMSCs	Human mesenchymal stem cells
i.e	Id est

IgA	Immunoglobulin A
IGF	Insulin-like growth factor 1
IHC	Immunohistochemistry
IL	Interleukin
LSFM	light sheet fluorescence microscopy
M-CSF	Macrophage colony-stimulating factor
MTT	3-(4,5-dimethylthiazol-2-yl)-2,5-Diphenyltetrazolium bromide
mRNA	messenger RNA
MSCs	Mesenchymal stem cells
MEM	Minimum essential media
µl	microliter
G	Gram
ml	mililiter
NO	Nitric oxide
P	Passage
P (LLA-co-CL)	Poly(L-lactide-co-caprolactone)
PBS-	Phosphate buffered saline (without magnesium and calcium ions)
PBS+	Phosphate buffered saline (with magnesium and calcium ions)
PFA	Paraformaldehyde
qPCR	Quantitative polymerase chain reaction

Ref	Reference
RNA	Ribonucleic acid
RQI	RNA quality indicator value
RT	Room temperature
RUNX2	Runt-related transcription factor 2
SD	Standard deviation
SPARC	Secreted Protein Acidic And Cysteine Rich(osteonectin)
SPP1	Secreted Phosphoprotein 1(osteopontin)
TERT	Telomerase reverse transcriptase
TGFβ3	Transforming growth factor β3
TNF	Tumor necrosis factor

1 Introduction

The field of tissue engineering has grown tremendously over the past two decades, taking us a step toward the repair and regeneration of damaged tissue—and organs, in some cases—with clinically relevant solutions[1]. Tissue engineering is a concept and technique that combines life science with engineering to develop transplantable tissues or organs. Tissue engineering can be used to generate almost every organ in the human body, and recent commendable attempts have been made to develop skin[2], cartilage[3], bones[3], corneas[4], blood vessels[5], and muscles[6]. Tissue engineering offers a promising solution to the growing need to replace either partially or completely damaged tissue and organs as life expectancy increases because it enables the *in vitro* fabrication of functional and compatible biological structures.

After blood, bone is the second most frequently transplanted tissue, with over two million bone grafting procedures performed annually worldwide[1]. Large bone defects due to ablative surgery, tumor resections, major trauma or injuries, poorly healed fractures, and pathological and physiological bone resorption represent a major challenge to bone healing therapies. Current clinical treatments to repair large bone defects are problematic and often yield poor results due to the complicated anatomy and physiology of the main skeletal tissue as well as limitations of medical technology. Transplanting autologous bone is still considered the gold standard[7], but large skeletal defects may require large volumes of bone, which leads to complications at the second surgical site[7]. Allogenic bone grafts from tissue banks are a secondary choice, but they include the risk of disease transfer and immunologic rejection[8].

Tissue-engineered bone implants have great potentional as a new treatment that avoids these issues. This thesis presents a novel bioreactor system for developing engineered bone tissue from autologous or allogeneic MSCs to achieve better bone regeneration.

The first step toward developing functional engineered tissue is understanding its the physiology and function. Tissue regeneration technology mainly depends on three important factors: 1) the cells that synthesize the tissue, 2) the scaffold that holds the cells together to create the tissue, and 3) the signaling mechanism that guides the cells to move toward the

certain phenotype[9]. All these are discussed in the following sections themes from the design perspective of the developed bioreactor.

1.1 Bone: the framework supporting the body

Bone is a hard and rigid form of connective tissue which supports the structure of the body. Skeleton system protects most of the organs present in the human body by surrounding or covering them. It is composed of several different tissues: bone tissue, cartilage, blood-forming tissues, blood vessels, adipose tissue, and nervous tissue. Each bone in our bodies is dynamic and constantly changes throughout our lives[10]. Bone functions together with skeletal muscles, ligaments, tendons, and joints to generate forces that bring about bodily movement.

Bone tissue consists of widely separated cells surrounded by large amounts of its matrix, which is made of the organic and inorganic phases. Bone mostly comprises collagen type 1 (organic) and calcium hydroxylapatite (inorganic)[11].

The connective tissue—particularly, the collagen-containing extracellular matrix (ECM)—plays an important role in force transmission and bone structure maintenance during different mechanical stresses such as walking and running. For example, cells isolated from osteoporotic patients secrete a small amount of collagen type 1, which results in weakening and fractures[12]. Besides collagen, bone ECM also contains minerals (*e.g.*, calcium), which support different body functions[13]. Calcium is required for the development, growth, and maintenance of the skeleton. It is one of the most important inorganic components of the bone ECM, providing strength and functioning as a scaffold. Several bone cells are involved in regulating calcium and mineral deposition in the bone tissue[14].

Three different bone cells produce and maintain the bone: osteoblasts, osteoclasts, and osteocytes. Osteoblasts originate from BM-MSCs, which are responsible for bone matrix synthesis and mineralization[15]. Osteoblasts are mononucleated and produce the matrix, which forms new bone layers. They are found on top of or next to existing bone. The molecules present in the matrix interact with each other to form osteoid, a flexible and rigid bone tissue mostly composed of collagen, a fibrous protein. Osteoblasts release receptor activator of nuclear factor kappa-B ligand (RANKL) and macrophage colony-stimulating factor (M-CSF) for

osteoclast differentiation. Osteoblasts also produce collagen protein fibers, which provide bone flexibility, and calcium phosphate, which provides bone rigidity.

Osteocytes maintain the balance between osteoblasts and osteoclasts. Osteoblasts produce and secrete the bone ECM components. Once osteoblasts become embedded in the ECM, they differentiate into osteocytes. In vivo mouse models show that apoptotic osteocytes induce a significant increase in bone absorption and decrease in bone formation[16]. By sensing the mechanical stress on the bone, osteocytes can regulate bone architecture according to the load applied to the skeleton.

Osteoclasts are large multinucleated cells that absorb and remove bone, which results in its maintenance, repair, and development. Osteoclasts also play a role in maintaining osteoblasts by releasing transforming growth factor-beta (TGF-β), insulin-like growth factor 1 (IGF), and bone morphogenetic protein (BMP). Osteoclasts continuously break down the old bone, while osteoblasts continuously build new bone structure.

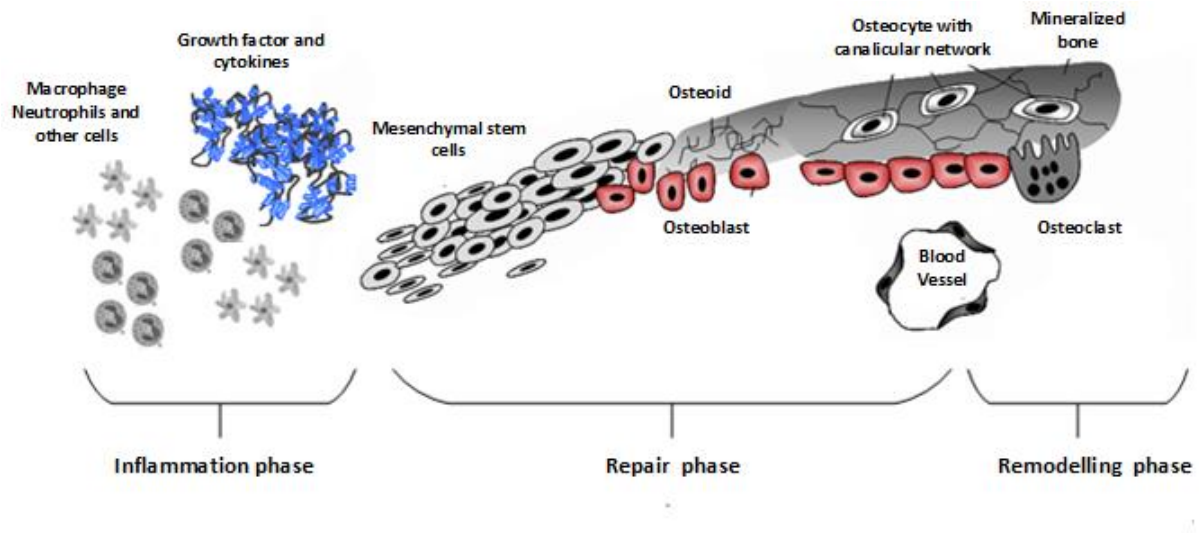

Figure 1-1: Schematic representation of bone healing process. Modified from Loi, F., et al [17].

Traumatic injuries cause bone fractures, which initiate healing. The healing process occurres over three phases: inflammatory, reparative, and remodeling[17]. Swelling, redness, and inflammation occur after an injury because the bone fracture not only damages the cells, bone matrix, and blood vessels but also the soft tissue around the area, such as muscles and nerves. Inflammation causes pain, allows new blood vessels to form, and recruits more macrophages, neutrophils, and other cells, proteins, cytokines, and growth factors to build

new bone. Next, the reparative phase occurs approximately 2 weeks after the fracture, when the injured site is still weak. MSCs are differentiated into osteoblasts, resulting in callus tissue developing around the fracture site to provide stability and stable union. This callus is then remodelled according to physical needs in the following phase.

In the final remodeling phase, the callus is being remodelled according to physical needs of the respectivwe anatomy into strong and healthy bone. The process occurs over several months (*i.e.*, the bone continuously repairs itself at the rate of 10–18% per year). The bone usually responds to mechanical force during this phase such that the healing process is accelerated. However, this process is affected when there is a critical size bone defect.

In humans, a bone defect of 10mm or more is considered to be critical size[18]. Such a defect disturbes the natural healing phases and prevents the bone from healing without surgical intervention. Instead, bone grafting—mostly autografts, allografts, or synthetic materials—is used to bridge the defect and assist the healing process.

1.2 Cells for engineering a bone tissue graft

Many studies have used different cell types, such as MSCs, pluripotent stem cells, adipose-derived stem cells, and human embryonic stem cells for bone regeneration or repair. MSCs are the preferred choice for bone tissue engineering because they are multipotent and can be easily differentiated into three different lineages—chondrogenic, osteogenic, and adipogenic—depending on growth factors and cytokines. MSCs are highly efficient at regenerating bone grafts when seeded in proper scaffold materials[19].

Embryonic stem cells are pluripotent and can differentiate into many lineages, such as osteogenic cells, vascular cells, osteoclast cells, and nerve cells[20]. This makes achieving a particular lineage commitment difficult. Furthermore, their usage is limited by a lack of availability due to political and ethical concerns. Although induced pluripotent stem cells (IPSCs) also exhibit pluripotency and do not face ethical or political issues, they are subject to safety concerns which remain to be addressed before they can be used in research for effective bone regeneration. Therefore, we employed MSCs in our experiments due to their safety and ease of availability.

1.2.1 MSC source

Frankenstein and colleagues identified adult MSCs in 1970[21]. They isolated MSCs from different adult tissues such as synovial tissue, tubercular bone, adipose tissue, skeletal muscle, the periosteum, blood, amniotic fluid, umbilical cord blood, the dental bulb, and hair[22]. BM-MSC became one of the main choice for bone tissue engineering. Previous research has shown that the age and health of donors affects the potency of MSCs.This potency also differs by gender[23]. MSCs can be cultured using *in vitro* models without spontaneously transforming into malignant cells. There have been no reports of tumors forming from cell cultured MSCs in human clinical trials.

1.2.2 MSCs and osteogenic differentiation

MSCs can be differentiated into osteoblasts, adipocytes, and chondrocytes. It is a known fact that osteoblasts play a major role in bone regeneration. MSCs can be differentiated into osteoblasts by estrogenic differentiation. As Figure 1-2 shows, *in vitro* estrogenic differentiation can be achieved by methods such as chemical, physical, and other biological factors[24].

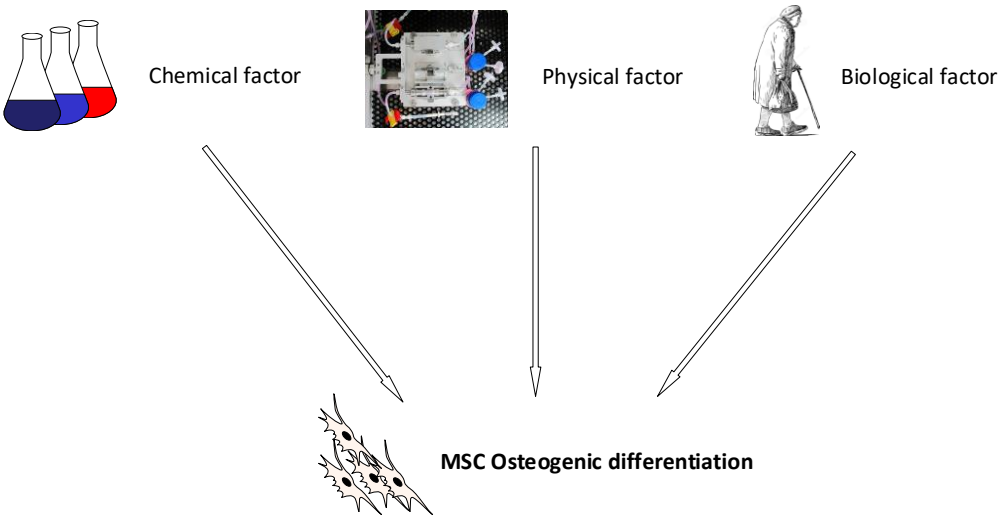

Figure 1-2 Schematic representation of chemical, physical and biological factors influencing MSCs osteogenic differentiation[24]

Chemical factors.

MSCs are cultured in an osteogenic differentiation medium consisting of dexamethasone, ascorbic acid, and beta glycerophosphate[25]. Dexamethasone is needed to achieve osteogenic commitment and achieve higher AP induction. Ascorbic acid helps the MSCs build the ECM, which further supports osteogenic differentiation. Finally, β-glycerophosphate provides a higher level of phosphate ions, which results in higher mineral deposition in the ECM[26].

Physical factors.

Previous research has shown that physical factors such as mechanical forces, cell shapes, the ECM, and the geometric structure of the scaffolds play an important role in stem cell lineage commitment[27]. Integrins can sense the mechanical forces applied to the cells by transducing mechanical signals to the actin cytoskeleton. Mechanical forces could also differentiate MSCs into osteogenic differentiation and inhibit the adipogenic lineage commitment.

Biological factors.

Aging leads to a decrease in the proliferation and differentiation capacity of stem cells. It decreases the osteogenic potential of BM-MSCs in humans, which decreases the number of osteoblasts and results in an imbalance between osteoblasts and osteoclasts. Osteoporosis is an age-related disease resulting from this imbalance[28].

After selecting proper MSCs from the above factors, they can be differentiated into osteogenic lineage commitments. These MSCs are then seeded into a scaffold, which can later be implanted into a patient suffering from a critical size bone defect.

1.3 Scaffolds

Scaffolds play an important role in the field of tissue regeneration and repair. Over the past two decades, much research has been done to develop appropriate scaffold materials for tissue engineering. These three-dimensional (3D) scaffolds perform many functions, such as promoting cell–biomaterial interactions, cell adhesion, and ECM deposition. They permit the sufficient transport of nutrients and regulatory factors to allow cell survival, proliferation, and

differentiation. The most challenging aspect is to produce a scaffold that biodegrades at a controllable rate to supports tissue regeneration without causing any degree of inflammation or toxicity.

Different materials such as natural polymer, synthetic polymer, and ceramics have been used to make scaffolds for bone implants[29]. The scaffolds are seeded with stem cells and later are differentiated into preosteoblasts. This is similar to the new bone formation in our bodies, where stem cells are recruited for bone regeneration. From a materials perspective, scaffolds for bone tissue engineering can generally be categorized into four classes: calcium phosphate-based ceramic bioactive scaffolds, bioactive glass-based scaffolds, polymer-based scaffolds, and composite scaffolds.

1.3.1 Calcium phosphate-based ceramic bioactive scaffolds

Many studies have shown that ceramic can be used as a substitute for bone implants. Most of the research has focused on beta-tricalcium phosphate (β-TCP), hydroxyapatite, or a combination of the two for bone tissue engineering[30]. Recent animal studies have shown that a β-TCP scaffold with greater than 60% porosity can increase not only osteoblast activity but also new bone formation. Other recent research has shown that a calcium phosphate-based scaffold also has a better dissolution rate, mechanical strength, and incompatibility in comparison to other scaffold materials. The presence of 0.5% silicon dioxide (SIO_2) and 0.25 % zinc oxide (ZnO) in the β-TCP scaffold has been reported to increase its compressive strength by 2.5% and cell viability by up to 92%. This composition also increases the collagen type 1 expression and extracellular signal-regulated kinase (ERK) expression and activtion that leads to osteoblast proliferation, differentiation, and morphogenesis.

1.3.2 Bioglass-based bioresorbable scaffolds

Bioactive glass-based scaffolds have excellent osteoconductivity. Scaffolds made from this material allow the cells to distribute evenly, and they exhibit controllable biodegradability. These advantages make a bioglass scaffold one of the most suitable choices for bone tissue engineering[31]. Many compositions have been tested. In vitro studies with 70% porosity have shown the formation of hydroxyl carbonate apatite on the scaffold, resulting from enhanced osteoblastic activity. In vivo studies have shown that the hydroxyl carbonate layer absorbs the

different proteins and soluble factors important for new bone formation. It also increases stem cell proliferation, differentiation, vascular endothelial growth factor (VEGF) secretion, and other gene expression related to bone development [32].

1.3.3 Polymer-based scaffolds

These types of scaffolds can be both biodegradable and bioactive. The most commonly used polymers in bone tissue engineering are silk, fibrin, collagen, and hyaluronic acid (HA). Degradable synthetic polymers such as polylactic acid, polyglycolic acid, and polycaprolactone are used to form the polymeric scaffold. The porous structure of these scaffolds plays a major role in cell adherence. Different techniques have been used to create a porous polymer scaffold, such as salt leaching, phase separation, modified lyophilization, various freezing temperatures, and electrospinning. Studies have shown that increasing pore size leads to improved cell proliferation, attachment, and viability[33].

1.3.4 Composite scaffolds

These scaffolds are made of two or more materials (*i.e.*, ceramic and polymer). The polymer in calcium phosphate increases the toughness and strengthens the scaffold. Similarly, adding calcium phosphate to the polymer leads to an increase in mechanical stability and makes the scaffold bioactive. Like the above-mentioned examples, different material composites have been tested to identify the most stable scaffolds. Current research is being done on combinations such as poly(glycolic acid) (PGA)/β-TCP 3D scaffolds, HA/poly(ester-urethane) (PU) composite scaffolds, biphasic calcium phosphate (BCP) porous scaffolds with HA/polycaprolactone (PCL) composite. Each of these composites has shown promise for bone tissue engineering. They move the cells towards osteoblastic differentiation by upregulating many gene expressions such as RUNX2, collagen type I, OC, and bone sialoprotein[34].

In this thesis, six scaffold types were used to develop of bone implants: poly(L-lactide co-caprolactone) (P(LLA-co-CL)), PP polymer, recombinant collagen peptide (RCP) (collagen type 1 peptide), RCP AP, and RCP AP Mg scaffolds. These scaffolds were developed with optimal characteristics such as strength, rate of degradation, porosity, and microstructure. One advantage of these scaffolds is that they are highly porous. The interconnected geometry of their structures allows for cell ingrowth and uniform cell distribution. Average pore size,

pore size distribution, pore interconnectivity, pore volume, pore shape, and pore throat size played important roles in designing the scaffolds. Furthermore, the mechanical properties of the scaffolds are critical to the success of bone implants. It is highly essential to retain the mechanical strength of the scaffold after implantation to facilitate bone reconstruction.

1.4 Bioreactors for bone tissue engineering

Previous studies have shown that blood vessels play a major role in bone healing. Efficient vascularization in bone leads to bone growth and remodeling[35]. This vascularization provides a proper supply of growth factors, cytokines, oxygen, and nutrients as well as removes the metabolic waste, which leads to healthy bone formation.

A bioreactor plays an important role in the development of new tissue by providing important signaling such as biochemical and physical regulatory signals to cells, and it guides the cells to differentiate into certain lineage commitments. There are many types of bioreactor systems such as spinner flasks, rotating walls, compression strain, and flow perfusion, which are used in various tissue engineering applications[36]. A bioreactor helps cells attain sufficient nutrient and metabolite transport, and homogenous distribution of cells in the scaffolds[37]. It also produces the extracellular matrix prior to *in vivo* implantations.

1.4.1 Spinner flask bioreactor

This type of bioreactor helps uniformly mix oxygen and nutrients throughout the medium. Cell-seeded scaffolds are attached to the ends of needles, where a magnetic stirrer is placed at the bottom of the bioreactor. The media in the bioreactor are constantly moved due to the presence of stirrer. This type of bioreactor is associated with turbulent and transitional flow, through which the media is transported to the center of the scaffolds[38]. The spinner flask usually consists of 120ml of cell culture media. Mass transfer in this type of bioreactor is not good enough to achieve homogeneous cell distribution.

1.4.2 Rotating wall bioreactors

In this type of bioreactor, cell-seeded scaffolds are free to move inside the bioreactor, which contains cell culture media. It is rotated such that the scaffolds are suspended in the media as the downward gravitational force and hydrodynamic drag force balance each other

out[39]. Dynamic flow generated by the rotating wall of the bioreactor helps improve the supply of nutrients and remove waste from the cells. Media exchange is achieved by stopping the bioreactor to remove the old media and replace it with new.

1.4.3 Perfusion bioreactors

Perfusion bioreactors have more advantages than other types, beginning with their ability to distribute cells in the scaffolds uniformly. They also have the best fluid transport, compared with other bioreactors available for bone tissue engineering[40, 41]. A perfusion bioreactor usually consists of a pump and scaffold chamber joined by tubes. Different scaffold materials are placed in the chamber, where fluid flows directly through the cell-seeded scaffold. The cell culture media is circulated constantly between the cell-seeded scaffold chamber and media reservoir. The efficiency of perfusion bioreactors is purely based on the flow rate of the media. Therefore, perfusion bioreactors should be standardized to maintain the proper balance between the media transport of nutrients and removal of waste products from the cells.

1.5 Mechanical force: the physical cue for bone regeneration

Different types of mechanical force can stimulate stem cells toward particular lineage commitments. In the 1980s, Harris et al. showed cell responses based on different types of force applied to them compared with unstimulated cells[42]. Many researchers have since shown that mechanical force plays an important role in bone regeneration[43].

Bone remodeling happens during skeletal development throughout our adult lives. Bone can adapt and sense different mechanical forces to modulate structural strength, shape, and mass[44]. During mechanical stimulation, cells can process and translate these forces into biochemical signals, which activates or upregulates different proteins and gene expressions. Most of the research has suggested that when mechanical force is imposed on bone, extracellular fluid is perfused through the network of canaliculi and lacunae. This fluid flow (or mechanical force) plays a major role in bone remodeling and repair[45].

In the human body, almost all the cells depend on mechanotransduction signaling for their normal functions. This mechanical force is transmitted through the ECM to the cytoskeleton and then to cell nuclei, which alters cellular functions such as autocrine and

paracrine factors, proliferation, migration, differentiation, hypertrophy, and apoptosis[42]. The force exerted by solid or liquid to create this stress is called mechanical stimulation. There are different types of mechanical stimulant, which are classified in Figure 1-.

Compression

Force applied to compress cells is called mechanical deformation or mechanical compression. This type of stress leads to the upregulation of gene markers related to bone, cartilage, and bronchial epithelial cells. Chu et al. showed that the compression force also activates epidermal growth factor receptor (EGFR) ligands[46].

Stretching

Force applied to stretch cells without tearing them is called mechanical stretching. This type of force is applied for better wound healing, tendon healing, skin regeneration, and cardiovascular regeneration.

Osmosis

Osmosis occurs when a solvent (such as water) moves through the semipermeable membrane of a living cell into a solution of higher concentration than inside the cell that tends to equalize the concentration on either side[47]. This type of force is applied for wound healing. Figure 1-3

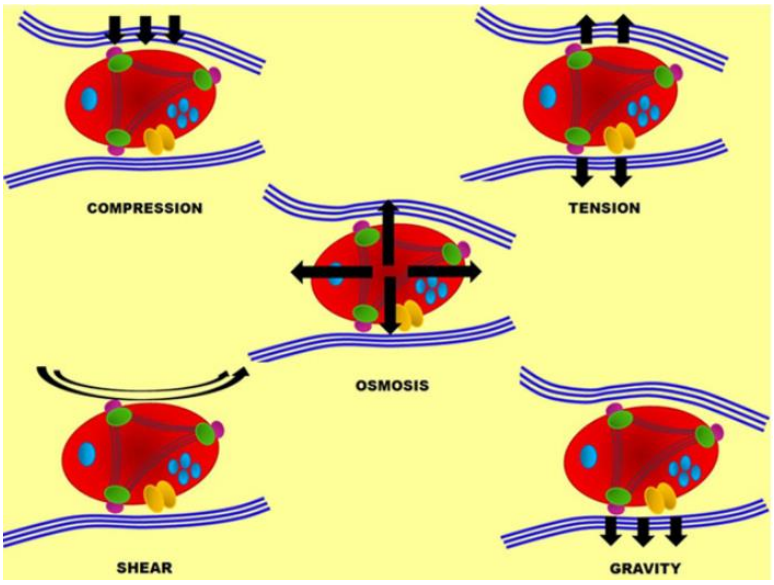

Figure 1-3 :Type of mechanical forces in cell biology [47]

Shear

Shear stress is created from the movement of fluid over the surface of the materials. It plays an important role in differentiating stem cells toward osteogenic lineage commitment[48]. Shear stress affects stem cell behavior at the molecular level, which leads to regulating their shape, proliferation, and differentiation. Du et al. showed that shear stress increases the amount of deoxyribonucleic acid (DNA) and alkaline phosphatase (ALPL) activity under oscillatory flow conditions[49]. They further suggested that continuous flow is advantagous because it allows the cells to migrate from one part of the scaffold to another.

Studies have shown that perfusion flow leads to the upregulation of osteogenic gene expression as well as matrix production, which results in the formation of quality bone tissue. The same study showed that shear stress in the 3D cell culture system leads to an increase in osteopontin and ALPL gene expression[48].

Gravity

Microgravity provides an environment in which intercellular forces become more evident because gravitational force is out of the picture. This type of stress is created by a rotational bioreactor, which stimulates a microgravitational environment. Studies have shown that a microgravity cell culture enhances the therapeutic effect of stem cell transplantation to various diseases in the cental nervous system, traumatic brain injuries, and visceral dieases. My PhD research work mainly focused on the perfusion bioreactor system due to the presence of shear stress in its culture condition. This helped the stem cells differentiate into osteogenic lineage commitment.

1.5.1 Mechanical deformation bioreactors

Mechanical deformation mainly depends on parameters such as the stiffness of the scaffold, type and elasticity of scaffold material, type of compression, type of stretching, type of frequency, type of amplitude, duration of treatment, shear stress, and type of cells. Different types of mechanical deformation forces are illustrated in Figure 1-4.

Simple compression strain.

This type of strain occurs when force is applied in one direction, compressing the 3D scaffold in that direction and stretching the orthogonal direction of the scaffold.

Pure uniaxial strain.

This strain happens when the scaffold is compressed in one direction while clamped on its orthogonal direction, inducing a pure uniaxial compression strain.

Biaxial strain.

In contrast with a uniaxial strain, a biaxial strain is achieved when the scaffold is compressed equally in both orthogonal directions.

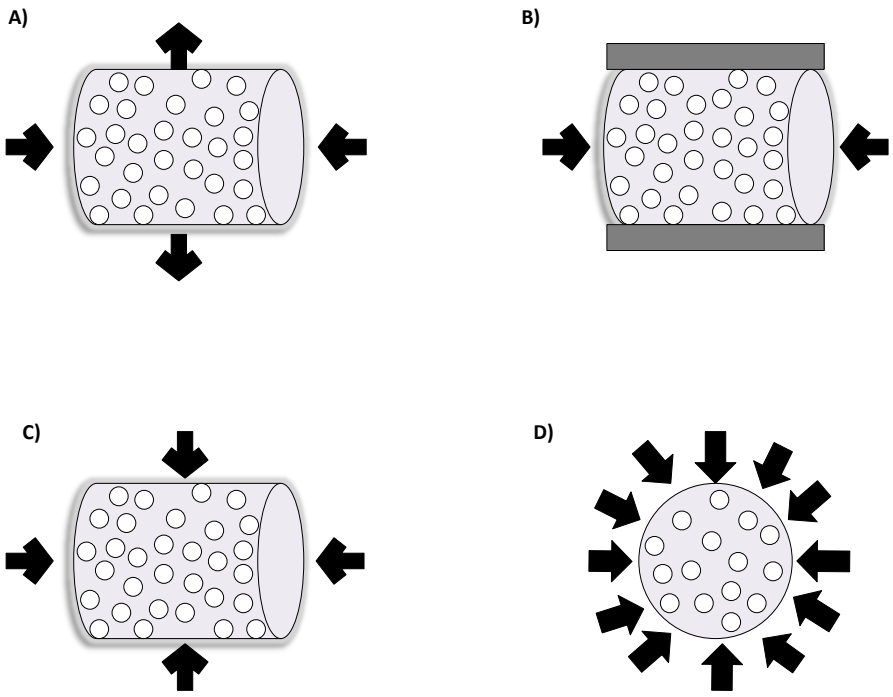

Figure 1-4 :Scheme of different compression variation (a) Simple compression strain, (B) Pure uniaxial strain, (c) biaxial strain (compressed in both direction), (D) Multi axial strain (compression is applied in all possible directions).

Multiaxial strain.

Multiaxial strain is induced when force is applied to the 3D scaffold in all possible directions.

In my PhD research, the vascubator was a custom-made incubator consisting of a mechanical stimulation bioreactor and a linear motor device. The experimental parameters of sinusoidal uniaxial scaffold deformation amplitude (%) and frequency of scaffold deformation (Hz) were used to apply mechanical deformation to the cells. The scaffold deformation experiments were conducted in the vascubator at combinations covering a range of 1–2% at 1–2 Hz[50, 51]. As the results of this mechanical force on the cells, different growth factors, cytokines, and gene expression are upregulated in the cells[52–54].

1.6 Signaling mechanism

Different growth factors and cytokines significantly impact bone regeneration. Dimitriou et al. showed that cytokines such as interleukin-1 (IL-1), interleukin 6 (IL-6), and tumor necrosis factor alpha (TNF-α) as wells as other factors such as TGF-β, BMPs, and fibroblast growth factor (FGF) play major roles in early bone regeneration[55]. Other studies have shown that in bioreactor cultures, different osteogenic genes such as osteonectin, OC, AP, early marker RUNX2, collagen type 1, and osteopontin are expressed under shear stress[56–58].

Cheung et al. showed that stem cells subject to shear stress express different genes such as osteopontin, collagen type 1, and OC after 35 days of 3D cell culture[59]. Bernhart et al. showed that stem cells under perfusion show an increase in AP, which is important for bone formation[60]. The studies have also shown that shear stress leads to the increased expression of collagen type 1 and osteopontin. Similarly, Bjerre et al. showed that shear stress increases the expression of ALPL, osteopontin, bone morphogenetic protein-2 (BMP2), RUNX2, and OC[61].

Recent bioreactor studies have shown that different mechanical forces result in the expression of different osteogenic gene markers. Matziolis et al. showed when mechanical deformation is applied for 1 day, it leads to an increase in osteopontin and TGF-β gene expressions[62]. Similarly, when mechanical compression is applied for 14 days to a stem cell-seeded collagen scaffold, it leads to increased ECM mineralization. In another study, a demineralized bone matrix scaffold was seeded with stem cells and 5% amplitude and one Hertz of mechanical compression were applied. This resulted in an increase to the proliferation of cells as well as changes to the microstructure inside the scaffold[64].

Liu et al. has also shown that when the polyurethane scaffold seeded with stem cells is compressed for 21 days of cell culture, it leads to a significant increase in ALPL, collagen type 1, and calcium gene expressions[63]. Some studies applied different types of mechanical stress, such as putting tension on the cells, which resulted in the upregulation of genes responsible for bone remodeling. Perter and Qin et al. have shown that stretching of stem cells for 7 days results in the upregulation of TGF-β and collagen type 1 gene expressions[64]. Yang et al. also showed that when mechanical stretching is done to stem cells, it leads to increased expressions of genes such as BMP2, RUNX2, osteonectin, and ALPL, which play a major role in osteogenic lineage commitment[65].

1.7 Toward an ideal bioreactor for developing bone grafts

Following immense progress in the field of bioreactor technology and significant advances to our knowledge of bone biology, growth factors, cytokines, signaling pathways, stem cell technology, and scaffold materials, several attempts have been made to develop bioreactors for bone graft development. But there has been no proper bone graft available in the market for clinical use until now. Recent studies have shown that mechanical forces play a major role in the development of bone thoughout the life cycle (*i.e.*, by releasing different growth factors and cytokines and upregulating different genes). Hence, I tested different types of mechanical stress on bone cells to achieve the highest osteogenic lineage commitment.

2 Aim and objectives

The aim of this thesis was to establish a technology for generating grafts with a minimum size of 10.5mm wide and 12.5mm tall, which is necessary for treating critical size bone defects. Bioreactor technology was developed to allow for standardized flow conditions both with and without mechanical stimulation on the different scaffolds. This bioreactor technology permitted mechanical stress to trigger the osteogenic differentiation of stem cells into osteogenic lineage commitment. Accordingly, the overall aim of this thesis was to determine the effect of different mechanical stress types on stem cells seeded onto each scaffold to achieve better osteogenic lineage commitment. This aim was addressed via the following objectives:

1) To evaluate the role of a mechanical shear stress bioreactor on different scaffold materials using patient-derived stem cells to efficiently generate cell-loaded bone substitute for critical size bone defects.

2) To study the effect of different types of mechanical deformation on cell-seeded scaffolds with respect to osteogenic lineage commitment at different intervals.

3) To identify whether mechanical shear stress or mechanical deformation is the main physical driver causing skeletal precursors to undergo osteogenesis in the early stage of bone regeneration.

4) To develop an *in vitro* osteoporotic test system for testing and evaluating osteoporotic drugs at the drug discovery stage to help prevent bone loss in osteoporotic patients.

These objectives addressed the role of different types of mechanical stress in enhancing osteogenic lineage commitment and sought to identify scaffold materials best suited to achieve better bone implants.

3 Materials and methods

3.1 Materials

In this section, the materials used to perform different experiments such as equipment, chemicals reagent, buffers, plastic disposal, primers and commercially available kits are described in details.

3.1.1 List of chemicals

Table 3-1 showing list of chemical used in the PhD research work.

Chemical	Product Number	Company name
3-(4,5-Dimethylthiazol-2-yl)2,5 diphenyltetrazoliumbromide (MTT)	20395	Serva, Heidelberg (GER)
Acetic acid	A6283	Sigma-Aldrich, Munich (GER)
Acetone (≥ 99.5% (v/v))	48358	Sigma-Aldrich, Munich (GER)
Chloroform	C2432	Sigma-Aldrich, München (GER)
Dimethyl sulfoxide (DMSO)	472301	Sigma-Aldrich, Munich (GER)
Descosept	00311-100	Dr. Schumacher, Malsfeld (GER)
Dulbecco's Modified Eagle Medium (DMEM)	61965-026	Life technologies, Darmstadt (GER)
Dexamethason	08168	Sigma–Aldrich, Munich (GER)
Ethanol, absolute	24102	Sigma-Aldrich, Munich (GER)
Fetal Calf Serum (FCS)	FCS.ADD.0500	Bio&SELL, Feucht (GER)
Hydrochloric acid	258148	Sigma-Aldrich, Munich (GER)
Isopropyl alcohol	278475	Sigma-Aldrich, Munich (GER)

Chemical	Product Number	Company name
L-ascorbyl-2-phosphate	A8960	Sigma-Aldrich, Munich (GER)
Paraformaldehyde (PFA)	A3813	AppliChem, Darmstadt (GER)
Penicillin/Streptomycin (100 x concentrated)	P4333	Sigma-Aldrich, Munich (GER)
Phosphate-buffered saline with calcium and magnesium (PBS+)	D8662	Sigma-Aldrich, Munich (GER)
Phosphate-buffered saline without calcium and magnesium (PBS-)	D8537	Sigma-Aldrich, Munich (GER)
RNAlater	76104	Qiagen, Hilden (G)
Na- pyruvate	08168	Sigma-Aldrich, Munich (GER)
l-proline	131547	Sigma-Aldrich, Munich (GER)
ITS^{+} (human insulin, human transferrin, and sodium selenite)	354352	BD
Trypan blue, 0.4%	T8154	Sigma-Aldrich, Munich (GER)
Tween®-20	P2287	Sigma-Aldrich, Munich (GER)
Tissue lysis reagent QIAzol	79306	Qiagen, Hilden (G)
Hygromycin B	10687010	Thermo Fisher Scientific

3.1.2 Cell Culture media and Buffer

List of different cell culture media used for experiment purpose and also the buffers used for washing the cells and staining are mentioned in this section.

Table 3-2 showing list of components used in the media preparation.

Media	Composition	Volume
MEM expansions media for TERT cells	MEM media	89%
	FSC	10%
	Penstrip	1%
	Hygromycin B	50 µg/ml
DEMEM expansion media for stem cells	MEM media	89%
	FSC	10%
	Penstrip	1%
Lonza medium expansion media for stem cells	Lonza media with supplement	97%
	FSC	2%
	Penstrip	1%

Table 3-3 showing list of components used in the buffer preparation

Buffer	Composition	Final concentration
Trypsin-EDTA 1x (cell culture)	PBS/EDTA	90% (v/v)
	Trypsin-EDTA (10x)	10% (v/v)
FACS buffer	PBS	
	EDTA 2mM	2mM
	BSA	0.5% (v/v)

3.1.3 Scaffolds materials used in the PhD research work

Table 3-4 showing list of scaffolds used in the thesis

S. No.	Name of the scaffold	University / Company	Contract person
1)	poly(L-lactide-co-caprolactone) scaffold	KTH VETENSKAP OCH KONST	Dr. Anna Fine Wistrand
2)	β-TCP scaffold	curasan Regenerative Medicine	Cursan Inc.
3)	Pppolymer scaffold	PPPOLYMER	Dr. Swaraj Paul (CEO)
4)	RCP scaffold	istec National Research Council of Italy Institute of Science and Technology for Ceramics	Dr. Gloria Ramirez Rodriguez
5)	RCP AP scaffold	istec National Research Council of Italy Institute of Science and Technology for Ceramics	Dr. Gloria Ramirez Rodriguez
6)	RCP AP MG scaffold	istec National Research Council of Italy Institute of Science and Technology for Ceramics	Dr.Gloria Ramirez Rodriguez

3.1.4 Commercially obtained kits and primers

List of all the commercially obtained kits and primers used for analyzing the experiments are mentioned below.

Table 3-5 showing commercially obtained Kits.

Name of kit	Description	Product no.	Company
Super Vision 2 HRPPolymer-Kit	Kit containing secondary mouse- and rabbitantibody, a polymer conjugated with HRP against	Cat. No PD000KIT	DCS Innovative Diagnostik System, Hamburg (GER)

Name of kit	Description	Product no.	Company
	secondary antibody, DAB concentrate, DAB substrate buffer		
Collagen I	(1:2000) rabbit	BP8028	Acris Antibodies, Herford (GER)
RNeasy Micro Kit	Rneasy MinElute Spin Columns Collection Tubes (1.5ml, 2.0ml) Buffer RLT Buffer RW1 Buffer RPE Rnase-Free Water	74004	Qiagen, Hilden (G)
The QuantiTect Reverse Transcription Kit	gDNA Wipeout Buffer Reverse-transcription master mix Quantiscript Reverse Transcriptase* Quantiscript RT Buffer, 5x RT Primer Mix	205310	cDNA Synthesis, Hilden (GER)
QuantiTect SYBR Green PCR Kit	SYBR green PCR Master Mix Primer Rnase-Free Water	204141	PCR kit, Hilden (GER)

Table 3-6 showing list of QIAGEN QuantiTect RT-PCR Primer Assay

S.No	Assay Name	Gene Symbol	Catalog no.
1	Hs_GAPDH_1_SG	GAPDH	QT00079247
2	Hs_BGLAP_1_SG	BGLAP	QT00232771
3	Hs_SPARC_1_SG	SPARC	QT00018620
4	Hs_RUNX2_1_SG	RUNX2	QT00020517
5	Hs_ALPL_1_SG	ALPL	QT00012957
6	Hs_SPP1_1_SG	SPP1	QT01008798
7	Hs_COL1A1_1_SG	COL1A1	QT00037793
8	Hs_BMP2_1_SG	BMP2	QT00012544
9	Hs_TGFB1_1_SG	TGFB1	QT00000728
10	Hs_VEGFA_1_SG	VEGFA	QT01010184

3.1.5 FACS Antibodies

Table 3-7 showing list of FACS antibodies used in the study

S.no.	FACS antibody	Company	Cat.no
1	CD73 –PE	BD, Heidelberg, Germany	561014
2	CD90-PE	Beckman Coulter,	IM1840U
3	CD105-PE	Beckman Coulter	A07414
4	CD14-PE	BD	345785
5	CD19-APC	BD	345791

S.no.	FACS antibody	Company	Cat.no
6	CD34 –FITC	BD	345801
7	CD45-APC	Beckman Coulter	A71117

3.1.6 Laboratory Equipment

Table 3-8 showing list of equipment used in lab.

Designation	Manufacturer	Specification
Aspiration system	VACUSAFE	Integra Biosciences,Biebertal (G)
Autoclave	Giessen (G) Systec, Wettenberg (G) H+P, Hackermoos (G)	Tecnoklav Biomedis, TableTop Autoclave Varioklav
Cell culture safety cabinet	Thermo Fisher Scientic, Dreieich (G)	Safe2020
Cell incubator 37°c,5% co2	Haraeus,Hanau (G)	
Centrifuge	Thermo Fisher Scientic, Dreieich (G)	Multifuge X3R
Cell counting chamber	Hartenstein, Würzburg (G)	
Real time PCR Detection system	Biorad,München (G)	CFX96
Cold storage room 4°C	Genheimer, Höchberg (G)	
Freezer -20 °C	Liebherr, Biberach (G)	
Freezer -80 °C	Kendro,München (G)	

Designation	Manufacturer	Specification
Fume hood	Prutscher Laboratory Systems, Neudör (AT)	
Immersion thermostat for Water Bath	Lauda, Lauda-Königshofen (G)	
Ice machine	Scotsman, Milan (I)	AF-80
Infinite 200 PRO NanoQuant	Tecan Deutschland	
Medical pump for cell seeding	Landgraf Laborsysteme Langenhagen, Germany	
Microbalance	Sartorius Stedium Biotech, Göttingen (G)	SE2 Ultra
Micro centrifuge	Eppendorf, Hamburg (G)	5417R
Microscope	Carl Zeiss, Jena (G)	AxioVision
Pipets	Eppendorf, Hamburg (G)	0.5-10µl, 10-100µl, 100-1000µl,
Pipetting aid pipetboy	Brand, Wertheim (G)	
PH meter	Mettler Toledo, Giessen (G)	
Multiplate for qPCR		Biorad, München (G)
PCR detection system		
Sonicator		
Vascubator		
Pump		

Designation	Manufacturer	Specification
Ph meter **Pressure sensor** **Mechanical stimulator** **Heat exchange** **Gas Exchange module**	Built in house at Lehrstuhl für Tissue Engineering und Regenerative Medizin, Würzburg	
Vortex Genie 2	Scientific Industries, INc., NY (USA)	
Liquid nitrogen storage tank	German-cryo, Jüchen (GER)	MVE 815 P-190
Thermocycler	SensoQuest, Göttingen (G)	
Vortex shaker	Scientic Industries via Carl Roth, Karlsruhe (G)	Vortex-Genie 2
Orbital shaker	Edmund Bühler, Hechingen (G)	KM-2 Akku
Bioreactor	Weckert Labortechnik, Kitzingen (GER)	
Freezing container "Mr. Frosty"	VWR, Darmstadt (GER)	
Water purification system	Millipore, Schwalbach (GER)	
TissueLyser LT	Qiagen(GER)	
Programmable Aladdin Syringe Pump	World precision instruments(GER)	Cell seeding into the bioreactor

3.1.7 Software

Table 3-9 showing list of software used to analysis the data

Application	Software	Company
SEM images	JEOL	JEOL GmbH
plate reader	Tecan i-control V 2.11	Tecan Deutschland
Recording PCR data	CFX manager 3.1	Bio-Rad
Statistics	Origin	Origin lab
	GraphPad Software Inc	GraphPad Prism

3.1.8 Laboratory materials and consumables

Table 3-10 Table showing list of laboratory materials and consumables.

Material	Manufacture	Specification
Beakers:	Schott, Mainz (GER)	250ml
Cell culture dish 35mm	Thermo Scientic Nunc, Dreieich (G)	
Cell culture multiwell plates	TPP, Trasadingen (G)	6 well, 12 well, 24 well
Cell Strainer EASYstrainer	Greiner Bio-One, Frickenhausen (G)	40 µm, 70 µm, 100 µm
Centrifuge Tubes	Greiner Bio-One, Frickenhausen (G)	CELLSTAR 15ml, 50ml
Cold protection gloves	VWR, Darmstadt (GER)	

Material	Manufacture	Specification
Forceps	Fine Science Tools, Heidelberg (G)	Standard, Dumont #3c, Dumont #5
Medical gloves	Kimberly-Clark, Koblenz (G)	
Microcentrifuge tubes	Eppendorf, Hamburg (G) PCR soft tubes, 0.2µl	Biozym, Hessisch Oldendorf (G) PCR clean 1.5ml, 2ml
Micro-spoon spatula	Hartenstein, Würzburg (G)	
Spoon spatula	Hartenstein, Würzburg (G)	
Multiplate for qPCR	Biorad, München (G)	Low-Profile 96-Well unscripted
PCR IsoFreeze Rack	LTF Labortechnik, Wassserburg (G)	with color indicator
PCR Tube Rack 96-Well with Cover	VWR, Darmstadt (G)	
Pipet tips	Nerbe plus, Winsen/Luhe (G)	0.5-10µl, 10-100µl, 100-1000µl
pressure sensor	HJK Sensoren/Syst. GmbH & Co. KG (D)	
Syringe	BD Biosciences, Heidelberg (G)	10ml Discardit II
Sterile filter	Hartenstein, Würzburg (GER)	

Material	Manufacture	Specification
Spray flask (Ethanol 70% (v/v), Descosept)	Hartenstein, Würzburg (GER)	
Stainless steel casting moulds for embedding tissue	Labonord, Mönchengladbach (GER)	
Sterile filter	Hartenstein, Würzburg (GER)	
Sterile filter Ø 50mm, pore size 0.2 µm	Sartorius Stedium Biotech (D)	
Laboratory bottles container for bioreactor: 50ml	Schott, Mainz (GER)	
Pump tubing for Bioreactor	ISMATEC, Wertheim(GER)	
Teflonband	Hydrasun Ltd (GB)	

3. 2 Methods

3.2.1 Stem cell isolation

Bone marrow stem cells were isolated with the approval of the local ethics committee (Vote IGBZSF-2012-078, vote 182/10) from bone marrow aspirate (Lonza, Walkersville, USA). The first three donors were from bone marrow aspirate (Lonza, Walkerville, USA) of two from male 24 & 25 years old and other one female from 45 years old healthy donor. Among the other three remaining donors, one were isolated from healthy donor i.e. male 76. The other two are isolated from osteoporotic disease donor women 70 and 77 years old. This bone marrow-MSCs were isolated from spongiosa biopsy samples received from the König-Ludwig Haus hospital. The biopsy sample was placed in the 50ml falcon tubes filled with 20ml DMEM media. Cells were obtained by briefly shaking, washing and centrifuging at 1200 rpm for 5 mins. The top layer of the supernatant in the flacon tube was discarded. The pellet obtained was washed again with 20ml of DMEM/F12 media and consequently pelleted until the biopsy bone becomes white. The cell pellet obtained was mixed with 30ml of DMEM supplemented with 10% FCS, 1% Penstrep and Ascorbate-2-phosphate and cultured in a T175 flask. The media was changed after 4 days and then every third day. Bone marrow-MSCs got confluent in about 5 to 7 days i.e. upon reaching 90% confluency the cells were either passaged again or frozen in liquid nitrogen for later use.

3.2.2 Freezing of cells

Long term cell storage was done with cryopreservation. The confluent flask was trypsinised and 1 million cells were dispensed in 1ml solution containing 10% dimethyl sulfoxide (DMSO) and 90% Fetal Calf Serum (FCS). Cells were transferred to cryotubes and stored in Mr Frosty at -80°C freezer for a duration of 24hours. Later, cryotubes were transferred into a liquid nitrogen storage tank for long term storage.

3.2.3 Thawing of cells

The cryotubes taken from the liquid nitrogen were thawed partially in a water bath heated up to 37°C. To remove DMSO, 2ml of FCS was added to the thawed cells and centrifuged at 1200 rpm for 5 mins. Cell pellet obtained was suspended into the fresh DMEM media and later they were transferred in a new cell culture flask.

3.2.4 Cell culture

The cell culture media was changed every third day to ensure proper nutrients and growth factor supply for the cells and to keep them in the exponential growth phase. The cells were cultured at 37°C with 5% CO_2. Media was changed by removing the old culture media present in cell culture flash and replaced with fresh media, which was prewarmed to 37°C.

Culture of TERT-AP1 cell line

TERT-AP1 cell line is basically Telomerase immortalized human mesenchymal stem cell line which were stabily transfected with luciferase reporter gene *luc2* (*Photinus pyralis*) clonned under AP1 response element. The AP1 response element have been shown to respond to mechanical strain. Thus this cell line produces luciferace reporter gene under mechanical stimulation. These cells were cultured in MEM expansions media containing 10% FCS and1% penicillin and streptomycin at 37°C with 5% CO_2. This cell line was given by Prof. Dr.Franz Jakob (Orthopedic Center for Musculoskeletal Research, Orthopedic Department, University of Würzburg, Würzburg, Germany) for this research work

3.2.5 Characterization of MSCs

Isolated stem cells were characterized for multipotency by assessing their ability to differentiate into osteogenic, adipogenic and chondrogenic lineages.

3.2.6 Osteogenic differentiation

15,000 MSCs were seeded per well in a 24 well plate and cultured with DMEM supplemented with 1% Penstrep and 10% FCS. After reaching confluency, cells were grown in the osteogenic differentiation media. The composition of osteogenic media for 50ml is described in the table below:

Table 3-11 Table showing composition of osteogenic media.

S.no.	Composition	Volume
1	DMEM 10%FCS 1%P/S	49.445ml
2	Ascorbat -2 phosphat	50µl
3	β-glycerophosphat	500µl
4	Dexamethason	5µl

Osteogenic differentiation media was refreshed every two days for 28 days. The alizarin red staining was done to confirm the differentiation process.

3.2.7 Alizarin red staining

Alizarin red staining is used to quantify the number of mineralized calcium deposits. After 28 days of post culture with osteogenic differentiation medium MSCs were washed with 1ml PBS. Cells were then fixed with 50% ethanol (room temperature) for 20mins. Afterwards, cells were stained by alizarin red dye solution at pH 6.4 for 30 mins under continuous shaking. Subsequently, cells were rinsed with water for three times. Then results were documented with microscopy.

3.2.8 Calcification assay

After osteogenic differentiation calcium content was quantified by dissolving the dye with the solution containing 0.5 M HCL and 5% SDS for 30 mins at room temperature. The Absorbance of the solvent was measured in the plate reader at 415nm (infinite M200, Tecan).

3.2.9 Adipogenic Differentiation

15,000 MSCs were cultured per well in 24 well plates. After reaching confluency, cells were grown in the adipogenic induction media. 50ml of Adipogenic induction media was set up as per table 3.12

Table 3-12 Table showing components of Adipogenic differentiation media

S.No	Composition	Volume
1	DMEM + 10% FCS	49.80ml
2	Dexamethason	50µl
3	IBMX	50µl
4	Insulin	50µl
5	Indomethacin	50µl

Adipogenic induction media was replaced every two days for 14 days. The oil red staining procedure was done to confirm the differentiation process.

3.2.10 Oil red staining

Oil red staining was done to quantify the lipid droplets obtained during adipogenic lineage commitment. After 14 days of induction of adipogenic differentiation, the cells were washed with PBS and fixed with 4% paraformaldehyde (PFA) for 20 mins. Thereafter, cells were washed with 60% of isopropanol for 5mins and oil red staining solution is added for 10 mins. Cells were once again washed with 60% of isopropanol followed by demineralized water. Hematoxylin was then added for 30 seconds and later washed tap water. Staining results were documented with microscopy.

3.2.11 Chrondrogenic differentiation

For chondrogenic differentiation at least one differentiation, assay and one negative control were made. 250,000 cells were centrifuged per assay in a 15ml centrifuge tube for 15 minutes at 1200 rpm. Pelleted cells were incubated overnight in the incubator and transferred into a 24 well plate (1 aggregate/well) the day after. 300µl differentiation medium were carefully added to the aggregate. The composition of the chondrogenic differentiation medium is presented in the table below:

Table 3-13 Table showing components of Chondrogenic differentiation medium

S.No	Content	Volume
1	DMEM	49.79ml
2	Ascorbat-2-Phosphat	50µl
3	Dexamethason	5µl
4	Na-Pyruvate	50µl
5	L-Proline	50µl
6	ITS+	5µl
7	TGF-β3	50µl

Chondrogenic differentiation medium without TGF-ß3 was used as a negative control and with TGF-ß3 was used as a positive control for the differentiation assay. Pellets are cultivated with the differentiation medium for 21 days and the medium was changed twice a *week TGIF*-ß3 is always added fresh to the medium before the medium is changed (1µl TGF-β3/2ml chondrogenic medium). After the differentiation protocol, Alcian blue staining was done to evaluate chondrogenic differentiation.

3.2.12 Alcian blue staining

For visualization of proteoglycans, which are abundant in cartilage, Alcian blue staining was performed. Sections were heated for 30 min at 60°C, and subsequently, deparaffinized using Roticlear®and decreasing ethanol concentrations. Washing in 0.1M HCl was performed for equilibration. Alcian blue solution containing1% w/v alcian blue 8 GX in 0.1M HCl was

added on the sections. For counterstaining, nuclear fast red solution was used to visualize cell nuclei. After dehydrating, sections were covered with mounting medium.

3.2.13 FACS

The fibroblast colony-forming units were characterized for their multipotent mesenchymal stem cells functions using a panel of cells surface markers according to ISCT guidelines (International society for cell therapy, 2006 position paper). The stem cells were characterized for the absence of hematopoietic markers and HLA-DR. Specific antibodies conjugated were used along with appropriate isotype controls.

MSCs were trypsinized, counted and 20,000 cells were placed per-flow tube. Cells were then with PBS Azide and spindown at 1800rpm for 5mins. 10µl of FC receptor (blocking agent) was added per 1ml of blocking buffer. 100µl of the blocking buffer was added to all the flow tubes, cells were resuspended and incubated on ice for 10mins. Appropriate antibodies shown in the table was added and incubated on ice for 1hour at 4°C.

Table 3-14 showing antibodies used for characterization of MSCs.

S.no.	Antibody
1	CD 73-PE
2	CD 90-PE
3	CD 105-PE
4	CD14-APC
5	CD 19-APC
6	CD 34-APC
7	CD 45-APC

Subsequently, cells were washed with PBS Azide and fixed with 300µl of 1% PFA for the whole day at 4°C. Following day all the flow tubes were run through BD FACSCalibur™ and 10,000 events were counted. The cells expressed either the positive or negative of markers based on their phenotype.

3.2.14 Population doubling of mesenchymal stem cells

The growth kinetics of MSCs was done to determine the growth rate of cells in each passage. This was done in passages ranging from p1 to p6. It is a useful method to understand the growth curve of stem cells under different passage.

15,000 cells per well were cultured in three wells in 24 well plates. After 3 days of culture, the cells were counted again after trypsinization. This was done from passage 1 till passage 6.

3.2.15 Bioreactor setup for autoclave

Bioreactor setup consisted of pump hose, silicon tubes, connectors, and bioreactor cartridge, air filters, septum, pressure sensor and media container. The bioreactor setup was made according to figure 3-1 described below

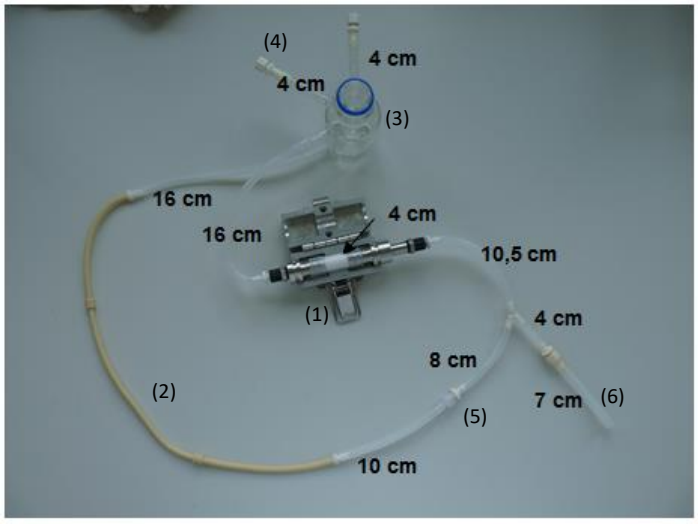

Figure 3-1 Bioreactor setup for Autoclave. (1) Bioreactor cartridge, (2) Pump housing tube, (3) bottle for media reservoir, (4) Provision for air filters, (5) Provision for pressure sensor, (6) Provision for cell seeding septum.[66].

The cell culture media reservoir is connected to the pump housing tube with connectors. This pump housing tube is connected to the bioreactor chamber and which is connected back to the media reservoir. After connections were made, the bioreactor was autoclaved for sterilization.

3.2.16 Cell seeding protocol

The different scaffolds cylinders were under the dynamic conditions in the perfusion bioreactor. In general, scaffolds were placed in the custom-made bioreactor cartridge and perfused by peristaltic pump for 1hour with the stem cell culture media before cell seeding.

The stem cells were harvested and resuspended at the concentration of 5 million cells in 10ml of stem cell growth medium. This stem cell suspended medium was transferred to a syringe (10ml) without air bubbles and injected through the sampling port with the help of a syringe pump at a flow rate of 0.5ml/min. The applied pressure in the bioreactor was measured by the pressure sensor and it is controlled in between 10 to 20mmHg. The cell suspension was pumped through the bioreactor chamber in the alternating cycle for 10s forward and 3 s backwards at a total of 1 hour at 1.6ml/ min. Once the seeding process was finished, the pump was stopped for 30 to 40mins in to allow the cells to be attached in the scaffold.

3.2.17 Computational fluid dynamic

To predict the shear stress distribution inside the scaffold, computational modelling was performed. Based on the bioreactor cartridge geometry, three-domain such as an inlet, outlet and the porous of the scaffold were generated by the computer-aided design (CAD). To simulate the flow regimes, COMSOL Multiphysics™ was used. The in- and outlet were defined as laminar flow domains, whereas, Darcy's law derived for creeping flows, i.e. for Reynolds numbers (Re)<< 1, was applied for the porous scaffold. When the flow rate was at 0.8ml/min, Re was approximately 214 [1/m] × pore diameter [m], in our system. Thus with pore diameters in the range of micrometres, Re was << 1 and Darcy's law held. The porosity of the scaffold was set as 90% in according to the µCT data we measured. By measuring the pressure difference at different flow rates, the permeability of the scaffold was determined as $1.72 \pm 0.2 \times 10^{-1}$ m^2. At the inlet, the total flow of 0.8ml/min was defined as a boundary condition. The outlet was set to ambient pressure[66].

3.2.18 3D culture conditions

3-dimensional cell culture was done at three different culture conditions, these are described below:

Static condition

The MSCs was seeded in the scaffolds as described in Cell seeding protocol. The dynamic cell-seeded scaffold was transferred from bioreactor into 50ml sterile glass bottle equipped with two filters (0.22µm) for gas exchange. They were cultured in stem cell growth medium at 37°C and 5% CO_2. Culture Medium was changed every two days and during experiments, no further MSCs were introduced into the system.

Dynamic condition

MSCs were seeded in the scaffold as described in Cell seeding protocol. The cells seeded scaffold in the bioreactor was perfused with the medium four times per hour for 5 mins at 0.8ml/min or two times per hour for 20 minutes at 1.6ml/min. The medium was changed every two days and during experiments, no further MSCs were introduced into the system.

Mechanical stimulation

After cell seeding into the bioreactor as described in 0, cyclic mechanical compression was applied through a period time of 48hours i.e. 1 hour in morning and evening for 2 days respectively. To ensure optimal cell culture conditions of 37°C and 5% CO2, during the mechanical stimulation, bioreactor and linear motion device were housed in the custom made incubator. Different types of forces are applied in this bioreactor based on experimental parameters comprised sinusoidal uniaxial scaffold deformation amplitude (%) and frequency of scaffold deformation.

3.2.19 Viability Assay (MTT assay)

MTT (3- (4,5-dimethyl-2-thiazolyl) -2,5-diphenyl-2H-tetrazolium bromide) test was done to check the viability of cells. 60mg MTT was dissolved in 20ml of demineralized water (3mg/ml) under sterile condition. Later the aliquot of MTT was stored in -20°C until further use. 2ml of an MTT stock reagent was thawed and mixed with 4ml of water to prepare a MTT working solution. For the viability assay, MTT solution was then added on the cells and they

were incubated for 30 mins at 37°C. Mitochondrial succinic dehydrogenase enzyme present in the viable cells metabolise MTT dye (yellow) to yield a purple formazan product. Presence and intensity of purple color indicates exsistance of viability and distribution of the cells on the scaffold.

3.2.20 Alizarin red staining for scaffolds

Alizarin red staining is used to quantify the number of mineralized calcium deposits. After the media was removed from the bioreactor, the cell-seeded scaffold was washed with PBS. Followed by fixation with 50% EtOH for 20mins. This fixed cell-seeded scaffold was stained by alizarin red at pH 6.4 for 30mins under continues shaking. Subsequently, cells seeded scaffold was rinsed with water for three times and photographed for documentation.

3.2.21 Calcification assay for scaffolds

Quantification of the calcium content of the scaffolds was done by dissolving Alizarin dye with 5ml solution containing 0.5 M HCL and 5% SDS for 30 minutes at room temperature. The absorbance of the solvent was measured in the plate reader at 415nm (infinite M200, Tecan).

3.2.22 Collagen type 1 staining

Expression of collagen type I by bone marrow stem cells cultured on scaffolds was determined by immunohistochemistry. Fresh samples of hybrid constructs were hydrated by washing them in PBS at 37°C. PBS was removed and samples were blocked with blocking buffer (BB) for 60 minutes at room temperature. Dilutions of the primary antibody were made in PBS with 10% blocking buffer. Samples were incubated with the primary antibody at 4°C for 16 hours and subsequently, they washed 3 times with PBS with 10% blocking buffer. Samples were incubated with a secondary antibody for 60 minutes at room temperature.

Samples were washed 3 times with PBS. Subsequently aDAB (3,3'-Diaminobenzidine) chromogen solution was prepared by adding 3 drops of DAB solution in 1ml of DAB buffer (buffer solution pH 7,5 DAKO). Samples were incubated in 100µl of DAB chromogen solution for 10 minutes at room temperature. Positive (goat bone) and negative (incubations without primary antibody and scaffolds without cells) controls were also included in this experiment.

3.2.23 Tissue rupture

100mg of the cell-seeded scaffold was taken in the 1.5ml microcentrifuge tube and 1ml of qiazol is added along with metal beads to rupture the cell-seeded the scaffold. The cell-seeded scaffolds were then ruptured by subjecting to oscillation mode of 50 for 10 mins in TissueLyser LT. This ruptured semi-liquid obtained was further for RNA isolation.

3.2.24 RNA Isolation

To the semi-liquid slurry obtained from after tissue rupture sees paragraph0. Chloroform (200µl) was added and centrifuged at 13,000 rpm for 15 mins at 4°C. The sample segregated into three layers, the top layer consisted of RNA, the middle layer consists of DNA and bottom layer consist of protein. To the aqueous phase containing RNA equal volume of 70% ethanol was added and the solution was transferred into a micro spin column with 2ml collection tube. 350µl of RW1 buffer from the RNA isolation kit was added to the spin column and centrifuged at 10,000 rpm for 15 seconds. Afterwards, the column was placed in a new collection tube and 500µl RPE buffer was added. The Column was centrifuged again at 10,000 rpm for 15 seconds. Subsequently, 500µl of 80% ethanol was added to spin column and the column was spun for 10,000 rpm for 2 mins. Finally, the column was centrifuged at full speed for 5 mins to remove ethanol and RNA was eluted in a fresh nuclease-free collecting tube with14µl of RNAase free water.

3.2.25 RNA quantification

RNA quantification was done in a Nanoquant plate with the Tecan M200 microplate reader. Nanoquant plate was wiped with water and 2µl of the RNA free water was pipetted on all quartz spots 'Quantify Nucleic Acid' program in the I-control software with individual blanking option was used for measurements. After blanking, 2µl of well-mixed RNA sample was loaded on the nano quant plate and RNA concentration was quantified by absorbance measurements taken at 260nm, 280nm and Ratio 260/280.

3.2.26 cDNA synthesis

For cDNA synthesis, Quantitect reverse transcription kit from QIAGEN was used. 2µl of cDNA wipeout buffer is added in 1 µg of RNA and RNA free water was added to total volume

to 14µl. It was then incubated for 2 mins at 42°C and then placed the sample on ice. Reagents described in the table below were then added sequentially.

Table 3-15 showing components of the cDNA reaction mix

Component	Volume
Reverse transcription master mix	1µl
Quantiscript RT Buffer	4µl
RT Primer Mix	1µl
Template RNA	14µl
Total	20µl

The reaction mix was incubated at 42°C for 15mins and 95°C for 3mins. The last incubation step was done to inactivate Quantiscript Reverse transcriptase.

3.2.27 RT-PCR

All the primer used in the real-time PCR were purchased from QIAGEN. Most of the primer assay used for gene expression markers for bone regeneration. *GAPDH, BGLAP, SPARC, SPP1, RUNX2, ALPL, Sp7, BMP2, BMP7, TGF-β, VEGFA and Col1A1.*

Table 3-16. Table showing components of RT PCR reaction mix

Component	Volume
QuantiTect SYBR Green master mix	25µl
Primer	3µl
cDNA template mix	1µl
RNA free water	21µl
Total	50µl

4 Results

4.1 Characterization of stem cells

As per the guidelines of the International Society for Cell Therapy, MSCs isolated from the bone marrow of six donors were characterized by their ability to differentiate into osteogenic, adipogenic, and chondrogenic lineage by subjecting them to an adipogenic differentiation medium for 14 days. The oil red O staining showed the presence of cytoplasmic droplets, indicating the commitment of the MSCs to adipogenic lineage. Similary, the MSCs were subjected to osteogenic and condrogenic media for 28 days and evaluated by Alizarin red staining and Alcian blue staining, respectively Figure 4-1.

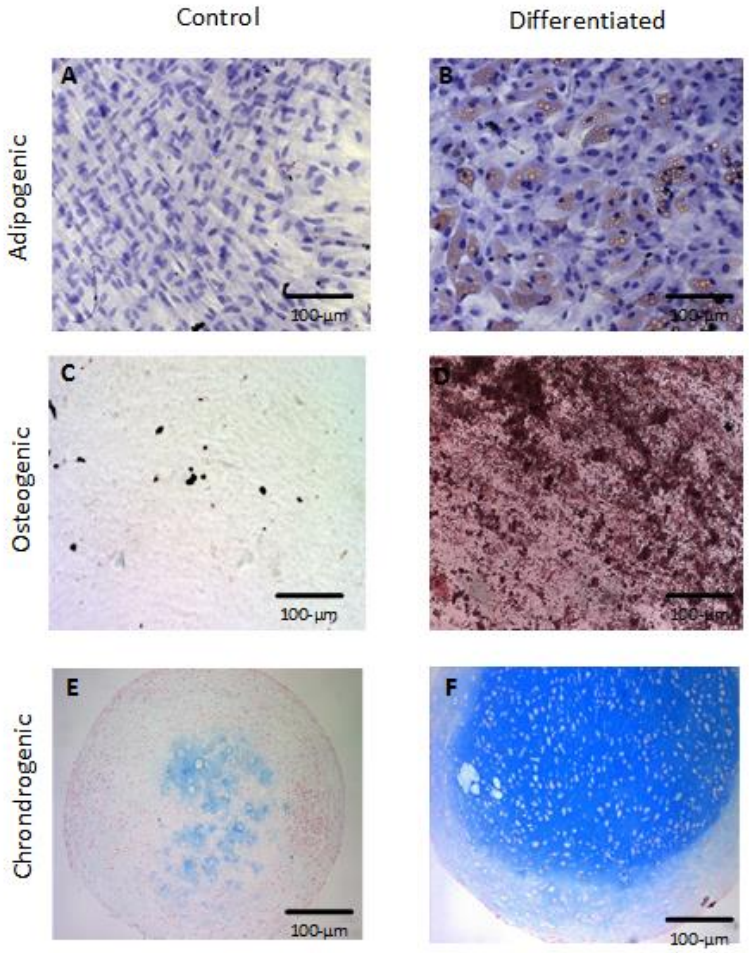

Figure 4-1: A representative figure showing characterization of the isolated MSCs into osteogenic, adipogenic and chondrogenic lineages. The formation of lipid droplets in adipogenic differentiated cells shown by oil red O staining on day 14 (A, B). Osteogenic differentiation was demonstrated by alizarin red staining on day 28 (C, D) The chondrogenic differentiation was performed on 28 days pellet cultures and detected by histological alcian blue staining (E, F) to verify the expression of glycosaminoglycans.

Following their characterization into three-lineage commitment, the MSCs were analyzed for the expression of different stem cell markers using fluorescent-activated cell sorting (FACS).

Table 4-1 describing the MSCs for the markers

Surface Markers	Positive	Negative
CD 73-PE	91.94%	8.06%
CD 90-PE	98.64%	1.36%
CD 105-PE	98.62%	1.38%
CD 14-APC	0.63%	99.55%
CD 29-FITCs	93.14%	6.86%
CD 44-APC	86.84%	13.16%
CD 45-APC	0.67%	99.32%

The expression of different stem cell (MSCs) markers shown in Table 4-1 further confirmed the identity of the isolated stem cells as MSCs. After this characterization, the growth kinetics of the MSCs was analyzed to determine growth characteristics of the MSCs from all the donors in different passages.

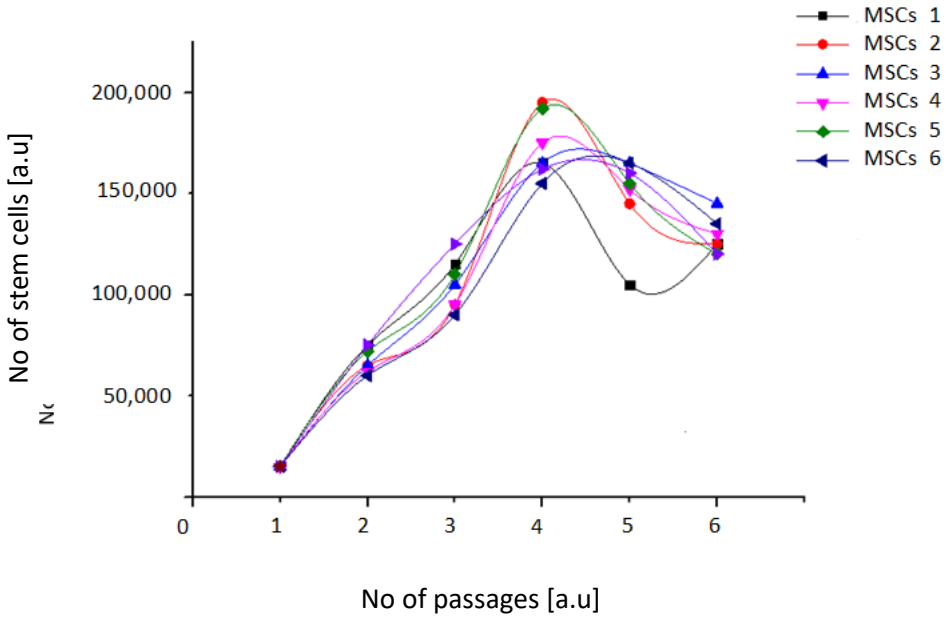

Figure 4-2: Growth kinetics of MSCs from six donors. The stem cells were cultured in 24 well plates and were passaged from passage 1 till passage 6. Fifteen thousand cells were seeded per well and counted with a hemocytometer after culturing for a duration of three days.

Stem cells from all the donors displayed log phase growth characteristics until passage 4. To ensure cells were in log phase further, the experiments were conducted with MSCs until passage 3 Figure 4-2.

4.2 Bioreactor development

A bioreactor system for a 3D cell culture was designed with bone scaffolds housed inside the cartridge, as shown in Figure 4-3 (A). Cells were introduced into scaffold through the septum. A pump constantly circulates media through the scaffold from the media reservoir via silicone tubing to maintain a constant supply of growth factors to the cells and remove waste from them. An air filter was attached to a medium reservoir to enable gas exchange. Finally, a pressure sensor was installed to monitor the pressure inside the bioreactor and avoid cell death caused by high pressure.

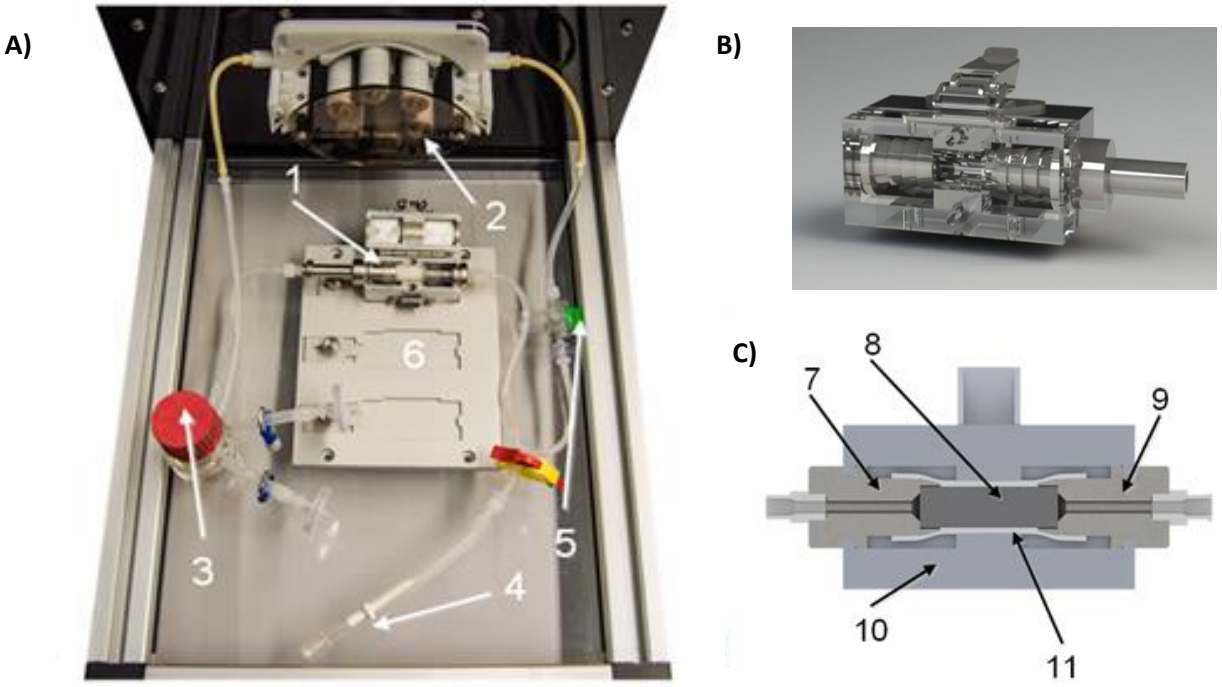

Figure 4-3 : Bioreactor set up (A) A bioreactor set up was composed of a bioreactor cartridge loaded with a poly(L-lactide co-caprolactone) (P[LLA-co-CL]) scaffold (1), a computer-controlled pump (2), a reservoir flask including air filters (3), a septum for cell seeding (4), an adapter to attach a pressure sensor (5), and a rack system that allows easy handling (6). (B) Bioreactor housing. (C) A cross-section shows the concept of the bioreactor cartridge. From an inlet (7),the cell culture medium was guided through the cylindrical P[LLA-co-CL] scaffold (8) to an outlet (9). The bioreactor housing (10), pressed a silicone tube (11) to the cylinder jacket surface of the P[LLA-co-CL] scaffold to ensure homogeneous flow conditions in the scaffold(66).

Next, the shear stress inside the bioreactor was analyzed by computational modeling. The bioreactor cartridge ensured homogeneous flow conditions inside the scaffold by pressing a silicon tube inside the cartridge (*i.e.*, the scaffold was present inside the silicon tube). The computational modeling of the bioreactor's fluid dynamics permitted the identification of the flow characteristics inside it. Average shear stress at the inflow rate of 0.8ml/min was calculated to be $7.6 \times 10^{-5} N/m^2$, as shown in Figure 4-4(A). When the cartridge was open (*i.e.*, it did not press the silicone tube), shear stress inside the bioreactor was reduced to 6.6×10^{-6} N/m^2,as shown in Figure 4-4(B).

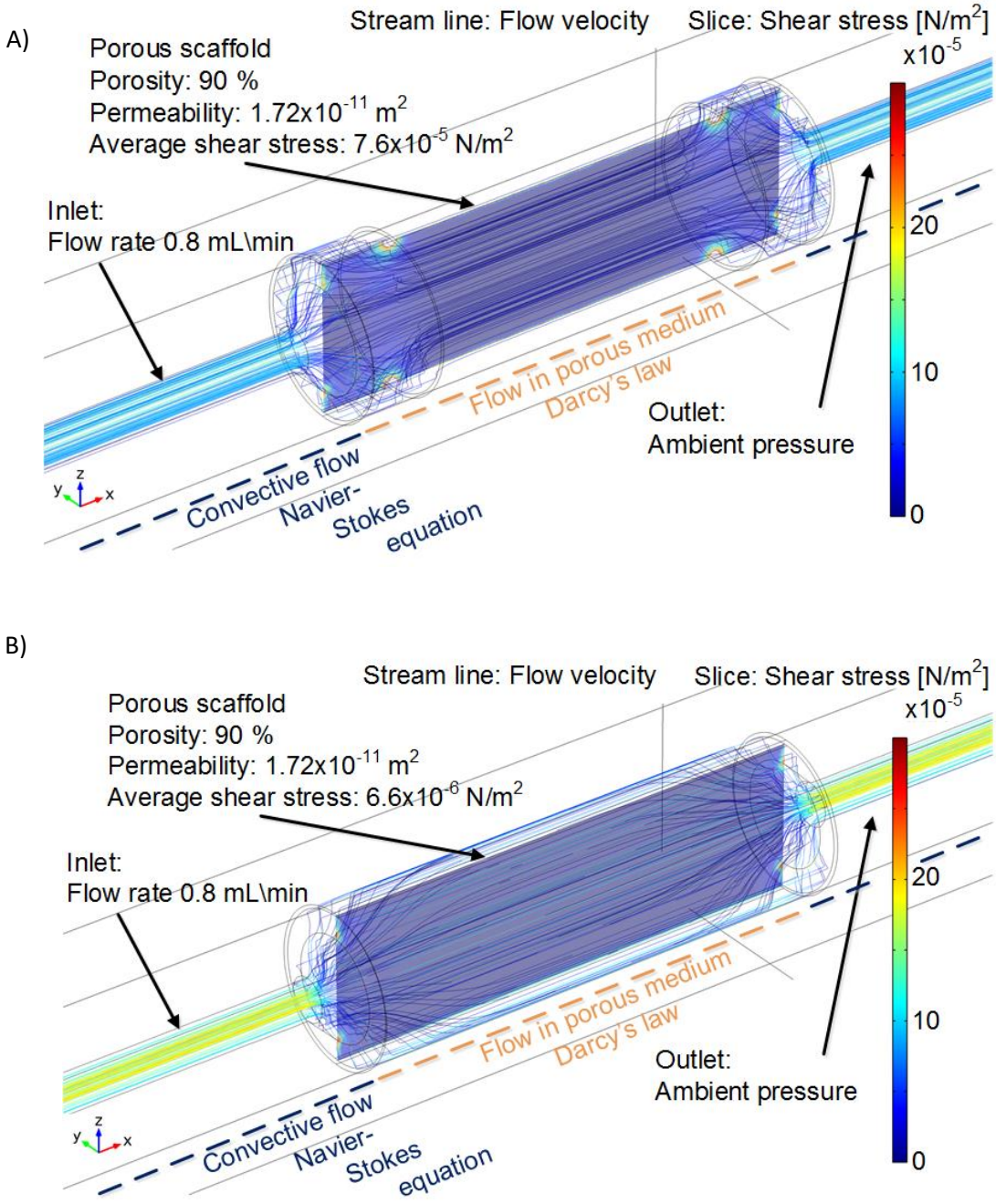

Figure 4-4: Computational Modeling (A) depicts the fluid mechanical conditions in the bioreactor and the scaffold. The average shear stress inside the scaffold was calculated to 7.6 × 10^{-5} N/m². Due to the sealed cylinder jacket surface, all streamlines stayed within the scaffold. In contrast, the open boundaries of the unsealed scaffold (B) reduced the number of streamlines inside the scaffold to a minimum. Except for regions close to the inlet and outlet, the scaffold was free of convective flow. This also resulted in low shear stress conditions of 6.6 × 10^{-6} N/m², 10-fold lower compared to the radially sealed scaffold. Computational simulation & modelling was done by my supervisor Prof Jan Hansmann (66).

The flow characteristics determined in the simulation were based on the P(LLA-co-CL) scaffold. The level of shear stress inside the bioreactor was also altered based on the porosity and structure of scaffold.

4.3 Different types of scaffolds and their mechanical properties

Six types of scaffolds were used for this research: ceramic, P(LLA-co-CL), PP polymer, RCP (collagen type 1 peptide), RCP AP, and RCP AP Mg. They were selected based on the two European projects (VascuBone & Bioinspire) involved in the study, and collaborations with different labs resulted in the testing of different scaffolds to develop better bone implants.

The mechanical properties of scaffolds plays a critical role in the success of bone implants. It is highly essential to retain the mechanical strength of the scaffold after implantation to facilitate bone reconstruction. Therefore, mechanical properties of these scaffolds was measured i.e. Force-deformation characteristics of scaffolds.

4.3.1 P(LLA-co-CL) Scaffold

The P(LLA-co-CL) scaffold is a copolymer composed of 75 mol% L-lactide and 25 mol% e-caprolactone. The 3D scaffold is made through solvent casting and salt leaching. A 4% (w/v) polymer solution was prepared in chloroform and later poured into a glass mold containing sodium chloride (NaCl) at the ratio to the polymer of 10% by weight. As shown in Figure 4-5, the pour size within the scaffold was obtained in the range of 90 to 500 µm, confirmed micro-CT scan. The postmanufacturing composition of P(LLA-co-CL) scaffold was verified by proton nuclear magnetic resonance.

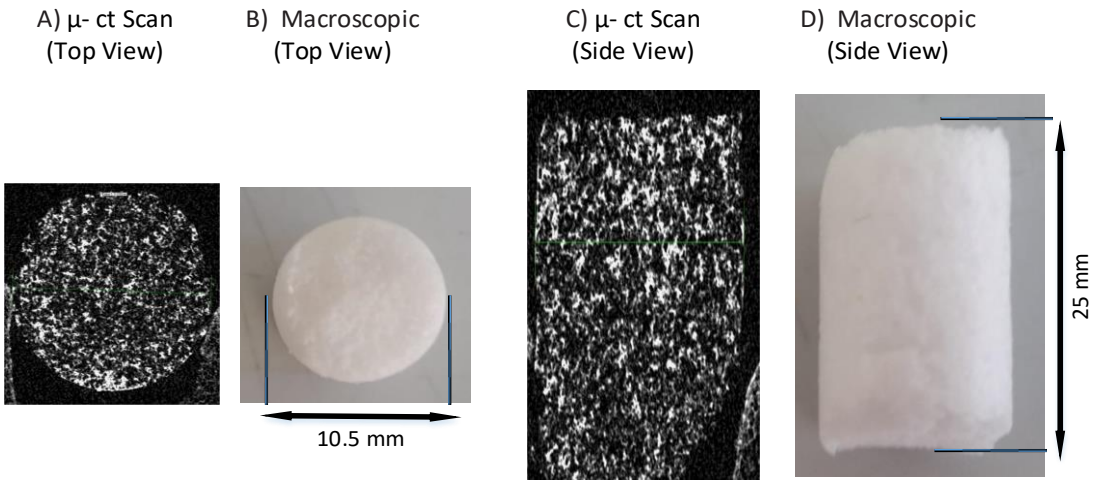

Figure 4-5: µ-CT scan of P[LLA-co-CL] scaffold. A and C show the top and side view of the µ-CT scan of P[LLA-co-CL] scaffold, B and D show the top and side view of the macroscopic image of the P[LLA-co-CL] scaffold.

Force-deformation characteristics of the P(LLA-co-CL) scaffold revealed high elasticity, as shown in Figure 4-6. The scaffold showed 50% deformation at a force of about 23 N, which demonstrates that the scaffold exhibits high elasticity. Furthermore, the Young's modulus, which describes the measure of stiffness of an elastic material, was determined to be 13.49 MPa.

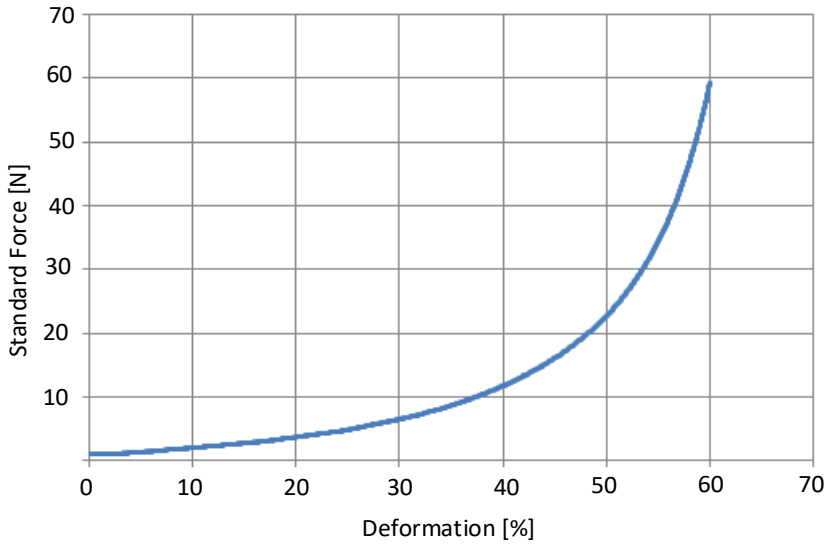

Figure 4-6: Force-deformation characteristics of the P[LLA-co-CL] scaffold . The mechanical deformation force was applied on the scaffold to determine the breaking point of the scaffold. The P[LLA-co-CL] scaffold showed high elasticity, hence different mechanical force can be applied on the scaffold seeded with cells to understand the role of mechanical stimulation on the bone cells.

After determining the force-deformation characteristics of the P(LLA-co-CL) scaffold, the stem cells were seeded in the scaffold using syringe pump, as described in section 3.2.16. Scanned electron microscopic (SEM) microscopy was done on cell-seeded and noncell-seeded P(LLA-co-CL) scaffolds to observe the difference with and without cell attachment inside them, as shown in Figure 4-7

.

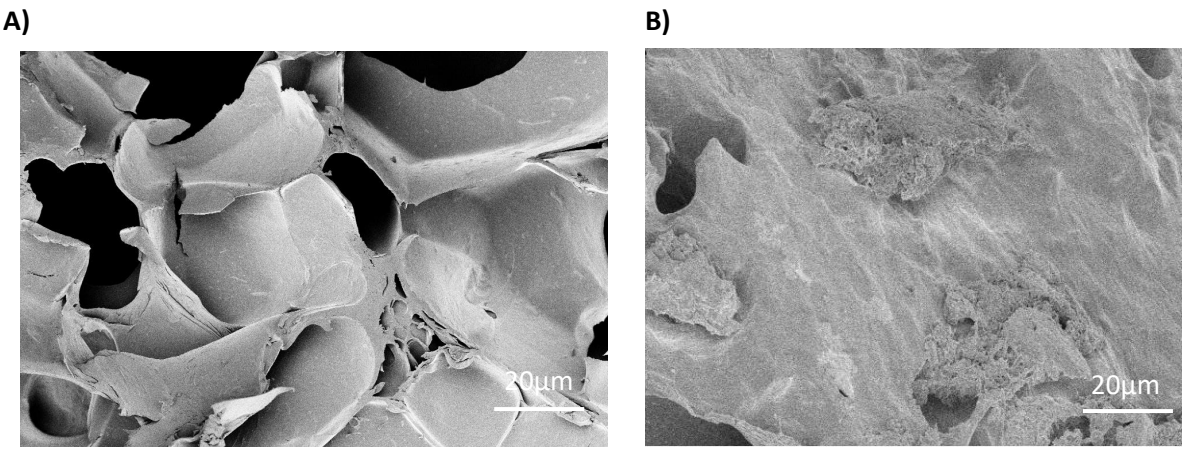

Figure 4-7: SEM of P[LLA-co-CL] scaffold. A) non-cell-seeded. scaffold (left), (B) cell-seeded scaffold (right). The scaffold shown in B was seeded with 5x10^6 Human mesenchymal stem cells (hMSCs), cultured for 7 days and scanned under SEM.

A next viability test (3-(4,5-Dimethylthiazol-2-yl)-2,5-Diphenyltetrazolium Bromide) (MTT)) was performed on the cell-seeded P(LLA-co-CL) scaffold after 1, 7, and 14 days of cell culture to check the viability and distribution of the stem cells inside the scaffold under both static and dynamic conditions, as shown in Figure 4-8.

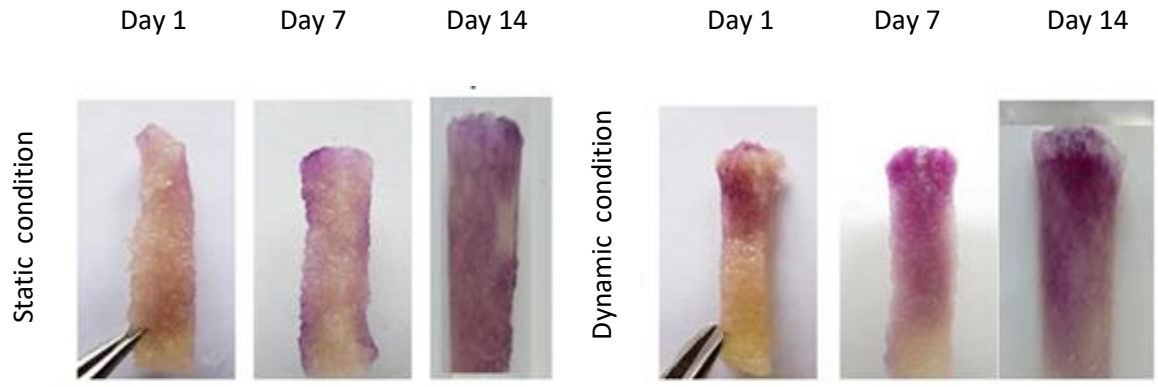

Figure 4-8: Evaluation of cell seeding efficacy and viability of cells in P[LLA-co-CL] scaffolds. 5x10^6 Human mesenchymal stem cells (hMSCs) were seeded on each scaffold and subjected to either static or dynamic culture condition. Cell seeded scaffolds were analyzed post one, seven and fourteen days of culture for cell viability with MTT assay (n=4) (66).

The cross-sections of the scaffolds at days 1, 7, and 14 under static and dynamic culture conditions show that hMSCs are viable under both shear and nonshear stress conditions. At days 1 and 7, homogeneous cell distribution only appeared in the dynamic culture condition. But on day 14, cell distribution in both the static and dynamic culture conditions was uniform. However, there were fewer cells present in the static culture condition compared with the dynamic culture condition. This difference in cell distribution can be attributed to the lack of supply of proper nutrients and growth factors in the static culture condition.

After ensuring the growth of hMSCs in the scaffold, the role of shear stress on osteogenic lineage commitment was investigated in both the static and dynamic culture conditions at three intervals (after 1, 7, and 14 days of culture). The Alizarin red staining revealed the cell-seeded scaffold under a dynamic culture condition to have higher calcification compared with the static culture condition, as shown in Figure 4-9.

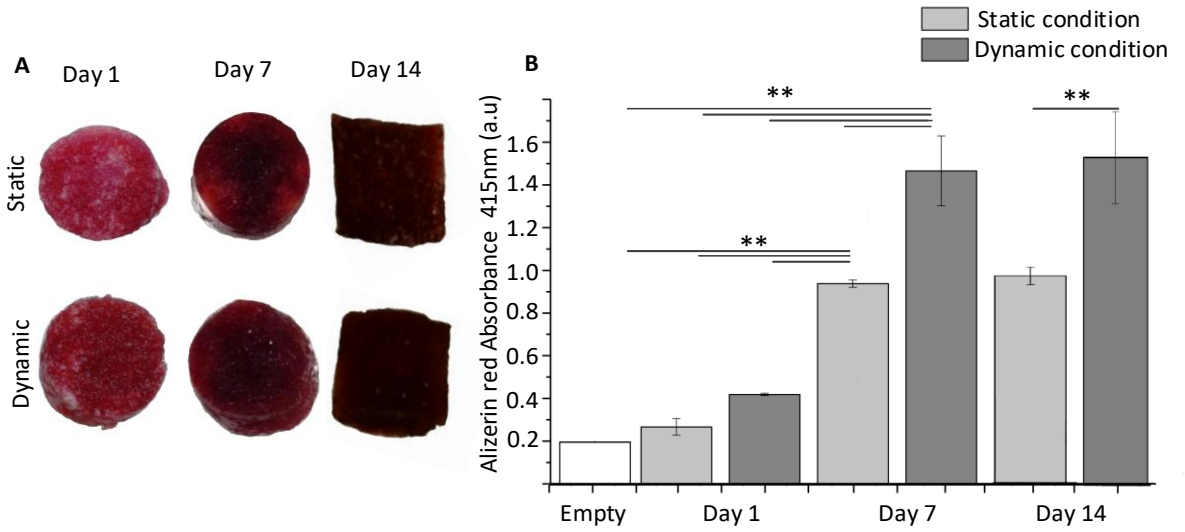

Figure 4-9 : Effect of shear stress on the level of calcification on the P[LLA-co-CL] scaffolds. Human mesenchymal stem cells (hMSCs) were cultured for one, seven days and fourteen days in proliferation medium under static or dynamic culture conditions. (A) Alizarin red staining was used to analyze mineralization. (n = 4) (B) Calcium concentration was measured quantitatively by dissolving alizarin red. **denotes a significant difference between culture conditions (p < 0.01). Legend Static- static culture condition; Dynamic- dynamic culture condition (66)**

An increase of calcification from day 1 to day 7 occurred in the dynamic cell culture condition, but there was no significant difference between days 7 and 14. A significant difference in calcification was detected between the static and dynamic culture conditions on day 7.

To analyze the influence of dynamic and static culture conditions on a molecular level, the expression of stress-related genes was determined by quantitative real-time polymerase chain reaction (qRT-PCR), as shown in Figure 4-10.

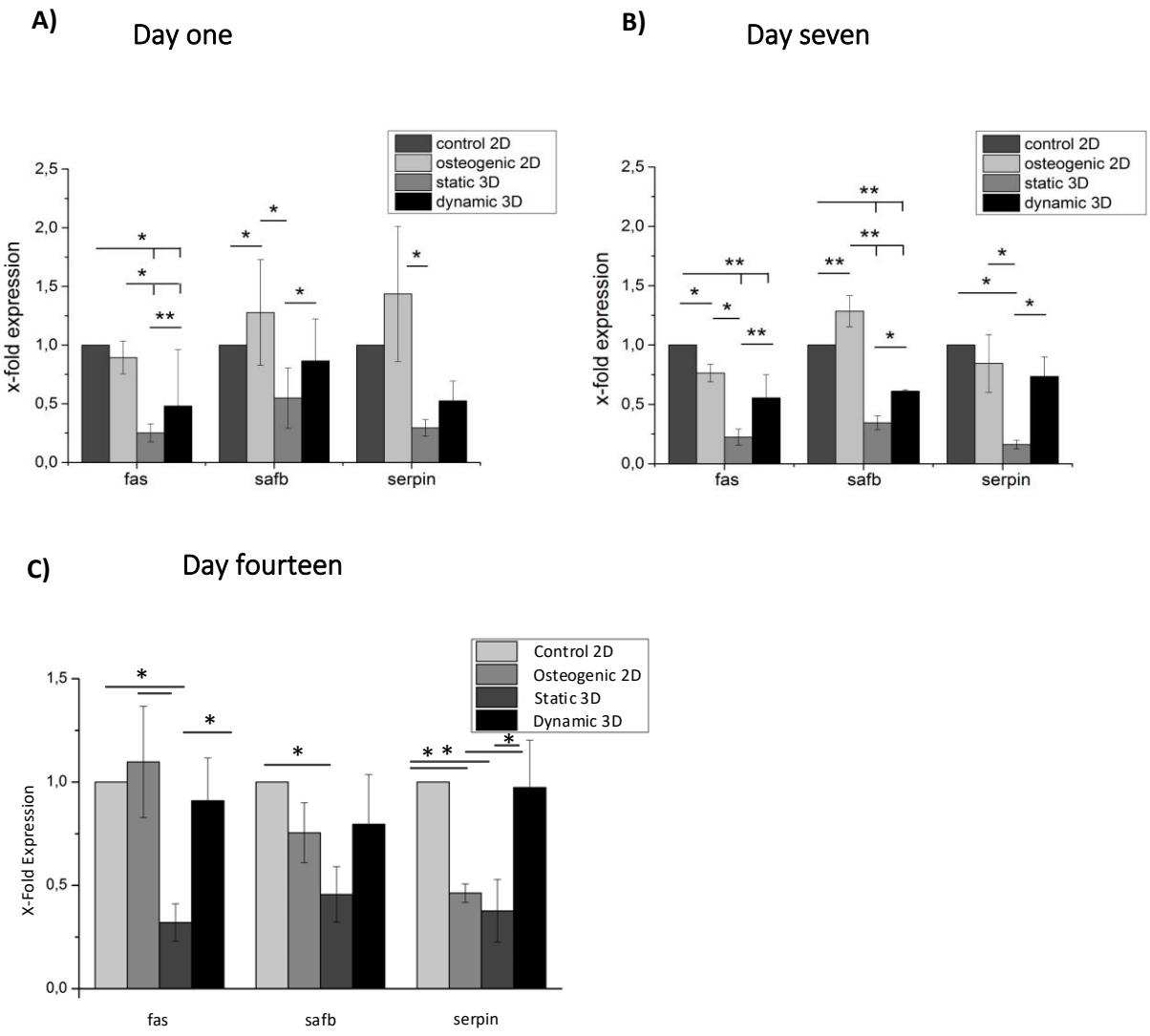

Figure 4-10: Detection of genes related to stress markers (*fas, Safb* and *serpinh 1*) via qRT-PCR after A)one, B)seven and C) fourteen days of culture in P[LLA-co-CL] scaffold. Time-fold gene expression were normalized to control cells in standard two-dimensional (2D) culture conditions. Legend: Control 2D: human mesenchymal stem cells (hMSCs) on standard tissue culture polystyrene using proliferative medium; Osteogenic 2D: hMSCs on standard tissue culture polystyrene using osteogenic differentiation medium; Static 3D: hMSCs in the 3D polymer scaffold using proliferative medium; Dynamic 3D: hMSCs in the 3D polymer scaffold exposed to shear stress employing the bioreactor system (n = 4). (Partial experiments on one and seven days was done by Kleinhans, C and Gabriele Vacun). *denotes a significant difference in gene-level expression between culture conditions (*p<0.05; **p<0.01), error bars represent standard deviation (66).

The stress marker genes *fas* and *SAFB* in the 3D dynamic culture conditions were upregulated compared with the 3D static culture conditions from day 1. The expression rates of *SAFB* and fas turned out to be significantly upregulated after 7 days of 3D dynamic culture compared with 3D static culture conditions. *SERPINH1* showed a significantly higher upregulation in 3D dynamic culture compared with 3D static culture conditions after 7 days.

On day 7, other than *SERPINH1*, all measured stress markers in 3D static and dynamic conditions were lower compared with the 2D cell culture condition. After 14 days of cell culture, all the stress gene markers were upregulated in the 3D dynamic culture compared with the 3D static culture conditions. Fewer gene markers were expressed in the 3D static condition compared with the other conditions.

Osteogenic gene-related markers.

Osteogenic gene-related markers—ALPL, collagen type 1, RUNX2, bone gamma-carboxyglutamate protein (BGLAP), and secreted phosphoprotein 1 (SPP1) were next analysed in hMSCs cultured in the scaffolds with and without perfusion. On day 1, all the osteogenic bone markers such as ALPL, RUNX2, and osteopontin were significantly upregulated under the dynamic culture condition. The expression of RUNX2 showed early osteogenic lineage differentiation.

When both static and dynamic culture conditions were continued for 7 days, collagen type 1 was significantly upregulated in the dynamic culture compared with the static culture condition, as shown in Figure 4-11.

On the day 14 of both the static and dynamic culture conditions, the important osteogenic markers such as ALPL (inorganic phase) and collagen type 1 (organic phase) were upregulated under the dynamic culture condition. The osteopontin gene marker was also significantly upregulated under the dynamic condition. These results show that shear stress influences the upregulation of collagen type 1 and osteopontin at all intervals

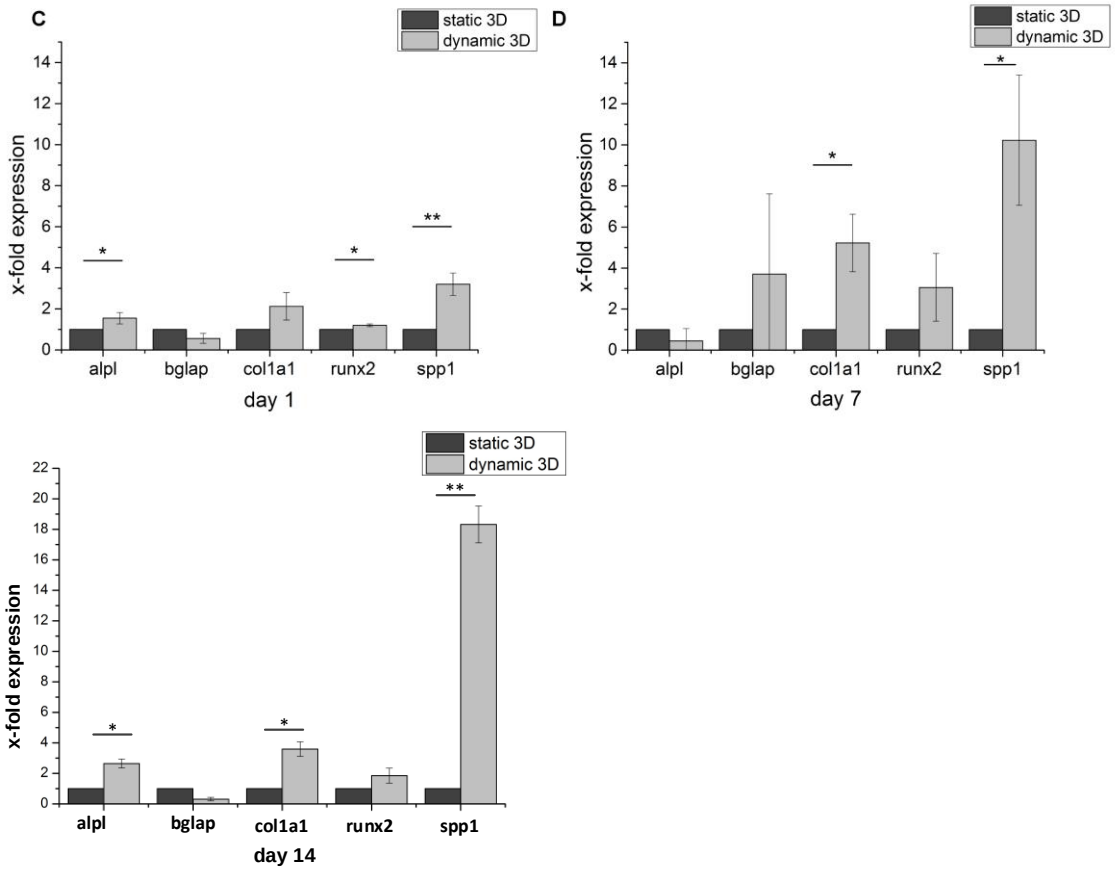

Figure 4-11: Osteogenesis were analyzed for one, seven and fourteen day's experiments on both static and dynamic 3D culture condition. *denotes a significant difference between culture conditions (*p<0.05; **p < 0.01). (Partial experiments on one and seven days was done by Kleinhans, C and Gabriele Vacun). Error bars depict standard deviation. Data are shown as average from four different donors; each donor comprises three internal replicates (66).

.P(LLA-co-CL) scaffolds showed increased calcification and upregulation of bone-regulated gene markers alakaline phosphate (ALPL) and collagen type I alpha 1 chain (Coll1A1)) under the 3D perfusion condition.

Because no difference was observed in the level of calcification from days 7 to 14 (Alizarin red staining), all the remaining experiment on different materials scaffolds were conducted for 7 days.

4.3.2 β-TCP Scaffold

β-TCP scaffolds are used the gold standard for bone implants. They are osteoconductive because osteoblasts adhere to them, causing bone tissues to be deposited on their surfaces. The scaffolds used in this study are made of tricalcium phosphate, calcium

sulfate, and hydroxylapatite. Calcium phosphate has a very high affinity toward proteins such as BMP2 and VEGF, which stimulate bone growth even in the nonbone formation area.

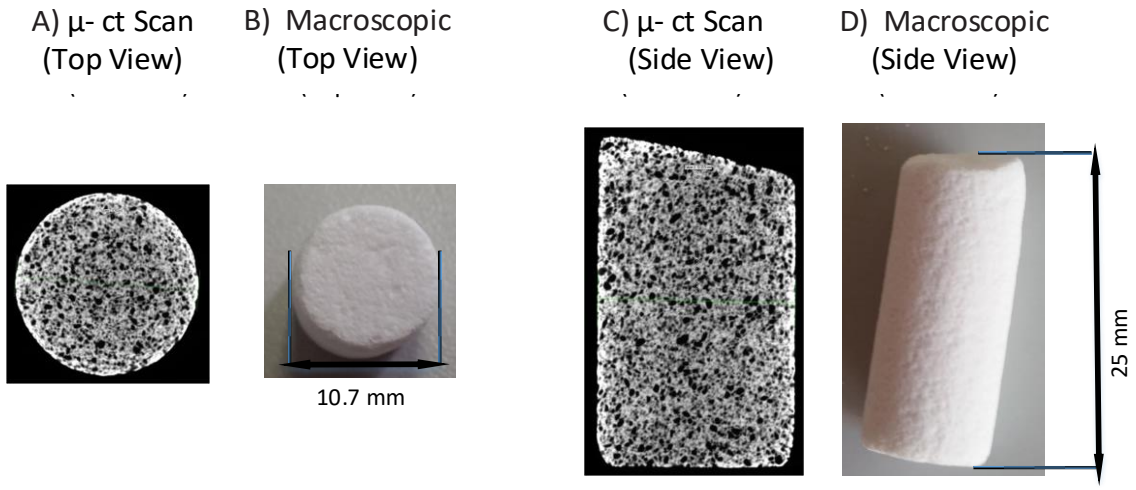

Figure 4-12: µ-CT scan of β-TCP scaffold, A and C show the top and side view of the µ-CT scan of β-TCP scaffold, B and D show the top and side view of the macroscopic of β-TCP scaffold.

Figure 4-12 shows the macroscopic and microscopic structures of the β-TCP scaffold. The µ-CT data show porous interconnectivity within the scaffold. Scaffold porosity was between 60–80%, and the pore size was between 100–500 µm. This scaffold was 20mm tall and 10.7mm wide.

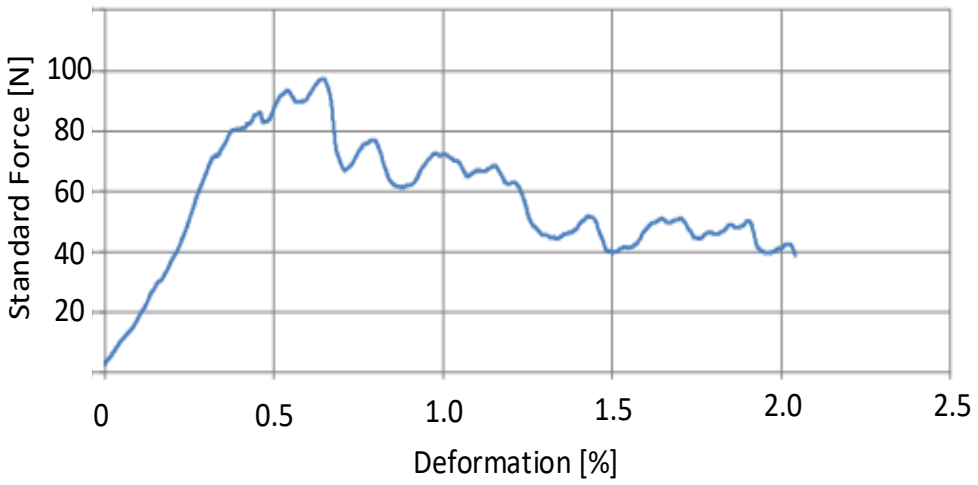

Figure 4-13: Force-deformation characteristics of the β-TCP scaffold. The mechanical deformation was applied on the scaffold to determine the breaking point of the scaffold. The β-TCP scaffold showed high tensile strength, hence it gives high mechanical support to the body.

Mechanical compression was applied to the scaffold to find its elasticity. As shown in Figure 4-13, when the scaffold was compressed more than 0.5% of its original size, it broke. The Young's modulus of the β-TCP scaffold was determined to be 67 MPa, indicating that these scaffolds are not elastic. This provides the β-TCP scaffold with both a unique advantage and disadvantage. The advantage is that it can withstand up to 80 N force, and the disadvantage is that its pores are not uniformly interconnected. Hence, achiving uniform cell distribution inside the scaffold is difficult.

To see hMSC attachment in the scaffold, 5 x 10^6 hMSCs were seeded into it and scanned after 7 days of cell culture with the SEM, as shown in Figure 4-14.

A) **B)**

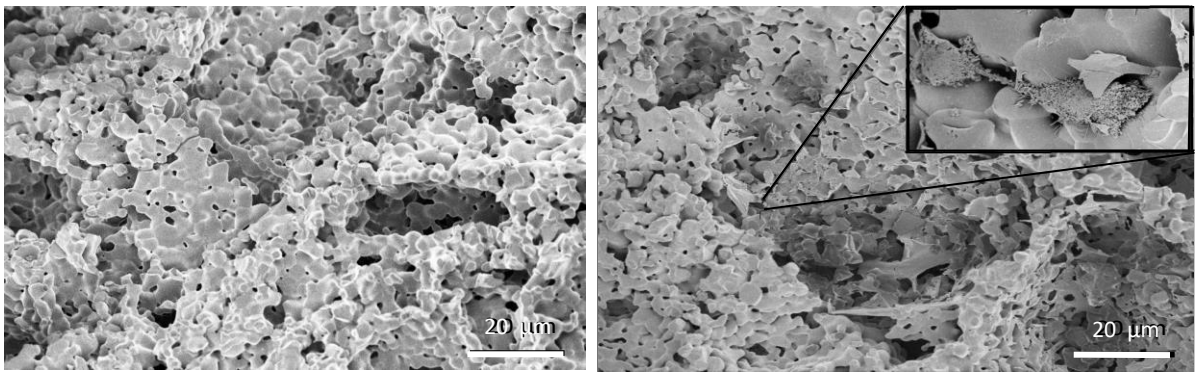

Figure 4-14 SEM of β-TCP scaffold. (A) Non-cell seeded scaffold (left), (B) cell seeded scaffold (right).The insert shows cells attachment to the β-TCP scaffold.

To see the viability of the cells inside the scaffold, a viability test (MTT) was performed after 7 days of cell culture in both the static and dynamic conditions.

Figure 4-15: Evaluation of cell seeding efficacy and viability of cells in β-TCP scaffolds. 5x10^6 Human mesenchymal stem cells (hMSCs) were seeded on each scaffold and subjected to either static or dynamic culture condition. Cell seeded scaffolds were analyzed post seven days of culture for cell viability with MTT assay (n=2).

Figure 4-15 shows cross-sections of the β-TCP scaffolds after 7 days of cell culture under static and dynamic culture conditions. While uniform distribution of stem cells was observed in the dynamic culture condition, nonuniform distribution of cells was observed in static culture condition.

Next, the level of calcification in the β-TCP scaffolds was determined after 7 days of static and dynamic cell culture via Alizarin red staining.

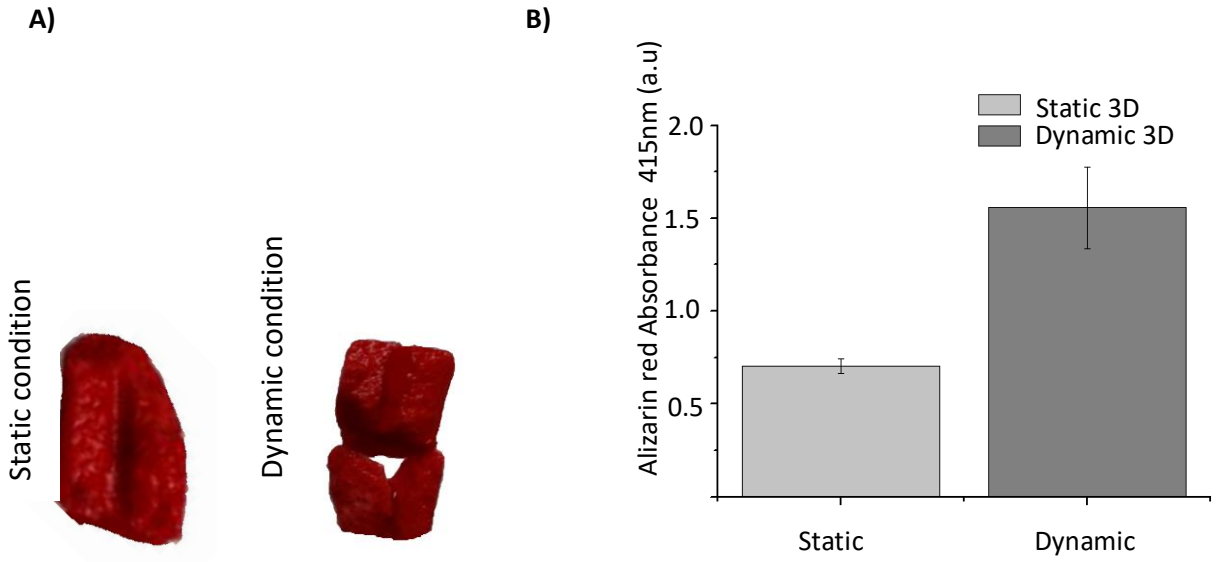

Figure 4-16: Effect of shear stress on the level of calcification on the β-TCP scaffolds. $5x10^6$ Human mesenchymal stem cells (hMSCs) were cultured for seven days in proliferation medium under static and dynamic culture conditions in β-TCP scaffold. (A) Alizarin red staining was used to analyze mineralization (n = 2). (B) Calcium concentration was measured quantitatively by dissolving alizarin red.

Under the dynamic culture condition (*i.e.*, perfusion), the bioreactor stimulated the hMSCs toward osteogenic lineage commitment, as shown in Figure 4-16. After 7 days of cell culture in the perfusion bioreactor, the β-TCP scaffold showed a significant increase in calcification compared with the static culture condition. To confirm this finding, qRT-PCR for osteogenic lineage markers was done.

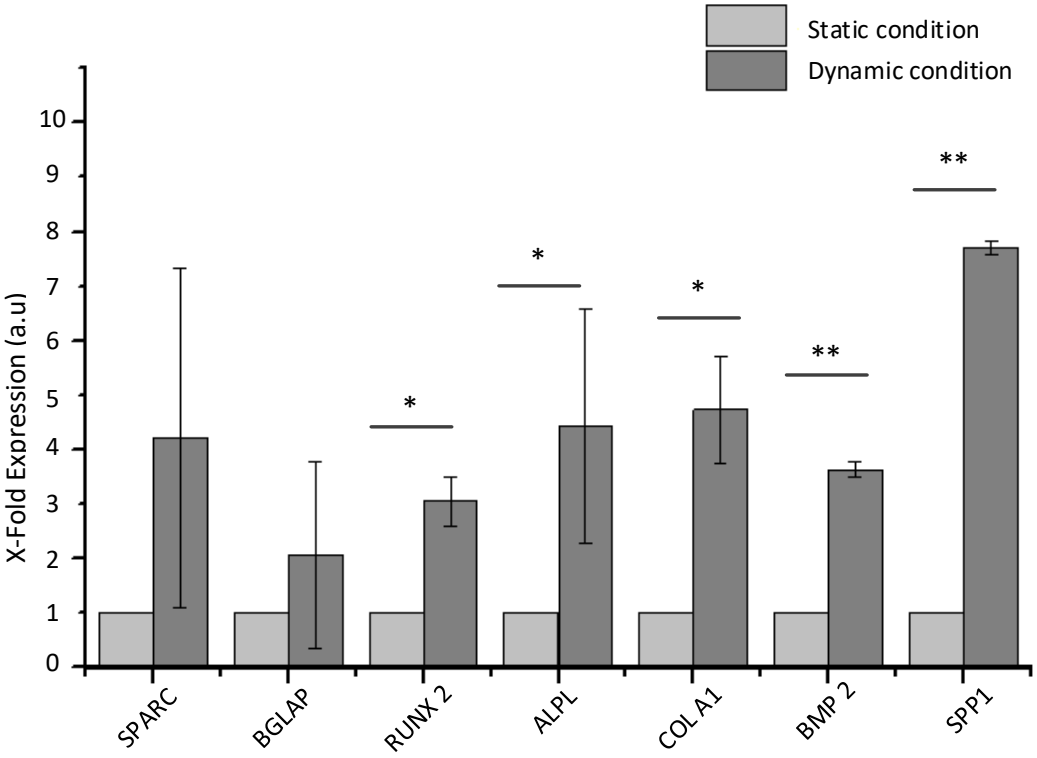

Figure 4-17 Osteogenic gene-related markers were analyzed for seven days of culture under both static and dynamic 3D culture condition in β-TCP scaffolds . Human mesenchymal stem cells (hMSCs) were cultured for seven days in proliferation medium under static and dynamic culture conditions in the β-TCP scaffolds (n=2). Osteogenesis related genes were analyzed by quantitative real-time polymerase chain reaction (qRT-PCR).

As shown in Figure 4-17, both the organic and inorganic gene bone makers (*i.e.*, *ALPL, RUNX2*, and *Col1A1* were significantly upregulated in the dynamic culture compared with the static culture condition. Moreover, other genes such as osteopontin and BMP2 were highly significantly upregulated in the dynamic culture condition.However, no significant change was seen in the expression of osteocalcin (*BGLAP*) or osteonectin (SPARC).

4.3.3 PP polymer scaffold

The PP polymer scaffolds were produced by PP Polymer AB. The scaffold's pore size is between 90 and 500 µm. The details of this scaffold were not disclosed because this scaffold is part of a pending patent application. Figure 4-18 shows both the macroscopic and microscopic nature of the scaffold. The µ-CT scan of this scaffold shows how the pores are interconnected within it.

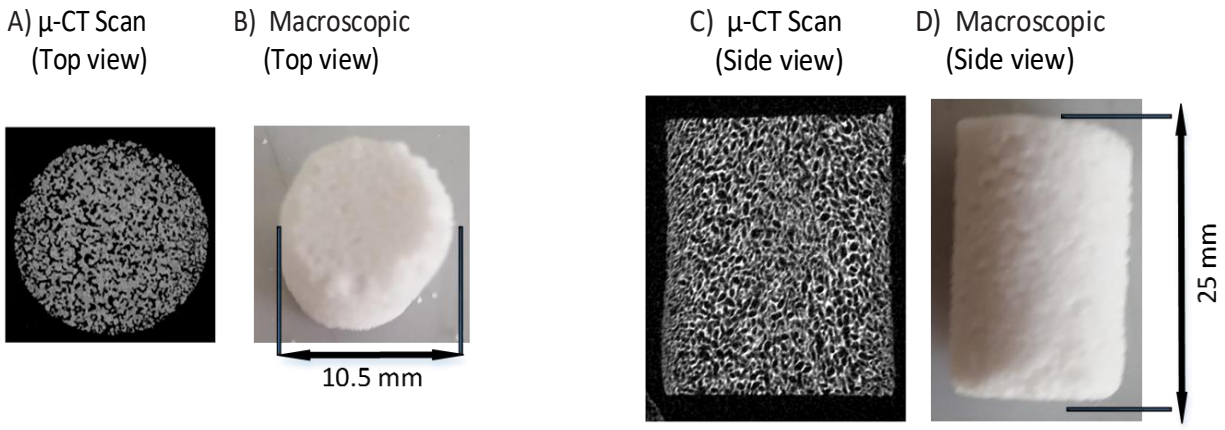

Figure 4-18: µ-CT scan of PP polymer scaffold. A and C show the top and side view of the µ-CT scan of PP polymer scaffold, B and D show the top and side view of the macroscopic of the PP polymer scaffold.

Afterwards, the stability of the scaffolds was tested by mechanical compression. Force was applied to measure the compression load the scaffold could withstand. This was done to verify the strength of scaffold so different types of mechanical deformation could be applied to mimic a real-time situation.

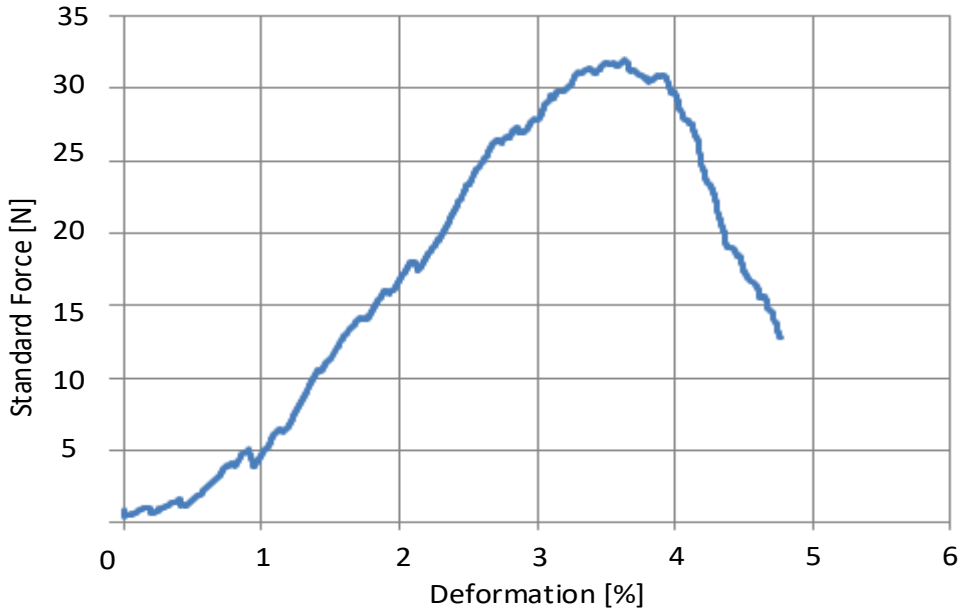

Figure 4-19: Force-deformation characteristics of the PP scaffolds.

As shown in Figure 4-19, the PP polymer scaffold breaks at 32 N. The Young's modulus for the PP polymer scaffold was 0.2284 MPa, revealing that PP polymer is brittle and breaks after 3.5% scaffold deformation.

Thereafter, PP scaffold was seeded with 5 x 10^6 hMSCs and cultured for 7 days. An SEM scan was conducted to verify cell attachment in the scaffold, as shown in Figure 4-20.

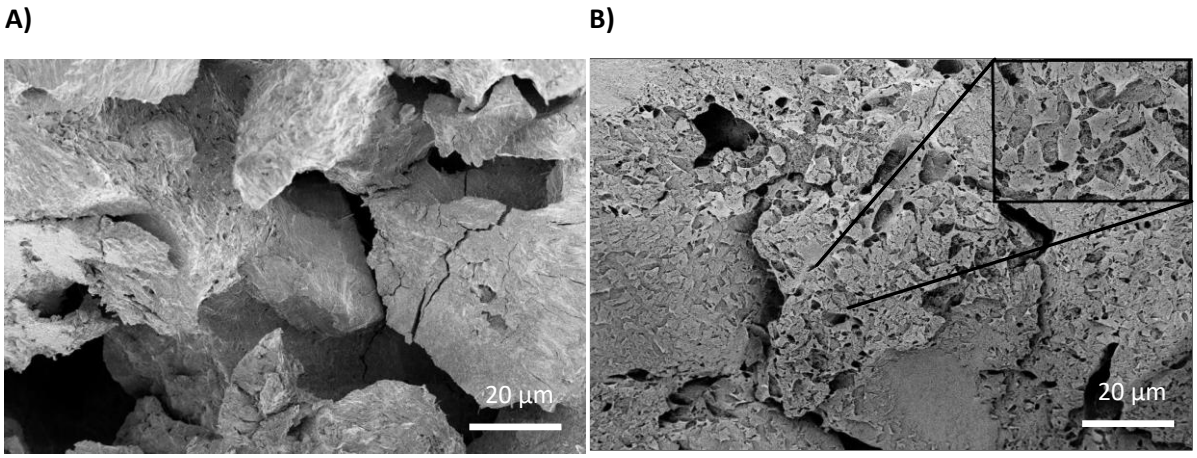

Figure 4-20: SEM of PP polymer scaffold. (A)non-cell seeded scaffold (left), (B) cell-seeded scaffold (right).

Figure 4-20 shows an SEM scan of the PP polymer scaffold in both noncell- and cell-seeded scaffolds. Cells were attached uniformly throughout the scaffold, as shown in Figure 4-20.

Subsequently, cell viability (MTT test) was analyzed after 7 days of cell culture in both the static and dynamic culture conditions.

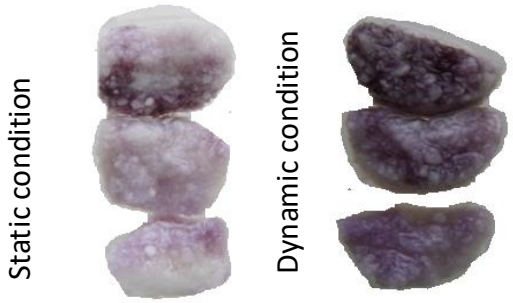

Figure 4-21 Evaluation of cell seeding efficacy and viability of cells in PP polymer scaffolds. 5x106 Human mesenchymal stem cells (hMSCs) were seeded on each scaffold and subjected to either static or dynamic culture condition. Cell seeded scaffolds were analyzed post seven days of culture for cell viability with MTT assay (n=2).

Figure 4-21 shows that cells were evenly distributed in the dynamic culture compared with the static culture condition. This shows that cells were growing better under the dynamic condition due to the constant supply of nutrition and growth factors.

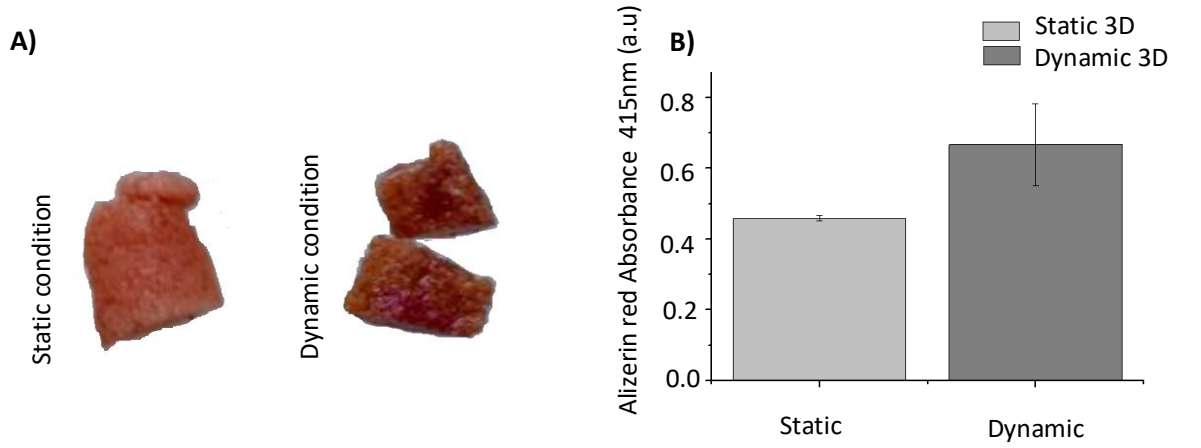

Figure 4-22: Effect of shear stress on the level of calcification on the PP Scaffold. 5x10^6 Human mesenchymal stem cells (hMSCs) were cultured for seven days in proliferation medium under static and dynamic culture conditions in the PP Scaffold . (A) Alizarin red staining was used to analyze mineralization. (n = 1) (B) Calcium concentration was measured quantitatively by dissolving alizarin red.

After 7 days of cell culture, both the static and dynamic culture conditions were evaluated for calcification. High Alizarin red staining was seen in the dynamic culture compared with the static culture condition, as shown in Figure 4-22(A). The calcifications assay was done for quantification purposes. Higher calcification was achieved under the dynamic condition, as shown in Figure 4-22(B). The experiment was done on only one donor because the scaffold started to dissolve in the dynamic condition due to stress.

Cell differentiation into osteogenic lineage commitment was evaluated by osteogenic gene marker expression using qRT-PCR, as shown in Figure 4-23. All the osteogenic gene markers displayed higher expression trends in the dynamic culture condition. However, this data could not be statistically evaluated due to the absence of biological replicates because the PP polymer scaffold was unstable and dissolved under perfusion. Thus, no further experiments were conducted with the PP polymer scaffold.

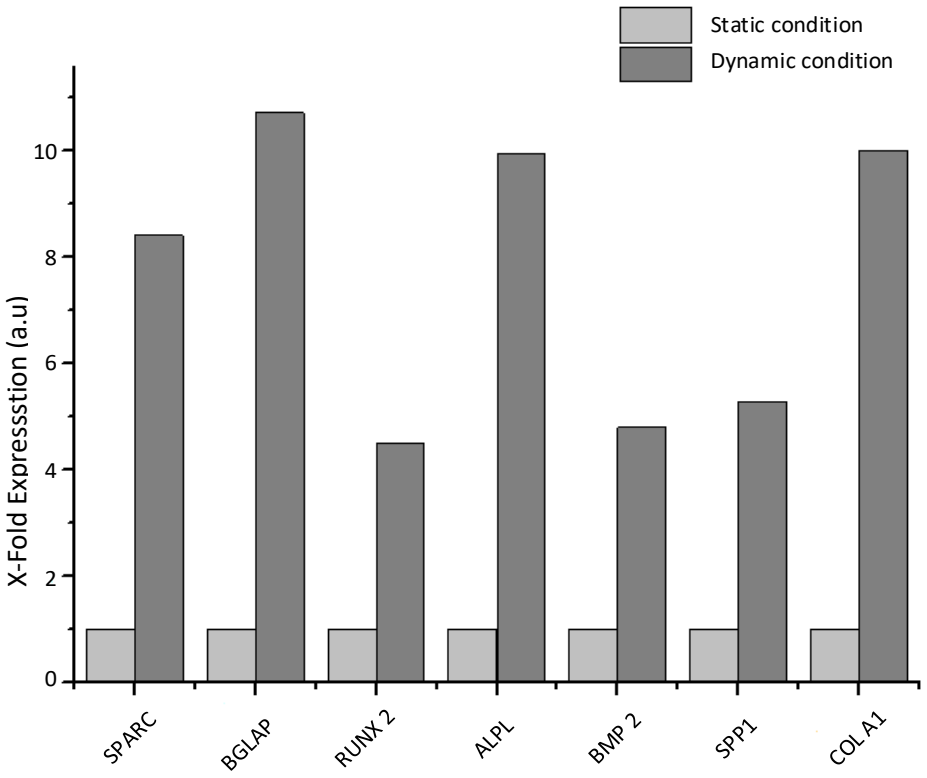

Figure 4-23: Osteogenic gene-related markers were analyzed for seven days of culture under both static and dynamic 3D culture condition in PP polymer scaffolds. Human mesenchymal stem cells (hMSCs) were cultured for seven days in proliferation medium under static and dynamic culture conditions in PP polymer scaffold (n=1). Osteogenesis related genes were analyzed by quantitative real-time polymerase chain reaction (qRT-PCR).

4.3.4 RCP Scaffold

The RCP scaffold is made of collagen type 1 and arginine glycine aspartate peptide (RGD). RGD is an important peptide for cell adhesion to ECM, blood, and cell surface proteins. This scaffold was supplied from the Institute of Science and Technology for Ceramics (ISTEC) in Faenza, Italy..

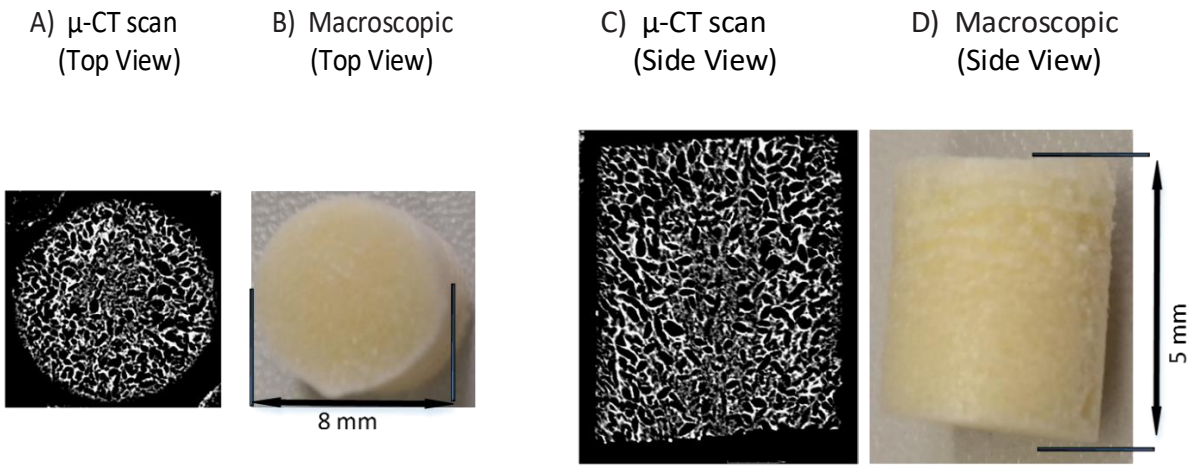

Figure 4-24 µ-CT scan of RCP scaffold, A and C showing the top and side view of the µ-CT scan of RCP scaffold, B and D showing the top and side macroscopic view of the RCP scaffold.

Figure 4-24 shows both macroscopic and microscopic images of the scaffold. The µ-CT scan shows the interconnection of pores within the scaffold, which allows cells to evenly distribute throughout it. Afterwards, mechanical deformation force was applied to the scaffold to determine its elasticity. .

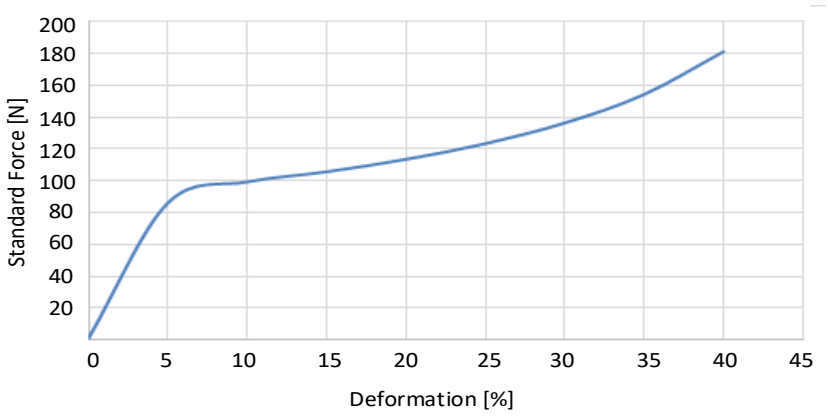

Figure 4-25: Graph showing force-deformation measurement of RCP scaffolds. The mechanical deformation was applied on the scaffold to determine the breaking point of the scaffold.

Young's modulus of the RCP scaffold was determined to be 5.18 MPa.This indicates that the RCP scaffold is very elastic. For example, at a high force of 85 N, the scaffold underwent only 5% deformation, and it could withstand deformation up to 40% at a force of 180 N.

Subsequently, to view cell attachments in the scaffold, 5 x 10^6 hMSCs were seeded into it. After 7 days of culture, SEM scans were taken of the cell-seeded scaffold, shown in Figure 4-26, revealing hMSCs attached evenly inside it.

A) **B)**

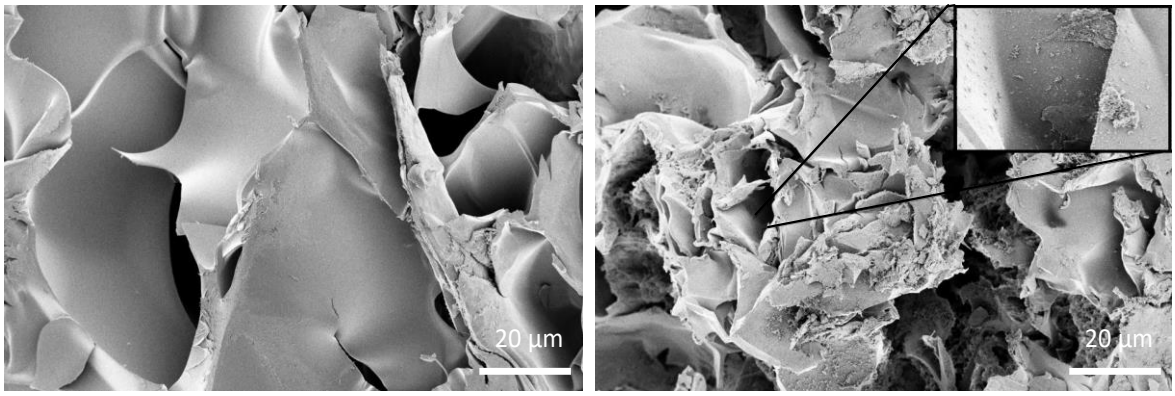

Figure 4-26: SEM of RCP scaffold. (A) Non-cell-seeded scaffold (Left), (B) Cell Seeded scaffold (Right), insert shows cells attached to the scaffold.

Next, cell viability and distribution was assessed in the scaffold under both static and dynamic culture conditions via an MTT test after 7 days of culture.

.

Figure 4-27: Evaluation of cell seeding efficacy and viability of cells in RCP scaffolds. 5x10^6 Human mesenchymal stem cells (hMSCs) were seeded on each scaffold and subjected to either static or dynamic culture condition. Cell seeded scaffolds were analyzed post seven days of culture for cell viability with MTT assay (n=3).

As shown in Figure 4-27, the cells were viable and evenly distrubuted in the RCP scaffold under both static and dynamic culture conditions. After testing the viability of the cells, both static and dynamic culture conditions were tested for collagen type 1 staining..

Figure 4-28: Collagen type 1 staining in the RCP scaffolds under both static and dynamic culture condition (n=3).

Collagen type 1 staining was higher under the shear stress condition (*i.e.*, the dynamic culture condition) compared with the static condition. This shows that under perfusion, collagen was expressed more in the RCP scaffold. The organic phase of bone is mostly made of collagen type 1, and this staining shows its expression under the influence of shear stress.

Osteogenic lineage commitment was then assessed by Alizarin red staining.

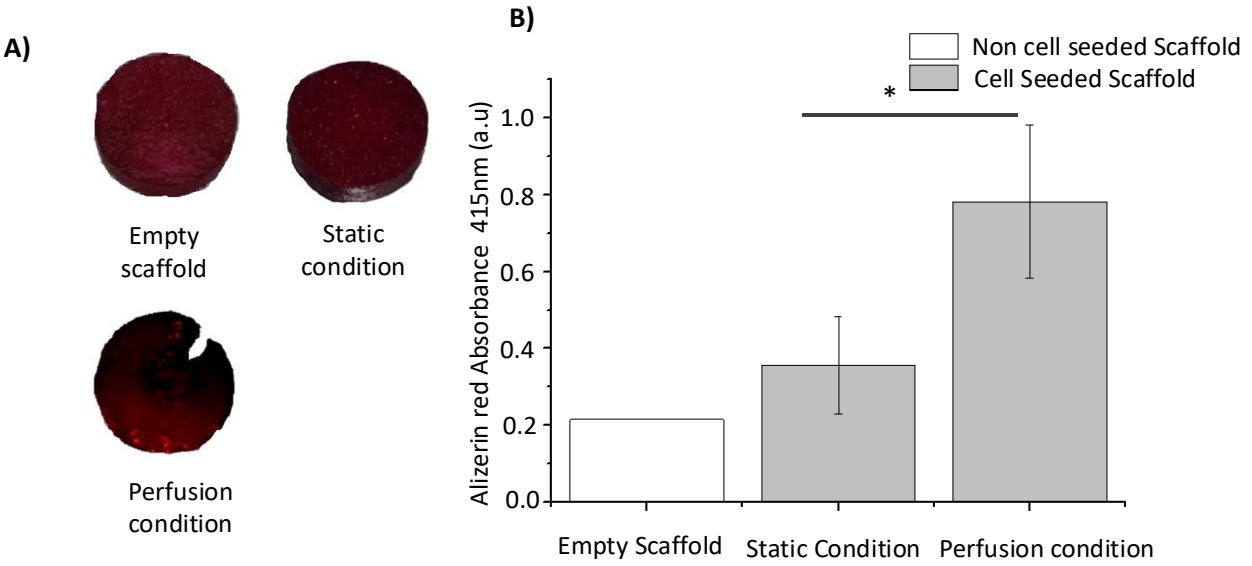

Figure 4-29: Effect of shear stress on the level of calcification on the RCP scaffolds. 5x10^6 Human mesenchymal stem cells (hMSCs) were cultured for seven days in proliferation medium under static and dynamic culture conditions in RCP scaffold. (A) Alizarin red staining was used to analyze mineralization. (n = 3), (B) Calcium concentration was measured quantitatively by dissolving alizarin red (n=3).

Higher Alizarin red staining was seen in the dynamic culture compared with the static culture condition. Later, quantification done by calcification assay showed significantly higher calcification in the dynamic culture compared with the static culture condition. This indicates that shear stress plays an important role in osteogenic lineage commitment, as shown in Figure 4-29.

The results of both collagen type 1 staining and alizarin red staining were confirmed by qRT-PCR. After 7 days of experiments, ribonucleic acid (RNA) was isolated, and qPCR was done for different gene markers related to osteogenic lineage commitment.

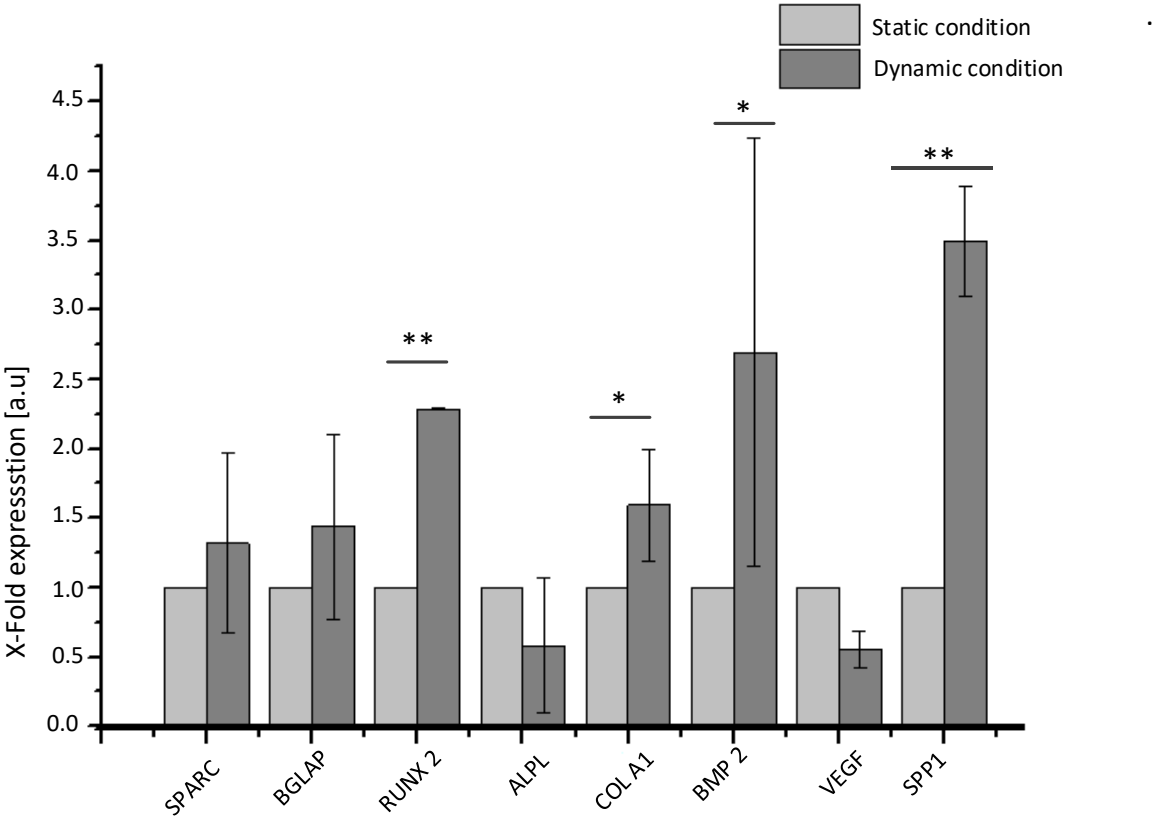

Figure 4-30: Osteogenic gene-related markers were analyzed for seven days of culture under static and dynamic 3D culture condition in RCP scaffolds. Human mesenchymal stem cells (hMSCs) were cultured for seven days in proliferation medium under static and dynamic culture conditions in the RCP scaffolds (n=3).Gene expression was measured by quantitative real-time polymerase chain reaction (qRT-PCR)., * denotes a significant difference between culture conditions (n=3) (*p<0.05, p< 0.01).**

Expressions of collagen type 1 and BMP2 were significantly upregulated under the dynamic culture condition. This shows that under shear stress, the RCP scaffold activates both collagen type 1 and BMP2 gene expressions. Furthermore, RUNX2 and osteopontin were highly significantly upregulated in the dynamic culture condition. It is well known that RUNX2

is an early osteogenic gene marker which plays a major role in activating ALPL, OC, and collagen type 1. However, no significant difference was seen in the expression of SPARC, BGLAP, ALPL, or VEGF genes, as shown in Figure 4-30.

4.3.5 RCP AP Scaffold

Like RCP scaffolds, RCP AP scaffolds are made of human collagen type 1 and RGD. They also contain AP, so they are called *mineralized scaffolds*. The RCP AP scaffold was also supplied by ISTEC.

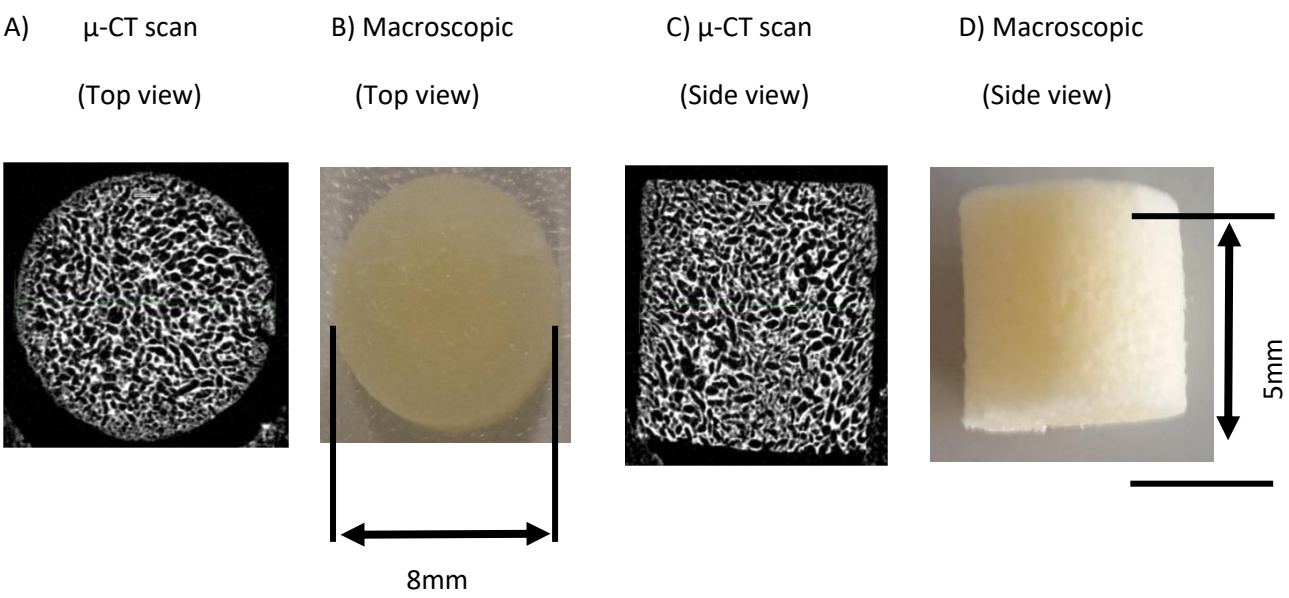

Figure 4-31: µ-CT scan of RCP AP scaffold, A and C showing the top and side view of the µ-CT scan of RCP AP scaffold, B and D showing the top and side macroscopic view of the scaffold.

Figure 4-31 shows both macroscopic and microscopic views of the RCP AP scaffold. These scaffolds are porous, and their pores are interconnected, which allows the cells to distribute throughout them. The scaffold's pore size was found to be in the range of 200 to 350 µm. Its porosity was 75 to 95% similar to cancellous bone. This scaffold can thus provide space for bone marrow and vessel development[67].

Next, force was applied to the RCP AP scaffold to determine its elasticity.

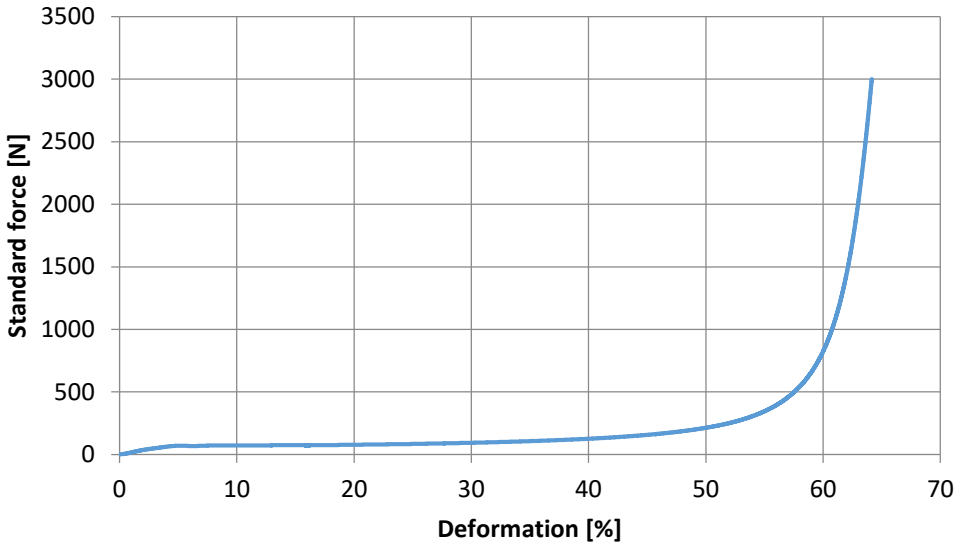

Figure 4-32: Graph represents a force-deformation measurement of RCP AP scaffolds. The scaffold showed elasticity when mechanical deformation was applied on the scaffold to determine the breaking point of the scaffold.

No breaking point was identified when mechanical force was applied to the scaffold, indicating its elastic nature. The Young's modulus for the RCP AP scaffold was determined to be 3.49MPa.

The RCP AP scaffold was then seeded with 5 x 10^6 hSMCs, and cell attachment and distribution was assessed by SEM scan after 7 days of culture.

A) **B)**

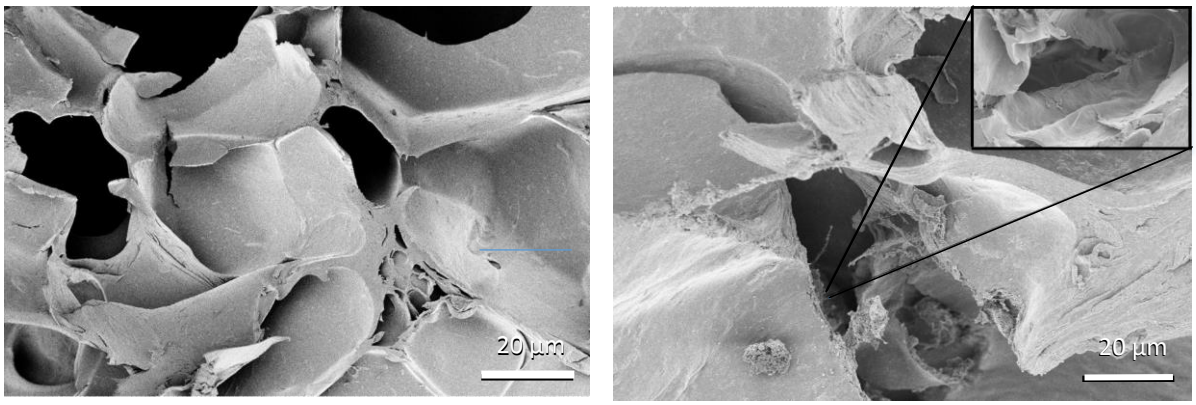

Figure 4-33 SEM of RCP AP scaffold. (A)Non cell seeded scaffold (left), (B) cell seeded scaffold (right)

SEM images of the RCP AP scaffold reveal its porous nature, as shown inFigure 4-33(A) shows the structure of the noncell-seeded scaffold, and Figure 4-33(B) shows the scaffold seeded with hMSCs. The cells were evenly disturbed inside it.

Next, the viability (MTT assay) and distribution of hMSCs in the scaffold were assessed in both static and dynamic culture conditions.

Figure 4-34: Evaluation of cell seeding efficacy and viability of cells in RCP AP scaffolds. $5x10^6$ Human mesenchymal stem cells (hMSCs) were seeded on each scaffold and subjected to either static or dynamic culture condition. Cell seeded scaffolds were analyzed post seven days of culture for cell viability with MTT assay (n=3).

Cells were viable and evenly distributed in both static and dynamic culture conditions, as shown in Figure 4-34.

Next, collagen type 1 staining was performed on cell-seeded RCP AP scaffolds subjected to both static and dynamic culture conditions.

Figure 4-35: Evaluation of collagen type 1 staining in the RCP AP scaffolds (n=3).

Collagen type 1 expression increased under the shear stress condition compared with the static culture condition. Its level of expression in the static culture condition was higher than the noncell-seeded empty scaffold (RCP AP is a collagen-based peptide scaffold). This shows that collagen type 1 expression increases upon the application of shear stress.

To check the osteogenic lineage commitment, Alizarin red staining was performed.

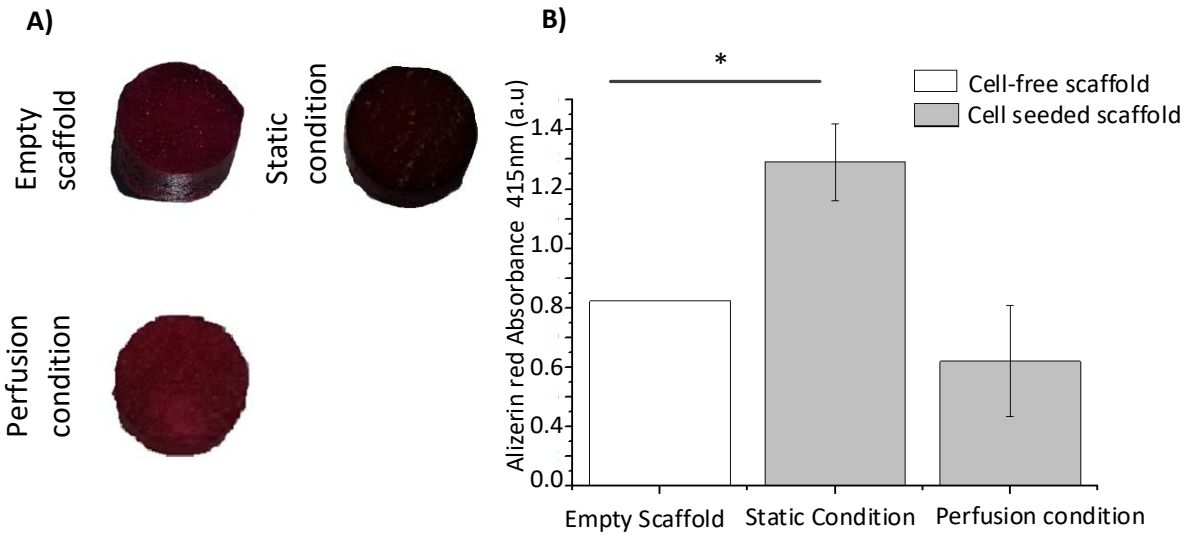

Figure 4-36: Effect of shear stress on the level of calcification on the RCP AP scaffolds. $5x10^6$ Human mesenchymal stem cells (hMSCs) were cultured for seven days in proliferation medium under static and dynamic culture conditions in RCP AP scaffold. (A) Alizarin red staining was used to analyze mineralization. (n = 3), (B) Calcium concentration was measured quantitatively by dissolving alizarin red.

Increased expression of Alizarin red staining was seen in the static culture compared with the perfusion culture condition. Quantification done by calcification assay showed a significant calcification increase in the static culture condition compared with the perfusion culture condition. The AP present in the scaffold helped the hMSCs differentiate into osteogenic lineage. However, the addition of shear stress caused the scaffold to leach minerals and AP, which decreased calcification, as was observed in the perfusion culture condition.

After 7 days of cell culture under both static and dynamic cell culture conditions, the expression of different osteogenic genes was assessed by qRT-PCR.

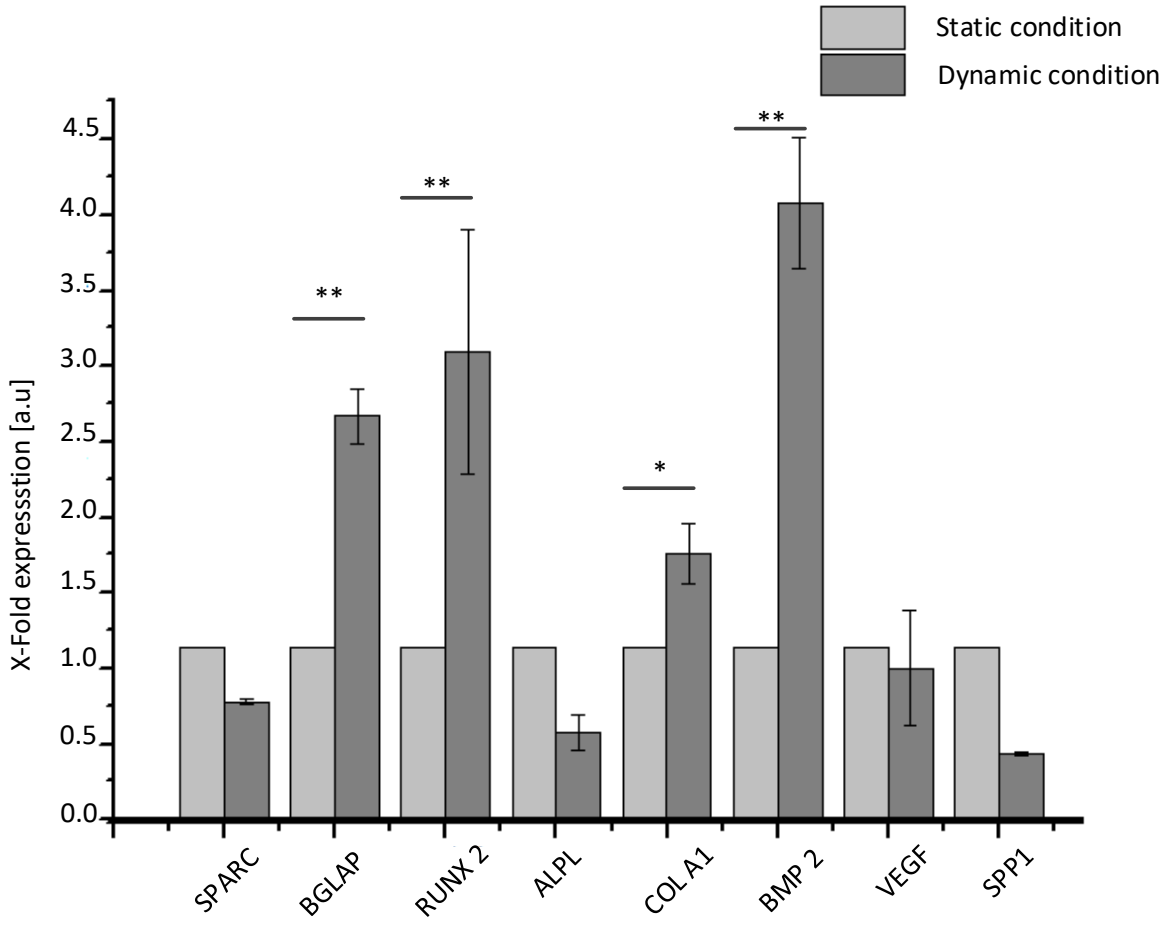

Figure 4-37: Osteogenic gene-related markers were analyzed for seven days of culture under static and dynamic 3D culture condition in RCP AP scaffolds. Human mesenchymal stem cells (hMSCs) were cultured for seven days in proliferation medium under static and dynamic culture conditions in the RCP AP scaffolds (n=3) Gene expression was measured by quantitative real-time polymerase chain reaction (qRT-PCR), * denotes a significant difference between culture conditions (*p<0.05).

The expression of the collagen type 1 gene was significantly upregulated in the dynamic culture compared with the static culture condition. *RUNX2, BGLAP*, and *BMP2* expression were highly significantly upregulated in the dymanic culture condition. In contrast, the expression of AP was downregulated in the perfusion condition compared with the static culture condition.

4.3.6 RCP AP MG scaffold

This scaffold is made of RCP (type 1 derived) mixed with AP and MG. It was also supplied by ISTEC.

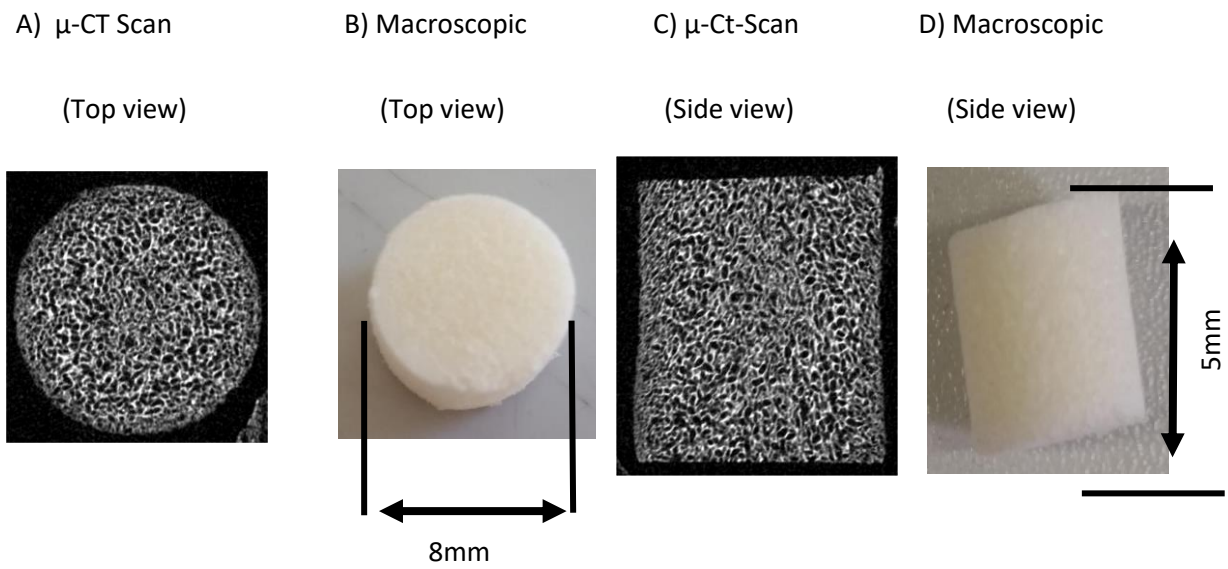

Figure 4-38 µ- CT scan of RCP AP MG scaffold, A and C showing the top and side view of the µ-CT scan of RCP AP MG scaffold, B and D showing the top and side view of the macroscopic of the RCP AP MG Scaffold.

Figure 4-38 shows both microscopic and macroscopic images of the RCP AP Mg scaffold. The macroscopic image shows its structure and shape, while the microscopic image shows the interconnection of pores within the scaffold, which helps cells distribute throughout it. Subsequently, mechanical deformation was applied to the scaffold to determine its elasticity.

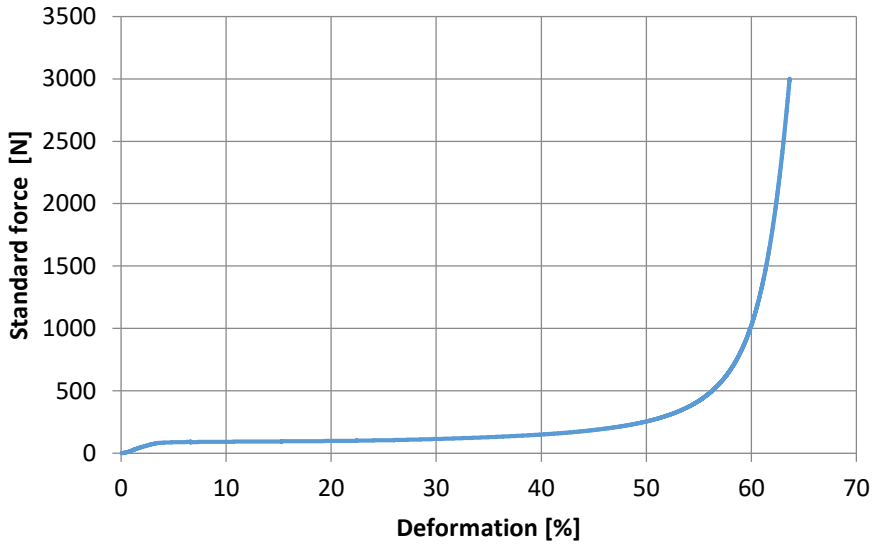

Figure 4-39 Graph represents a force-deformation measurement of RCP AP MG scaffolds. The scaffold showed elasticity when mechanical deformation was applied to the scaffold.

No breaking point was identified when mechanical deformation was applied. The scaffold endured 50% demormation at a force of 250 N. Young's modulus for the RCP AP Mg scaffold was determined to be 3.69 MPa, indicating that the scaffold is elastic.

To view cell attachment, the cell-seeded RCP AP Mg was scanned with an SEM.

A) **B)**

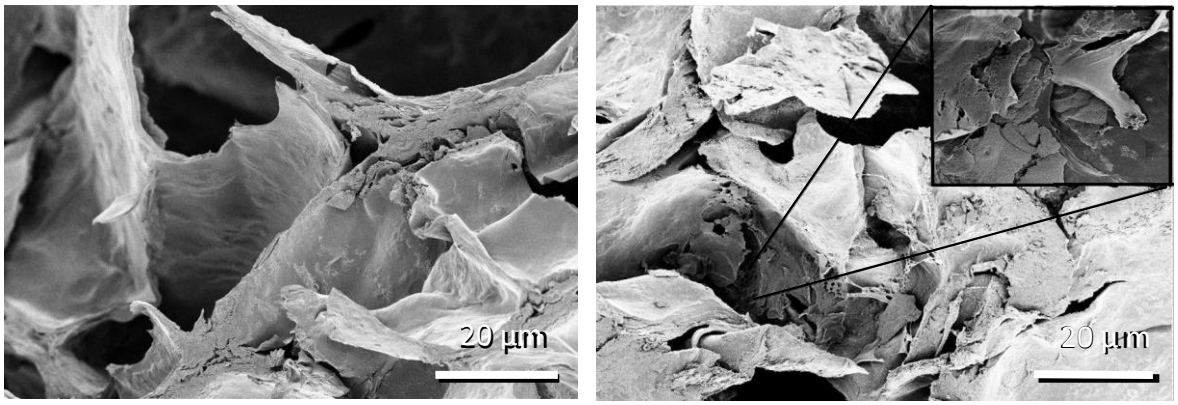

Figure 4-40: SEM of RCP AP MG scaffold. (A) Cell-free scaffold (left), (B) cell-seeded scaffold (right).

The SEM scan of the scaffold further confirmed its porous nature. Figure 4-40 reveals that cells were growing throughout it.

To access hMSC viability and distribution, an MTT assay was performed on 5 x 10^6 hMSCs seeded on the RCP AP Mg scaffold and cultured under static and dynamic conditions for 7 days.

Figure 4-41 Evaluation of cell seeding and viability of cells in RCP AP Mg scaffolds. 5x10^6 Human mesenchymal stem cells (hMSCs) were seeded on each scaffold and subjected to either static or dynamic culture condition. Cell seeded scaffolds were analyzed post seven days of culture for cell viability with MTT assay (n=3).

The purple color observed indicated the presence of viable cells in RCP AP Mg scaffolds cultured under both static and dynamic culture conditions, as shown in Figure 4-41.

Following the MTT test, both static and dynamic culture conditions were tested for collagen type 1 staining

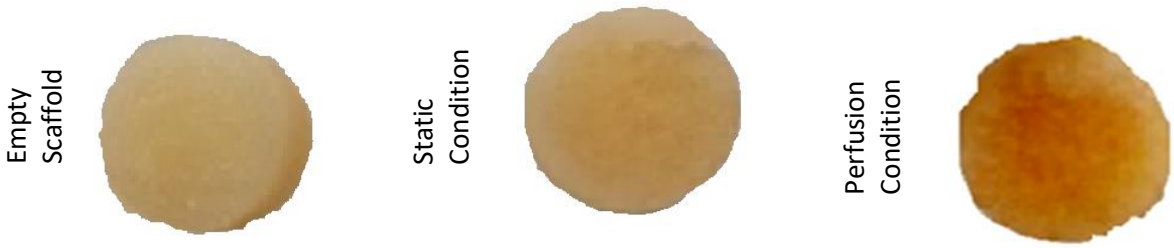

Figure 4-42 Evaluation of collagen type 1 staining in the RCP AP Mg scaffolds (n=3).

In static culture condition the expression of collagen type 1 was observed more than the empty scaffold. The expression of collagen type 1 further increased under shear stress i.e. under perfusion culture condition staining of collagen type 1 increased compared to static culture condition Figure 4-42. This shows that shear stress increases the expression of collagen type one in RCP AP Mg scaffold.

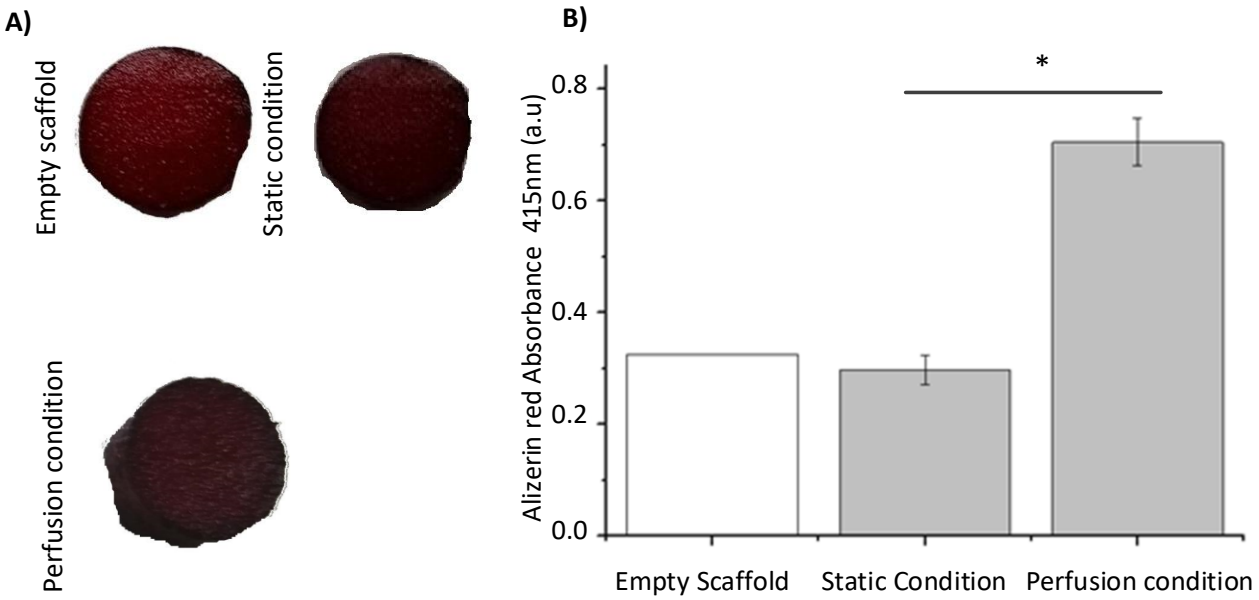

Figure 4-43: Effect of shear stress on the level of calcification on the RCP AP Mg scaffolds. 5x10^6 Human mesenchymal stem cells (hMSCs) were cultured for seven days in proliferation medium under static and dynamic culture conditions in RCP AP MG Scaffold. (A) Alizarin red staining was used to analyze mineralization, (B) Calcium concentration was measured quantitatively by dissolving alizarin red (n=3).

Increased Alizarin red staining was seen in the dynamic culture compared with the static culture condition. Later, quantification was done by calcification assay in both conditions. Twofold higher calcification was seen in the dynamic culture compared with the static culture condition. This shows that shear stress induces stem cells to move toward osteogenic lineage commitment. The results of both Alizarin red staining and collagen type 1 staining were confirmed by qRT-PCR.

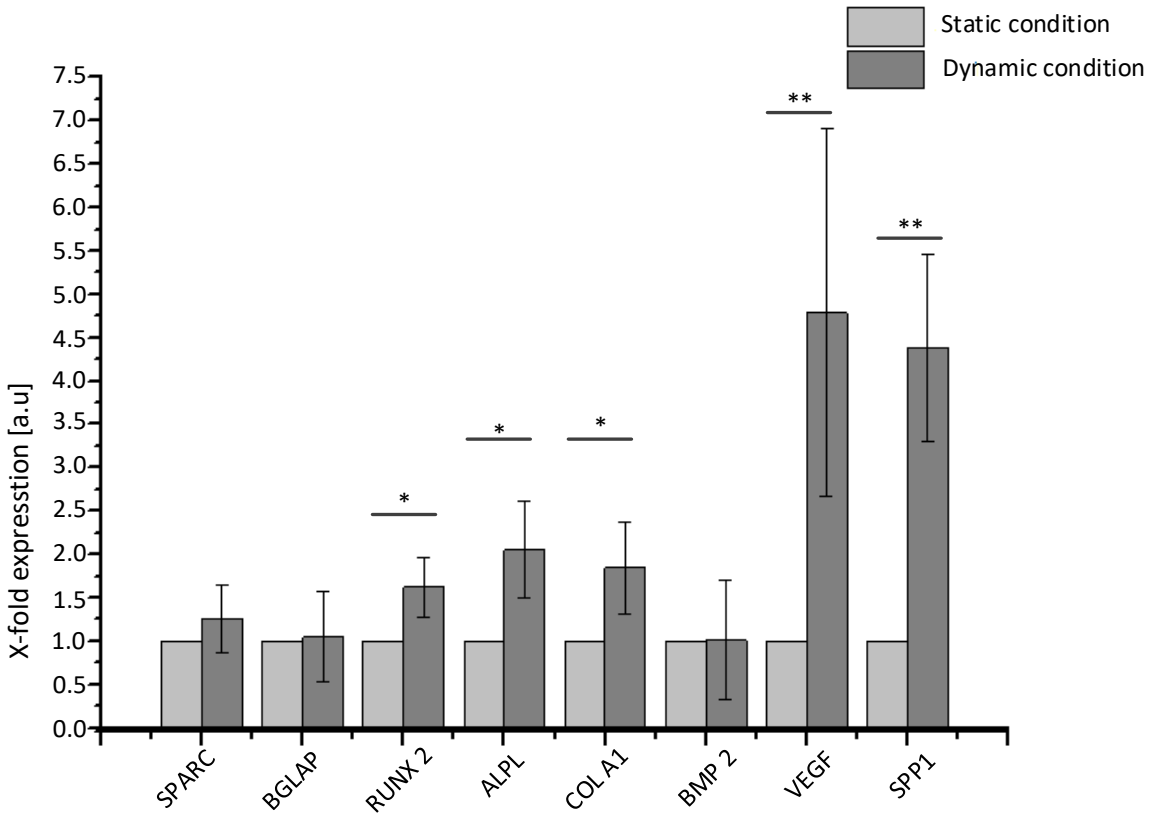

Figure 4-44: Osteogenic gene-related markers were analyzed after seven days of culture under static and dynamic 3D culture condition in RCP AP Mg scaffolds. 5x10^6 Human mesenchymal stem cells (hMSCs) were cultured for seven days in proliferation medium under static and dynamic culture conditions in RCP AP Mg scaffolds. Gene expression was measured by quantitative real-time polymerase chain reaction (qRT-PCR), * denotes a significant difference between culture conditions (n=3) (*p<0.5, **p<0.05).

After the 7 days of cell culture in both static and dynamic conditions, different osteogenic gene markers were evaluated by qRT-PCR. Under shear stress, a significant increase in the expression of AP, RUNX2, and collagen type 1 was observed. Other markers such as VEFG and osteopontin were also significantly upregulated under the dynamic culture compared with the static culture condition. However, no difference was observed for the expression of SPARC, BGLAP, or BMP2, as shown in Figure 4-44.

4.3.7 Selection of suitable scaffold for mechanical deformation

To address the effect of different types of mechanical deformation on cell-seeded scaffolds for osteogenic lineage commitment, a scaffold with high elasticity, stability under perfusion, and cell viability was sought. Furthermore, the scaffold needed to provide a condusive environment for hMSCs to differentiate into osteogenic lineage commitment.

Among all the tested scaffolds, only four scaffolds showed high elasticity (*i.e.*, P(LLA co-CL), RCP, RCP AP, and RCP AP Mg). Of them, the RCP AP scaffolds were not stable under perfusion because the AP leached out out under the perfusion culture condition. Although the hMSCs exhibited good cell viability and homogenous distribution on all three remaining scaffolds, the highest calcification under shear stress was obtained with the P(LLA-co-CL) scaffold. Thus, P(LLA-co-CL) scaffolds were used in further experiments to address the mechanical stimulation of hMSCs for osteogenic lineage commitment.

4.4 Effect of different types of mechanical stimulation on the stem cells for osteogenic lineage commitment

To evaluate the effects of different types of mechanical stimulation on hMSCs for osteogenic lineage commitment, a bioreactor platform was developed in which a 3D cell culture can be performed under both perfusion and mechanical deformation conditions. The bioreactor consists of a stem connected to a pump through which different types of mechanical stimulation can be applied to a cell-seeded scaffold based on frequency and amplitude. The pump moves in a uniaxial direction, so uniaxial force with shear stress can be applied to 3D cell cultures, as shown in Figure 4-45

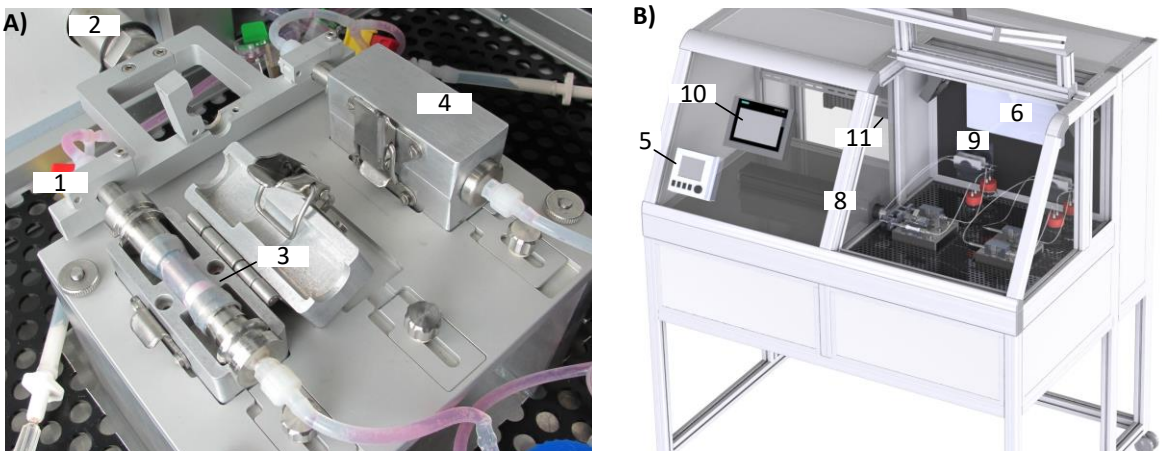

Figure 4-45:Bioreactor technology for the physiological culture of hMSCs seeded scaffold for osteogenic lineage commitment. (A) A stem (8) was used to superimpose mechanical loading (9) onto the scaffolds (10) placed inside bioreactor chambers (11). (B) The incubation system comprises monitoring of pH (1) and allows oxygen, carbon dioxide, and temperature (2) control. Bioreactors were hooked onto a stage (3), and mechanical loading was applied via a linear motion device (4). Moreover, the simultaneous perfusion of multiple bioreactors was achieved through µ-control-regulated roller pumps (5). System performance was monitored and adjusted by the user interface (6) embedded into the front panel. The corresponding control modules (7) are situated in the back of the incubator (45).

This custom-made bioreactor was placed in an incubator consisting of a linear motion device and pressure sensor to ensure optimal cell culture conditions (*i.e.*, 37°C and 5% CO_2).

Cells were seeded into the porous P(LLA-co-CL) scaffolds and allowed to attach for 30 minutes without any perfusion of media or application of mechanical deformation, after which perfusion was applied. Thereafter, mechanical deformation at 1% amplitude and 1%

frequency was applied to the cell-loaded scaffold for 1 hour twice a day over two intervals (1 and 7 days). Cell viability and distribution were similar under both mechanical and perfusion conditions, as shown in Figure 4-46.

Figure 4-46: Evaluation of viability of cells in the scaffolds under mechanical deformation. 5x106 hMSCs were seeded on P[LLA CO-CL] scaffolds and cultured under perfusion and mechanical deformation condition for a period of 1 day and 7 days. Cell viability and cell distribution were assessed by MTT assay. Perfusion culture condition without any mechanical deformation was used as control.

The application of mechanical deformation led to significantly higher calcification at both intervals compared with the perfusion culture condition, as shown in Figure 4-47.

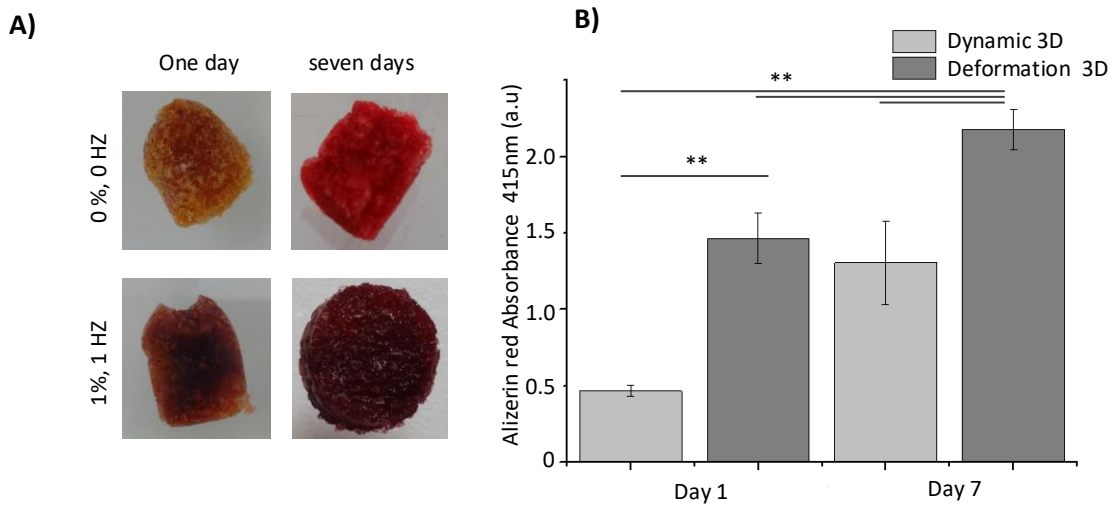

Figure 4-47: Effect of mechanical stimulation on the level of calcification the scaffold. (A) Alizarin red staining, (B) calcification assay was done on stem cell-seeded P[LLA CO-CL] scaffolds, cultured under mechanically stimulated for the duration of one and seven days, ** $p<0.05$ (n=3). Perfusion culture condition (dynamic) without any mechanical deformation was used as control.

A threefold increase in calcification under mechanical deformation was observed on day 1 and a 1.6-fold increase on day 7 compared with the perfusion culture condition at each respective interval. From day 1 to day 7, a 1.5-fold increase in calcification under mechanical

deformation was observed. These findings indicate that MSCs differentiate toward the osteogenic lineage in a shorter period under the influence of mechanical deformation compared with shear stress. This was further confirmed by assessing the expression of genes related to osteogenic lineage commitment, as shown in Figure 4-48 and Figure 4-49.

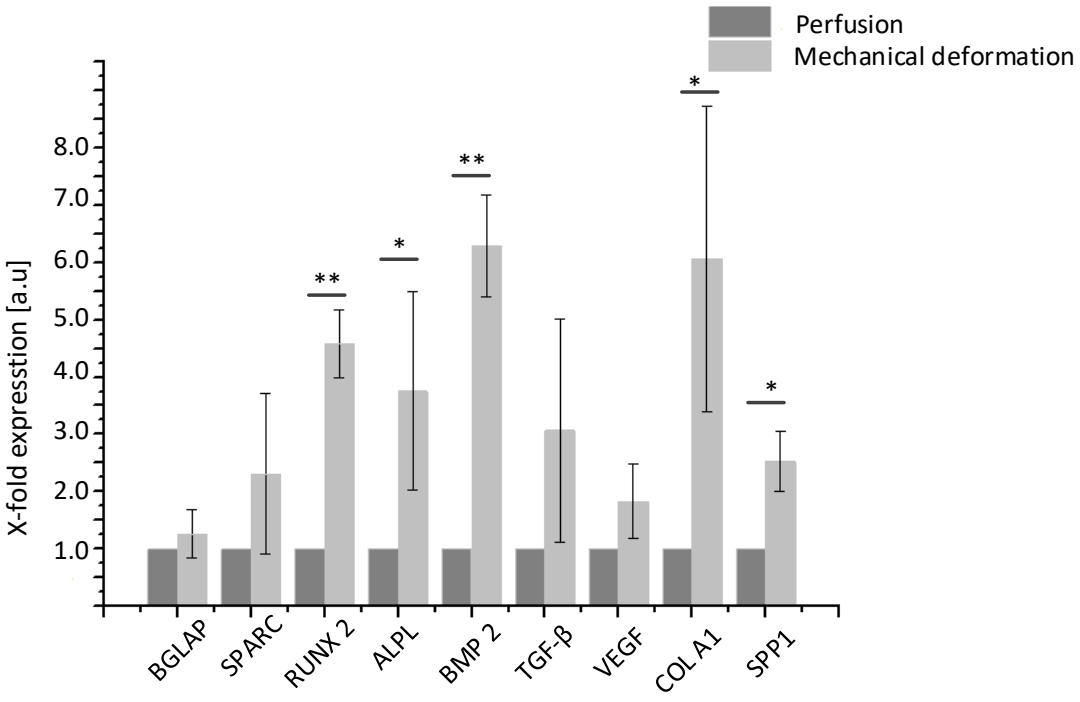

Figure 4-48: Expression of genes related to osteogenic lineage commitment under mechanical stimulation post day one of culture. 5x10^6 hMSCs stem cells were cultured in P[LLA CO-CL] scaffolds for a period of one day under perfusion and mechanical deformation conditions. Osteogenesis related genes were analyzed after one day of culture. *denotes a significant difference between culture conditions (*p<0.5) (* p< 0.05) (n=3).

The expression of different gene markers for osteogenic lineage commitment was observed in both perfusion and mechanical deformation cell cultures after 1 day. Under the influence of mechanical deformation, *RUNX2* and *BMP2* expression were highly significantly upregulated compared with the perfusion condition. The expression of other gene markers such as *ALPL, COL1A1, and SPP1* were also upregulated under mechanical deformation compared with shear stress alone, as shown in Figure 4-48.

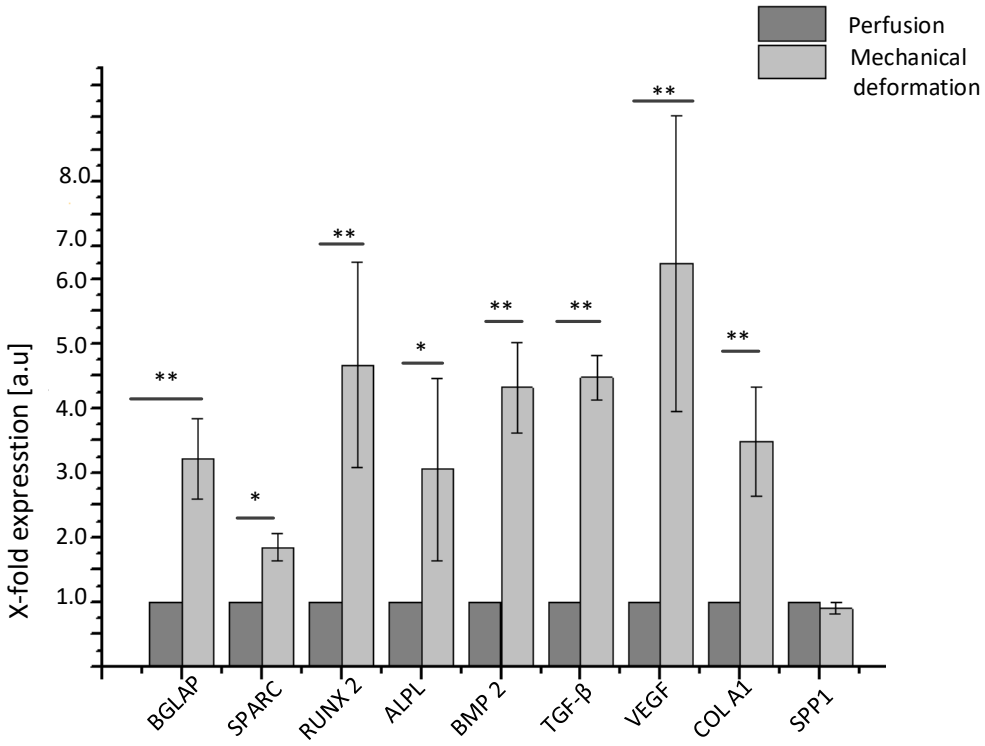

Figure 4-49 : Expression of genes related to osteogenic lineage commitment under mechanical stimulation post day seven of culture. 5x10^6 hMSCs stem cells were cultured in P[LLA CO-CL] scaffolds for a period of seven days under perfusion and mechanical deformation conditions. Osteogenesis related genes were analyzed after seven days of culture. *denotes a significant difference between culture conditions (*p<0.5) (* p< 0.05) (n=3).

Gene markers for osteogenic lineage commitment such as RUNX2, OC, BMP2, VEGF, TGF-β, and collagen type 1 were highly significantly upregulated under mechanical deformation compard with the shear stress condition, as shown in Figure 4-49. Other genes such as osteonectin and AP were also significantly upregulated under mechanical stimulation, as Figure 4-49 shows. Genes such as BGLAP, SPARC, TGFβ, and VEGF showed significant upregulation from days 1 to 7 under mechanical stimulation. Contrary to this, SPP1 was downregulated under mechanical stimulation during the same period, as shown in Figure 4-48 and Figure 4-49. These findings further support the evidence that mechanical force influences the upregulation of genes that are key to osteogenic lineage commitment.

After establishing that mechanical stimulation plays an important role in differentiation of hMSCs into osteogenic lineage, the type of force required to achieve this differentiation was determined (*i.e.*, deformation). To identify the ideal combination of

deformation force needed to effectuate high osteogenic lineage commitment, such force was applied in varying amplitudes and frequencies to a TERT-AP1 cell line, which expresses the luciferase reporter gene in response to mechanical defomation (additional information about TERT-AP1 cell lines is provided in section 3.2.4).

TERT-AP1 cells were cultured in the bioreactor and subjected to different combinations of force based on frequency (1–2%) and amplitude (1–2%). The mechanical deformation was induced over 2 days for 1 h twice a day. Cell viability and cell distribution inside the scaffold was determined by an MTT assay.

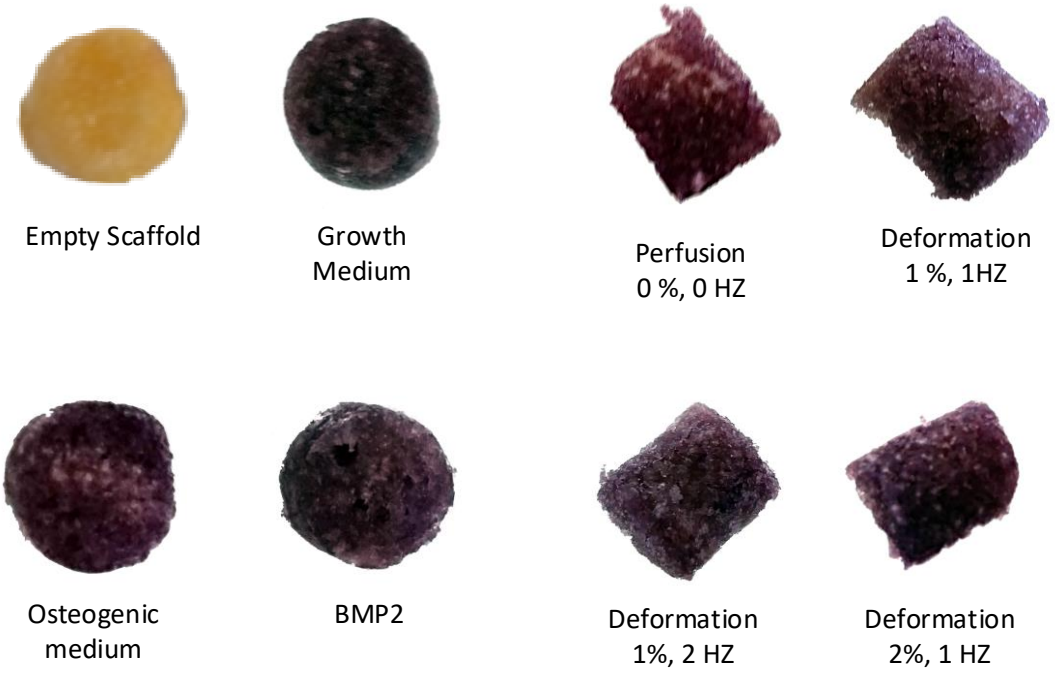

Figure 4-50: Evaluation of cell viability in the scaffolds. The scaffolds seeded with TERT AP1 cells were cultured for two days under various conditions. Cells grown under static conditions in the growth medium, osteogenic differentiation medium, growth medium with BMP2(10 ng/ml) served as controls. In addition to this, cells cultured under perfusion conditions in growth medium without mechanical deformation also served as control. TERT AP1 cells were subjected to different type of force based on frequency (1-2%) and amplitude (1-2%). After 48 hours cells were stained by MTT (n=4) (45).

TERT-AP1 cells were viable in the static culture conditions without any shear stress or mechanical deformation. Cells were evenly distributed and viable at the end of the 2 days. Likewise, cells cultured under shear stress and different mechanical deformations were also viable and evenly distributed. Thus, no difference were seen in terms of cell viability under these different conditions

Next, Alizarin red staining and a calcification assay were done to measure the level of calcium content present in the TERT-AP1 cell-seeded scaffolds

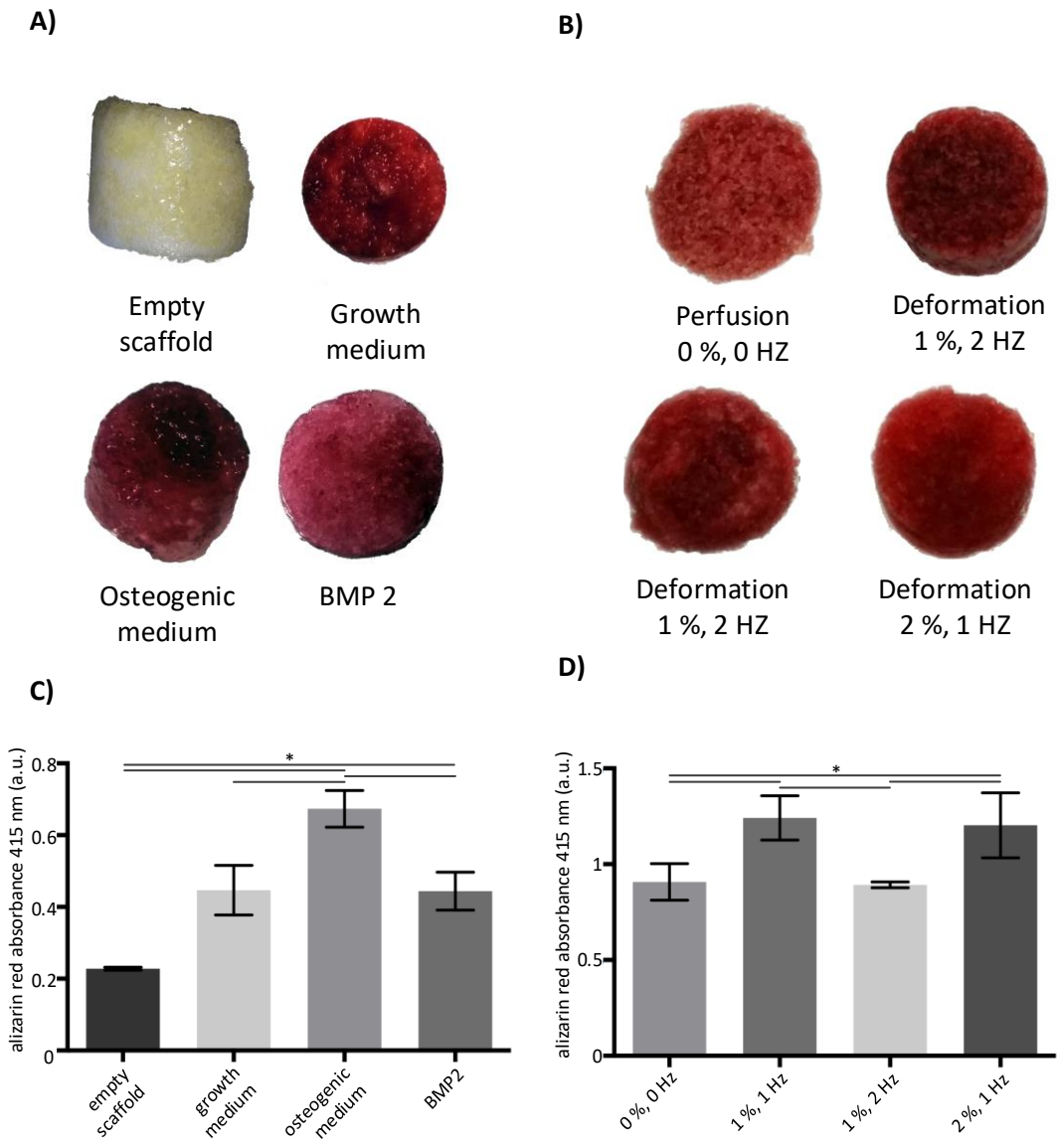

Figure 4-51: Alizarin red staining on the scaffolds. The scaffolds seeded with TERT AP1 cells were cultured for two days under various and conditions. Cells grown under static conditions in the growth medium, osteogenic differentiation medium, and growth medium supplemented with BMP2(10 ng/ml) served as controls. In addition to this, cells cultured under perfusion conditions in growth medium without mechanical deformation also served as control. TERT AP1 cells were subjected to different type of force based on frequency (1-2%) and amplitude (1-2%). (A-B) After 48 hours of culture Alizarin red staining was done to analyze the level of calcium present in the scaffold after the experiment (n=4). (C-D) Higher the intensity of alizarin red shows higher the level of calcium present in the scaffold construct. (n=4) *denotes a significant difference between culture conditions (*p<0.05) (45).

As shown in Figure 4.51(A, C), in the control group, the highest level of calcification was observed with the cells cultured in the osteogenic medium in comparison to either with

the growth medium or the growth medium supplemented with BMP2. Cells cultured under shear stress or different mechanical force showed even higher calcification than cells grown in the osteogenic medium under the static culture condition. Further, cells stimulated with shear stress showed less calcification than cells stimulated with mechanical force—except when they were stimulated at a frequency of 2 Hz. However, other conditions of mechanical deformation, such as 1 Hz with 1% amplitude and 2% amplitude with 1% Hz, showed a higher level of calcification in the scaffolds Figure 4.51(B, D). These findings demonstrate that cells mechanically stimulated by higher amplitude tend to differentiate toward the osteogenic lineage commitment. To confirm the results of Alizarin red staining, qRT-PCR was performed.

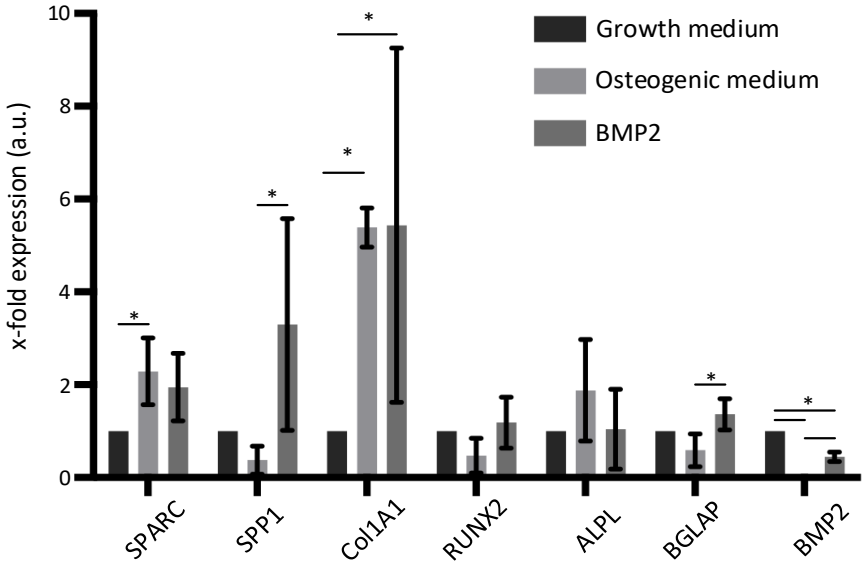

Figure 4-52: Expression of genes related to osteogenic lineage commitment under different static culture conditions. Data were expressed as mean values ± standard deviation and analyzed by one-way analysis of variance followed by Fisher's LSD test. * denotes a significant difference between two experimental groups (*p < .05). n = 4. "A.U." abbreviates "arbitrary unit." ALPL = alkaline phosphatase; BGLAP = osteocalcin; BMP-2 = bone morphogenic protein-2; Col1A1 = collagen type 1 alpha 1; RUNX2 = runt-related transcription factor 2; SPARC = osteonectin; SPP1 = osteopontin (45).

When the cells were cultured under the osteogenic medium, there was significant upregulation of osteonectin and collagen type 1 compared with the growth media culture condition. But when BMP2 was added to the growth media, there was significant upregulation of osteopontin and the *BGLAP* gene compared with the growth media and osteogenic media culture conditions. BMP2 expression was downregulated in both the osteogenic and BMP2

supplemented growth medium culture conditions compared with the growth medium culture condition, as shown in Figure 4-52. Furthermore, in the initial 2 days of cell culture, the presence of neither BMP2 nor growth factor influenced the expression of *ALPL*, as shown in Figure 4-52.

Subsequently, the cell-seeded scaffolds stimulated either by shear stress or mechanical deformation were analyzed for different gene markers through qRT-PCR.

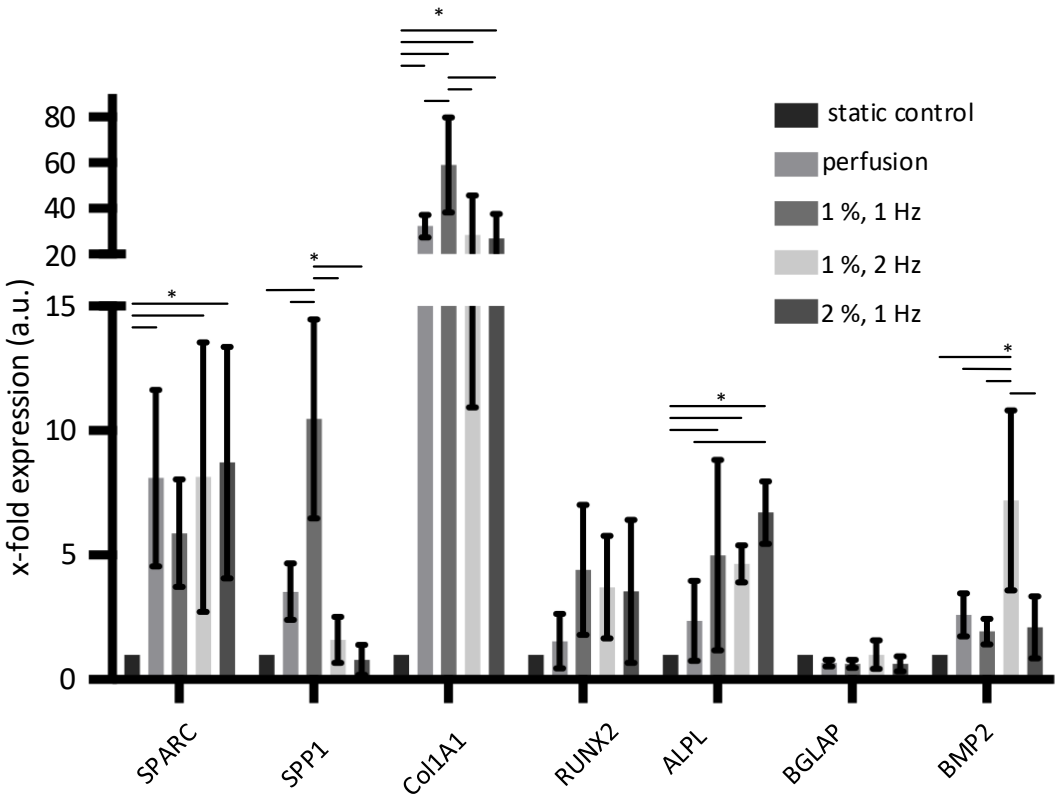

Figure 4-53: Expression of genes related to osteogenic lineage commitment under different mechanical stimulation culture conditions. Data were expressed as mean values ± standard deviation and analyzed by one-way analysis of variance followed by Fisher's LSD test. *denotes a significant difference between two experimental groups (*p < .05). n = 4. "a.U." abbreviates "arbitrary unit." ALPL = alkaline phosphatase; BGLAP = osteocalcin; BMP-2 = bone morphogenic protein-2; Col1A1 = collagen type 1 alpha 1; RUNX2 = runt-related transcription factor 2; SPARC = osteonectin; SPP1 = osteopontin (45).

After the 2 days of experiment under perfusion and different mechanical stimulations concluded, qRT-PCR was done for different gene markers to identify the best mechanical deformation condition for improving osteogenic lineage commitment.

Figure 4.43 hows that 1 Hz and 1% amplitude of mechanical deformation resulted in the upregulation of alkaline phosphate, collagen type 1 and osteopontin in comparison to static condition or perfusion condition. Similarly, when the frequency was increased to 2%, the upregulation of osteonectin, AP, collagen type 1, and BMP2 expression compared with the static condition was observed. When the amplitude was increased to 2%, there was an upregulation in osteonectin, AP, and collagen type 1 gene expression compared with the static conditions. These results show that under mechanical stimulation, there were upregulations of AP (inorganic phase of the bone) and collagen type 1 (organic phase of the bone) gene expression compared with the static condition. AP gene expression was significantly upregulated when the amplitude was increased in mechanical deformation.

4.5 Effect of mechanical deformation versus deformation-induced shear stress on the stem cells for osteogenic lineage commitment

Mechanical compression applied to the scaffold can lead to shear stress inside it. A computational simulation was conducted to evaluate the roles of mechanical deformation and deformation-induced fluid–flow shear stress in osteogenic lineage commitment. Shear stress induced by mechanical deformation was measured inside the bioreactor by the computational model of the fluid dynamics

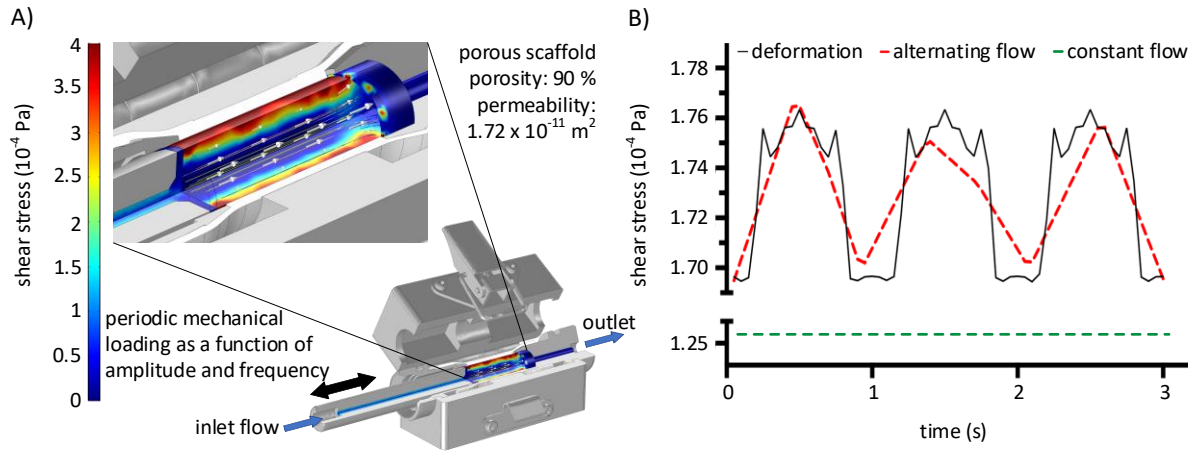

Figure 4-54: Characterization of shear stress-induced by mechanical loading. (a) A computational model of the fluid dynamics inside the bioreactor chamber. Stem motion was modelled by defining the porous scaffold domain as moving mesh. Fluid flow was achieved by generating inlet and outlet boundaries as indicated. Multiphysics computations conveyed shear stress data occurring inside the porous scaffold while under perfusion and simultaneous compression. Shear stress levels are designated by colour range. (where colder (blue) color indicate low shear stress and warmer (red) color indicate higher shear stress) (b) The computational model facilitated the identification of a flow profile resulting in a

similar shear stress pattern compared with average shear stress induced by mechanical deformation. (Computational simulation & modelling was done by the colleague: Ivo Schwedhelm) (45).

The compression of the scaffold was simulated for 1 Hz and 2% amplitude, and the shear stress was extracted from the modeling based on factors such as porosity and the mechanical deformation of the scaffold. The initial shear stress was computed to be 1.26×10^{-4} Pa for the constant flow, with an average increase to 1.73×10^{-4} Pa under shear stress when the mechanical deformation was performed in the bioreactor. This computational model allowed us to measure the alternating perfusion flow profile, which helped us compare the shear stress pattern caused by mechanical deformation in the scaffold. Figure 4-54 shows the comparison of shear stress caused by deformation or alternating fluid flow in the scaffold. Accordingly, shear stress generated by mechanical deformation can be isolated to understand the independent role of mechanical deformation.

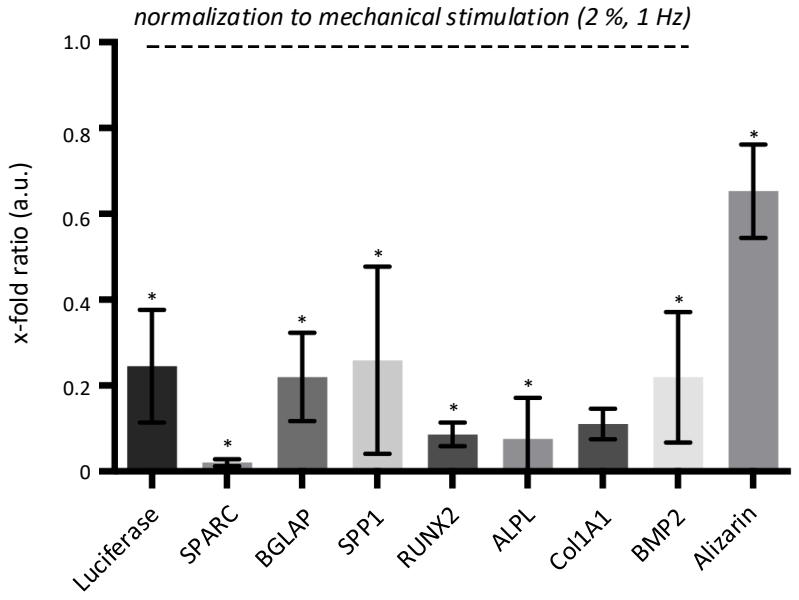

Figure 4-55: Expression of genes related to osteogenic lineage commitment under periodic flow of shear stress because of mechanical deformation normalized to mechanical deformation alone . The qRT- PCR genes expression data was expressed as mean values ± standard deviation and analyzed one-way analysis of variance followed by Fisher's LSD test (GraphPad Prism, GraphPad Software Inc., La Jolla, USA). * denotes a significant difference between two experimental groups (*p < .05). n = 4. "a.U." abbreviates arbitrary unit. ALPL = alkaline phosphatase; BGLAP = osteocalcin; BMP-2 = bone morphogenic protein-2; Col1A1 = collagen type 1 alpha 1; RUNX2 = runt-related transcription factor 2; SPARC = osteonectin; SPP1 = osteopontin (45).

After 2 days of culturing cells in the bioreactor under the periodic flow of shear stress caused by mechanical deformation and by mechanical deformation alone, qRT-PCR was

performed to evaluate the expression of the osteogenic gene markers. The results obtained were normalized to the data obtained from mechanical deformation.

TERT-AP1 expresses luciferase under the AP1 response element, which gets activated under mechanical strain. TERT-AP1 cells can thus identify general stress as they express luciferase under different mechanical stress. The luciferase expression was reduced under the periodic flow of shear stress compared mechanical deformation strain. This shows that AP-1 responded more strongly to mechanical deformation than shear stress itself. The level of calcification seen under the periodic flow of shear stress was less than the mechanical deformation condition. Furthermore, the expression of all the osteogenic genes, such as osteonectin, OC, osteopontin, RUNX2, ALPL, and collagen type 1, was significantly downregulated under shear stress (generated by mechanical deformation) compared with the mechanical deformation condition.

These findings indicate that mechanical deformation strain plays a greater role in osteogenic lineage commitment than shear stress strain.

4.6 *In vitro* osteoporosis drug test system

After standardizing the mechanical stimulation, hMSCs isolated from osteoporotic patients (OMSCs) were tested in a bioreactor with the application of mechanical deformation. The effects of the osteoporotic drug strontium ranelate, marketed under name Protelos®, was determined on OMSCs with respect to osteogenic lineage commitment. hMSCs from healthy donors were cultured under different concentrations of Protelos® for 7 days to determine optimal drug concentration for high cell viability and calcification. One mM of Protelos® induced higher calcification with high cell viability, as shown in Figure 4-56..

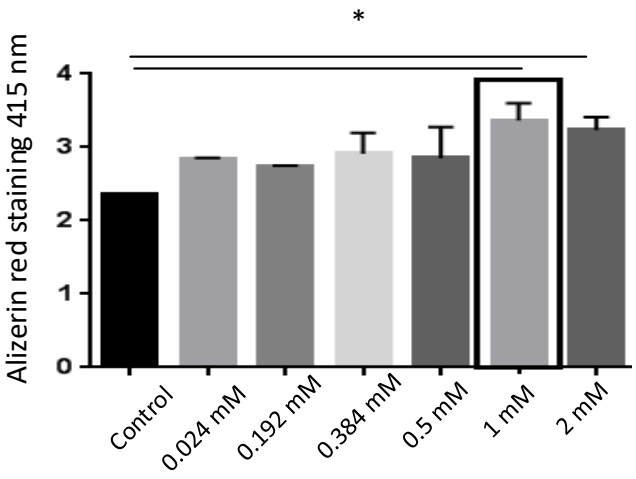

Figure 4-56: Effect of different concentrations of Strontium Ranelate (marketed under name Protelos®) on osteogenic differentiation stem cells isolated from healthy donors. MSCs were cultured with different concentration of Strontium Ranelate under 2D culture for seven days. Alizarin red staining and calcification assay were done to determine cell viability and calcification.*denotes a significant difference between culture conditions (n=3)(*p<0.05).

OMSCs were cultured in a mechanical deformation bioreactor for f 7 days, and the viability of the cells after drug–cell interaction was determined via an MTT assay. Stem cells from healthy donors and OMSCs not receiving Protelos® treatment were cultured in the bioreactor as controls. No difference in cell viability was observed between the different conditions, showing that Protelos® treatment did not affect it. The cells were viable and evenly distributed in the scaffold, as shown in Figure 4-57.

Figure 4-577: Effect of Strontium Ranelate on OMSCs under the condition of mechanical deformation. OMSCs, MSCs and OMSCs with 1mM Strontium Ranelate were cultured in mechanical deformation bioreactor for seven days in KTH Scaffold.MTT assay was performed to determine cell viability (n=2).

Organic and inorganic phases of bone were evaluated with Alizarin red and collagen type 1 staining.

Figure 4-58: Effect of Strontium Ranelate on Collagen type 1 expression under the condition of mechanical deformation. OMSCs, MSCs and OMSCs with 1mM Strontium Ranelate were cultured for seven days in growth medium under mechanical deformation culture conditions in P[LLA-co-CL] scaffolds. Seven days post culture, the cell-seeded scaffolds were stained for collagen type 1 (n=2).

MSCs under mechanical stimulation produced collagen type 1, but it was highly diminished in the OMSCs, as shown in Figure 4-58. However, Protelos® treatment restored the expression of collagen type 1 in the OMSCs, as shown in Figure 4-58. This shows that the osteoporotic diseased cells started to express collagen type 1 and behave like the healthy MSCs in the cell-seeded scaffold.

.

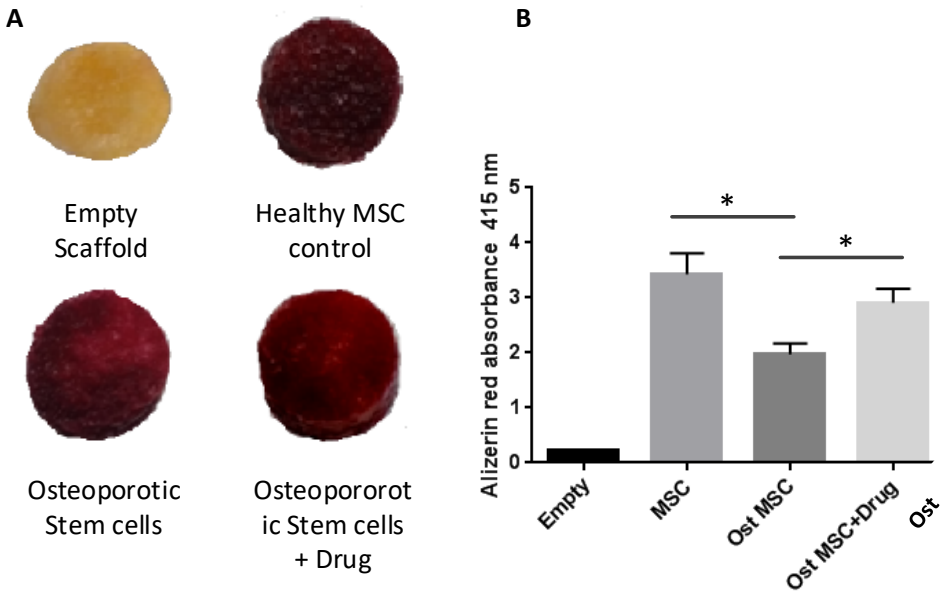

Figure 4-59: Effect of Strontium Ranelate on calcification under the condition of mechanical deformation. OMSCs, MSCs and OMSCs with 1mM Strontium Ranelate were cultured for seven days in proliferation medium under mechanical deformation culture conditions in P[LLA-co-CL] scaffolds. Seven days post culture, (A) Alizarin red staining was used to analyze mineralization. (n = 2) (B) Calcium concentration was measured quantitatively by dissolving alizarin red (n=2).

Higher calcification was seen in MSCs compared with OMSCs with or without drug treatment. Strontium ranelate treatment of OMSCs increased calcification levels compared with the nondrug-treated OMSCs. These results show that OMSCs displayed less calcification compared with MSCs, but the level of calcification could be improved by strontium ranelate.

To confirm the results obtained from collagen type 1 and the calcifcation assay, qRT-PCR was conducted on different osteogenic markers.

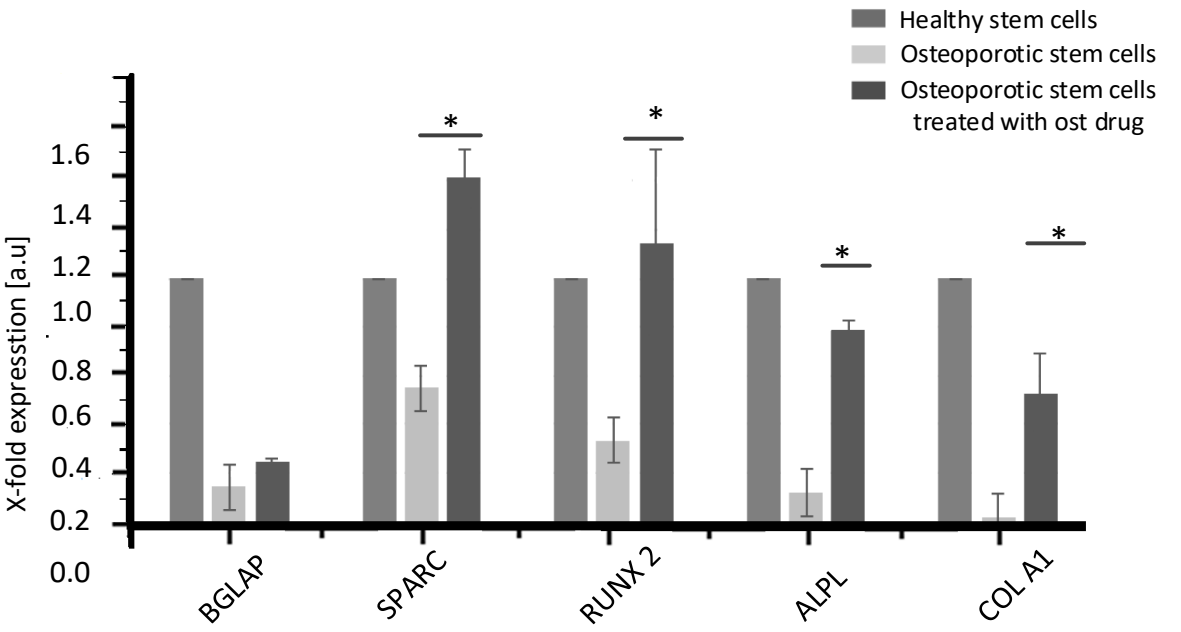

Figure 4-60: Effect of Strontium Ranelate on the expression of genes important for bone regeneration.OMSCs, MSCs and OMSCs with 1mM Strontium Ranelate were cultured for seven days in proliferation medium under the mechanical deformation culture conditions in P[LLA-co-CL] scaffolds. Seven days post culture osteogenesis related genes were analyzed (n=2, two donors).

The expression of genes important for bone regeneration such as BGLAP, SPARC, RUNX2, ALPL, and COLA1 were downregulated in the OMSCs compared with the healthy hMSCs, as shown in

Figure 4-60. Strontium ranelate treatment led to the upregulation of gene expression, including SPARC, RUNX2, ALPL, and COLA1 in OMSCs. This shows that strontium ranelate leads to the upregulation of osteogenic gene markers in treated OMSCs.

This model may thus be used to screen drugs for osteoporosis and can be further developed into an *in vitro* osteoporotic drug testing system.

5 Discussion

Tissue-engineered bone grafts offer a promising treatment for large and critical size bone defects[68], [69], [70]. The demand for bone implants is ever increasing due to fractures caused by trauma, tumors, and infectious bone diseases. The standard line of treatment involving bone allografts causes secondary trauma and increases the risk of associated morbidity and poor healing. Although allogeneic bone implants[71] offer an attractive solution, they carry their own risks of immune system reaction and implant rejection. Therefore, developing tissue-engineering technology to deliver bone grafts which can enhance healing after implantation is the need of the hour.

The tissue-engineering approach to developing bone implant involves seeding stem cells in synthetic biomaterial scaffolds to create an efficient osteogenic implant and achieve graftable bone tissue. To this end, several praiseworthy attempts have been made to optimize scaffold materials as well as their shape and structure, and much research has also been done on selecting the right type of stem cells, optimizing growth media and conditions, and developing bioreactor technology to support the growth of such bone implants[72].

In this thesis, state of art scientific knowledge concerning scaffolds, cells, and bioreactor technology was employed to develop a bioreactor which provides optimal conditions for developing cylindrical bone implants 10mm tall and 12mm wide to treat critical size bone defects. Furthermore, this bioreactor system can be used to screen osteoporotic drugs.

In the following paragraphs, the impact of the development of this bioreactor and the bone implant it generated is discussed, including drawbacks.

5.1 Critical size bone defects and their regeneration

Bone is a dynamic organ undergoing continuous remodeling throughout adult life, depending on the mechanical loading of the limbs as well as hormones and calcium and phosphate levels in the blood. Bone also has an inherent regenerative capacity which allows fractures to heal, restorating its preexisting properties without formating scar tissue such that newly formed bone is eventually indistinguishable from adjacent, uninjured bone.

However, natural bone regeneration is not effective beyond a certain defect size. The minimal dimension of a critical size bone defect depends on the animal. For rabbits, it is a length of 6mm; for mice, it is a length of 4mm[73]; and for humans and larger animal models, it is a length of more than 12mm and a diameter of more than 10mm[74], [18].

Our understanding of bone regeneration at the cellular and molecular levels has advanced enormously. It is well known that bone regeneration is a complex, physiological process comprising a well-orchestrated series of bone induction and conduction events which rely on several cell types and intra and extracellular molecular signalling pathways, all occurring in a definable temporal and spatial sequence[75]. Bone tissue engineering combines knowledge from biology, physics, material science, and engineering to develop bone implants[76]. In essence, progenitor cells such as MSCs (native or expanded) of mature cells (for osteogenesis) are seeded in 3D biocompatible tissue-like scaffolds with appropriate growth factors to generate bone implants [77]

Two clinical studies have shown that MSCs seeded on a hydroxyapatite ceramic scaffold and implanted in patients exhibited stronger osteogenic ability and more effective bone formation under computed tomography images with no side effects for the patients, who were suffering from critical size defects[78]. Another excellent long term study was conducted on hydroxyapatite ceramics scaffold for a longer period about seven years showed promising results and improvement in the repair of criterial size long bone defect[79].

Despite two decades of rigorous research and development, there is no proper solution to the problems posed by bone implants. Overall, bone tissue engineering is in its infancy, and there are many issues of efficacy, safety, and cost to be addressed before its general clinical application can be achieved.

5.2 Problems in the development of ideal artificial bone implant

Optimal cell selection raises many safety concerns. But hMSCs are the first choice for developing tissue-engineered bone implants because they can easily be obtained from donors and are free of ethical issues. After harvesting, hMSCs can be expanded under good manufacturing practice (GMP) culture conditions for seeding onto scaffold implants[80]. Studies have reported that culture-expanded cells may have mutations or epigenetic changes

that could increase the risk of tumors[81]. However, *in vitro* and *in vivo* evidence suggests that this risk is minimal with MSCs[82]. For example, 41 patients (45 joints) were tracked for up to 11 years and 5 months after receiving autologous bone marrow-derived hMSC transplants to repair cartilage[83], and they reported no cases of tumor formation. But the tumor-forming potential of MSCs still needs to be thoroughly evaluated before such technology can become part of the clinical practice.

One of the major problems artificial bone implants face is how to achieve even cell distribution within the scaffold and maintain the cells with high viability[84]. To achieve a critical size bone implant close to native bone, we must culture the cells in 3D scaffolds. The 3D cell culture environment seems to provide more physiological conditions in terms of mechanical properties, cell orientation, and cell communication via soluble factors compared with the 2D culture[85]. Maintaining a constant supply of nutrients and soluble factors while allowing for gas exchange to keep the cells alive in the 3D environment is a constant challenge. However, the perfusion of media into this environment ensures nutrient supply and gas exchange. Furthermore, direct perfusion in the bioreactor can be employed to trigger specific lineage commitment because perfusion leads to shear stress that triggers cell differentiation[86].

In the initial development phase of the bioreactor, there was no uniform distribution of cells in the scaffolds. But uniform high cell densities were achieved in later development phases by dynamically seeding cells. The cell suspension was pumped through the bioreactor chamber in alternating cycles for 10 s forward and 3 s backward over 1h at 1.6ml/min. Following this, the pump was stopped for 30 mins to allow for cell adhesion. Automated dynamic cell seeding can thus help achieve a high-density cell population in the scaffold.

Although high cell densities were achievable and low-stress marker levels were observed in the developed bioreactor system, one foreseeable drawback is that the post-*in vivo* transplantation nutrient supply of the implant will be impaired because no provision for perfusion of the implant *in vivo* has been designed. Native bone tissue receives nutrients from the periosteum, which is highly vascularized. Thus, introducing artificial periosteum tissue is an important aspect to be considered for future development.

5.3 Different scaffold materials for bone implant in a bioreactor

In this thesis, scaffolds were constructed from P(LLA-co-CL), PP polymer, ß-TCP, RCP, RCP AP, and RCP AP Mg in minimum sizes 10mm wide and 12mm long to meet the requirements for critical size defects in large animals and humans[18]. These bone implants are biocompatible (*i.e.*, the scaffolds are free from toxicity, teratogenicity, hemolysis, and other inflammatory reactions). Thus, all the scaffolds used in this study are safe to implanting in the human body.

An ideal scaffold should have further interconnected pore networks to provide better oxygen and nutrient supply. Studies have shown that scaffolds with higher porosity and larger surface area promote cell adhesions, cell growth, nutrient and oxygen supply, and waste removal, and they better support the ingrowth of blood vessels and nerves[87]. Recent studies have shown that the ideal diameter of scaffold pores should be in the range of 200µm to 400 µm[88]. All the scaffolds used in this studies have pore diameters in the range of 200µm to 250 µm, other than the ß-TCP scaffold. Uniform cell distribution was not observed in the ß-TCP scaffold, with pore diameters ranging from 100 µm to 500 µm. This was further confirmed by the MTT test as described in the results section and shown in Figure 4.15.

5.4 Optimal bioreactor in bone tissue engineering

Different types of bioreactors are available in the field of tissue engineering, such as stir type, spinner flask, rotating wall, and perfusion[36],[89],[90]. Other than the perfusion bioreactor, most bioreactors cannot receive a constant supply of growth factor, cytokines, oxygen, and nutrients due to mass transfer limitations resulting in low cell viability inside them[91].

Perfusion bioreactors can be further classified based on the stress or strain induced on the cells within the 3D scaffold (*i.e.*, mechanical compression or stretching). Many research studies have shown that mechanical compression plays a major role in ideal bone tissue engineering [92].

5.5 Preparing critical size bone implant under a 3D perfusion bioreactor

Many studies indicated improved bone formation from synthetic bone substitutes when the scaffold was seeded with stem cells before implantation into the animal or human subject[93],[94]. Osteoblasts and osteoclasts are key to both bone remodeling and regeneration[95]. Because stem cells can differentiate into osteoblasts, MSCs were isolated from a healthy patient in this research to culture them in the 3D scaffold implant.

Studies have described different strategies for seeding cells onto scaffolds, such as incubation in centrifugation[96] and cell suspension[97]. Furthermore, one study claimed that shaking increases seeding efficiency with uniformly distributed cells within a scaffold[98]. In this thesis, a seeding protocol was established that employed bioreactor technology to allow for the homogeneous distribution of hMSCs in different cylindrical scaffolds.

Oscillating flow for seeding has already been described as the most efficient way to achieve cell viability[98],[99],[49]. However, for the different scaffold types used in this thesis, optimal parameters for seeding conditions were identified. In contrast to previously published protocols, scaffold seeding was already accomplished after 1h rather than 2h. Further, the seeding parameters exhibited a higher dynamic in terms of flow velocity (0.15 or 1.0ml/min vs. 1.6ml/min) and oscillating frequency (5min vs. cycles for 10s forward and 3s backward). The seeding process was performed fully automatically with no manual intervention, making it thus more reproducible and reliable [66]. Furthermore, controlling the pressure during the seeding prevented cell death caused by uncontrolled high pressure.

5.6 Viability potential of bone scaffold implants using perfusion bioreactors

MTT staining the cross-sections of P(LLA-co-CL) scaffolds showed viable cells after 1 day, 7 days, and 14 days of perfusion cell culture. The scaffold started to show uniform cell distribution from day 7 under the perfusion condition. Hence, all the other scaffolds were cultured for the duration of 7 days, followed by MTT tests.

Homogenous cell distribution was found in the core regions of the P(LLA-co-CL), PP polymer, RCP, RCP AP, and RCP AP Mg scaffolds. But homogeneous cell distribution was not present in the ß-TCP scaffold due to the presence of smaller pores. This data supports recently

published research work showing that smaller pore sizes make it more difficult to distribute stem cells throughout the scaffold.

5.7 Optimal shear stress conditions for 3d cell culture scaffolds

In a perfusion bioreactor, the flow rate of the medium is important because a low rate leads to sufficient nutrient supply and waste removal, while a high rates can lead to cell death. In this thesis, the ideal flow rate was identified to be between 0.8mL/min to 1.6ml/ min during the culture. This value was calculated based on the computational modeling conducted based on three domains such as inlet, outlet, and the porous nature of the scaffold. It was also confirmed experimentally by alternating different media flows in the 3D cell-seeded scaffolds; for example, decreased cell densities were observed in the P(LLA-co-CL) scaffold at a higher flow of more than 1.6ml/min, probably due to cell death. This correlates to previously published data by Cartmell et al.[100]. Hence, a flow rate between 0.8ml/min and 1.6ml/min during cell culture is sufficient for efficient nutrient supply and waste removal.

5.8 2D vs 3D cell culture conditions in terms of shear stress factor

3D cell culture provides better mechanical properties, cell orientations, and cell communication via soluble factors than 2D cell culture[101],[102]. In our published data, stress gene marker levels under both static and perfusion conditions were low in 3D cell cultures compared with 2D cell cultures[66]. Furthermore, in this thesis, stress markers—fas, SAFB, and SERPINH1—showed an increased gene expression on one day post culture in the 2D cell culture compared with perfusion cell cultured in the scaffolds. Even after 7 days of flow exposure, the gene level expression remained on similar levels and did not increase further.

It is remarkable to see that cells cultured under the 3D static condition showed less expression of stress markers compared with cells cultured under the 3D condition with perfusion. The expression profile of SERPINH1, which is correlated to general stress[103], was highly upregulated on days 1 and 7 under the 3D perfusion culture condition, and it displayed the effect of shear stress on the cells. Upregulation was also detected for the stress marker SAFB, which contributes to stress regulation and differentiation processes. This gene was also reported to be upregulated when the endothelial cells were under fluid shear stress[104].

Although shear stress is an important factor that drives cell differentiation, it remains unclear whether increased stress markers caused by shear stress are beneficial for the process.

5.9 Role of shear stress on different scaffold materials for achieving higher osteogenic lineage commitment

This thesis once again establishes that shear stress plays an important role in osteogenic lineage commitment. Other than the RCP AP scaffold, all the scaffolds used in this study showed higher calcification in the 3D perfusion culture compared with static 3D cultures condition as shown in Table 5-1. An increase in the level of calcification was observed up to day 7 in cells cultured under perfusion, but an increase in calcification was not seen when the duration was increased to 14 days. Hence, the interval 7 days) with the highest calcification was relied on for further experiment in the different scaffolds. This also indicates that the role shear stress plays in osteogenic lineage commitment is time dependent.

Table 5-1 Calcification level of scaffolds used in this study under 7 days of static or dynamic culture

Scaffold Material	**3D culture conditions**	
	Static	**Perfusion**
P(LLA-co-CL) scaffold	1.0	1.5
ß-tcp scaffold	0.75	1.5
PP polymer scaffold	0.45	0.7
RCP scaffold	0.4	0.8
RCP AP scaffold	1.3	0.6
RCP AP Mg scaffold	0.3	0.7

Both the P(LLA-co-CL) and ß-TCP scaffolds showed the same level of calcification under 7 days of the dynamic culture condition. No significant difference was seen in PP polymer in either the static or dynamic conditions, and the level of calcification observed on this scaffold was significantly lower than the P(LLA-co-CL) and ß-TCP scaffolds. The collagen (RCP) scaffolds generally also showed higher calcification under shear stress compared with the static culture condition. However, for the collagen scaffold coated with AP (the RCP AP scaffold), the level of calcification found in the static condition was much higher than dynamic culture condition; this is due to the leaching of AP under the dynamic condition. The RCP AP scaffold was also coated with Mg (the RCP AP Mg scaffold). For this scaffold, the level of calcification increased under shear stress. The level induced in all three scaffolds (RCP, RCP AP, and RCP AP Mg) was lower than the level induced in the P(LLA-co-CL) and ß-TCP scaffolds under the dynamic condition. This shows that under shear stress, both the P(LLA-co-CL) and ß-TCP scaffolds induce higher calcification compared with the remaining scaffolds (the PP polymer, RCP, RCP AP, and RCP AP Mg scaffolds) under the 7-day culture condition.

5.10 Expression of collagen type 1 on scaffold implants

Collagen type 1 plays an important role in bone strength. It is well known that 90% of the organic phase in the bone is made up of collagen. In our research, we unfortunately could not do collagen type 1 staining on the PP polymer and β-TCP scaffolds due to the unavailability of the Lonza stem cell medium from the market. In coming to the P(LLA-co-CL) scaffold, we could perform the staining only for experiments done under mechanical stimulation conditions. We performed this staining for other collagen-based scaffolds due to presence of collagen peptides.

The level of collagen present in the RCP, RCP AP, and RCP AP Mg scaffolds was analyzed before and after the cell cultures. The expression of collagen type 1 increased when the cell-seeded scaffolds were cultured under the perfusion condition. Under the static culture condition, the expression of collagen was higher in the RCP and RCP AP scaffolds compared with the empty scaffold. For the RCP AP Mg scaffold, there was no difference in the expression of collagen between the static condition and the empty scaffold. Under the dynamic condition, the RCP and RCP AP scaffolds exhibited higher collagen expressions than the RCP AP Mg scaffold and other static conditions.

5.11 Osteogenic lineage commitment gene expression for different scaffold implants

Osteogenic lineage gene markers on cell-seeded scaffolds were assessed. The early core transcription factor RUNX2 is a critical factor in the osteogenic lineage commitment, and it was significantly upregulated under shear stress in the ß-TCP, RCP, RCP AP, and RCP AP Mg scaffolds after 7 days of cell culture conditions. However, *RUNX2* was unregulated in the P(LLA-co-CL) scaffold after 1 day of cell culture under shear stress. This shows that in most of the scaffolds described in our study, the *RUNX2* gene was activated under the shear stress condition.

Bone is made of organic and inorganic phases (*i.e.*, it is mostly made of collagen type 1 (organic) and *ALPL* -dependent hydroxylapatite (inorganic))[105]. Hence, we checked for *ALPL* and the collagen type 1 gene in all the cell-seeded scaffolds after 7 days of culture conditions. The expression of the *ALPL* gene was significantly upregulated in the ß-TCP and RCP AP Mg scaffolds after 7 days of cell culture under shear stress, whereas the P(LLA-co-CL) scaffold expressed higher *ALPL* after 1 day and 14 days of the dynamic cell culture condition.

Col1A1 gene expression was upregulated significantly in all the cell-seeded scaffolds under the dynamic conditions after 7 days of cell culture. This shows that *Col1A1* is upregulated under shear stress better than static culture conditions. Similarly, when the P(LLA-co-CL) scaffold was cultured for 14 days, the collagen type 1 gene expression was significantly upregulated in the dynamic condition compared with the static condition.

The *BMP2* gene is also important for bone regeneration[106]. Under the shear stress condition, the *BMP2* was significantly upregulated in the ß-TCP, RCP, and RCP AP scaffolds. But in other scaffolds, there was no significant difference between dynamic and static culture conditions.

The OC (*BGLAP*) gene was significantly upregulated in the RCP AP cell-seeded scaffold under shear stress, while no effect was seen in other cell-seeded scaffolds. Osteopontin also plays an important role in bone remodeling, and it is activated under shear stress. Under 7 days of the dynamic culture condition, osteopontin was highly significantly upregulated in all the scaffold conditions. This shows that shear stress significantly impacts the activation of osteopontin expression.

Similarly, osteonectin gene expression was verified in all the cell-seeded scaffolds. There was no significant difference between the static and dynamic cell culture conditions. This shows that shear stress did not influence the upregulation of osteonectin gene expression.

Shear stress leads to osteogenic lineage commitment, as indicated by the upregulation of osteogenic gene markers. Several studies conducted in bioreactor system with perfusion have shown the upregulation of RUNX2, osteonectin, OC, and COL1A1 gene expression when cultured for periods of 7 and 14 days[107] [108],[109],[110],[111]. Bjerre et al. showned that a perfusion bioreactor with osteogenic media for 21 days leads to the increased upregulation of ALPL and BMP2, osteopontin, and RUNX2gene expression compared with the static culture condition[61]. Similarly, Filipowska et al. have shown that a perfusion bioreactor with an osteogenic medium for 21 days leads to increased VEGF, BMP2, and RUNX2 gene expression[91]. Together with the results presented in this thesis, all these studies support a finding that shear stress strongly influences the osteogenic lineage commitment of MSCs when seeded on a 3D scaffold.

Many *in vivo* implantation studies have also shown the better performance of scaffold implants in terms of osteogenic lineage commitment when cultured under shear stress/perfusion conditions. For instance, Gomes et al. have shown that rat MSCs cultured on the scaffold in the bioreactor showed increased expression of ALPL and OC postimplantation in mice [112]. In a separate study, Yeatts et al. have also shown an increase in the formation of new bone when a bioreactor cultured implant was transplanted into a rat[113]. Wang et al. also reported similar results, where bone marrow stem cells isolated from a rabbit and cultured in a perfusion bioreactor in the presence of an osteogenic medium resulted in blood vessel formation during *in vivo* studies conducted in rabbit [114]. These effects were consistent and reproduced in a large animal study conducted by Gardel et al. using goats. They showed that goat MSCs cultured in the bioreactor in the presence of an osteogenic medium for 14 days resulted in the expression of higher calcium in implanted constructs during an *in vivo* study of goat with new bone formation[115].

Pore size also influences the expression of genes related to osteogenic lineage commitment. Pisanti et. al conducted studies on three pore sizes—100 µm, 250 µm, and 500

µm—under a perfusion bioreactor with an osteogenic medium[116]. They reported that stem cells cultured in the 250 µm pore size resulted in increased BMP2 and ALPL gene expression compared with other pore sizes. Another study reported an increase of cell viability, ALPL, and OC expression after implanting a bioreactor-cultured implant with a pore size between 300 µm and 500 µm into mice[34].

The bioreactor technology developed in this thesis allows for generating cell-loaded bone substitutes to treat critical size bone defects by overcoming limitations of waste removal and nutrient supply in a complex 3D scaffold. Dynamic culture conditions enhance calcification and the expression of osteogenic-related genes after 1 week of culture in most of the scaffold materials studied. Furthermore the technology presented in this thesis achieved early osteogenic lineage commitment solely by shear stress, without the addition of growth factors. The omission of soluble factors supports the development of processes compliant with GMP guidelines and may accelerate technology translation in clinical applications.

5.12 Mechanical deformation influence on osteogenic lineage commitment

Mechanical force can meaningfully enhance bone remodeling, and there are different types such as stretching and compressing. As discussed in the Results section, these types are further divided into uniaxial, biaxial, and multiaxial categories. To apply mechanical force, the scaffold should possess elastic stiffness, strength, and toughness. These properties are important because a postimplantation scaffold should be able to bear the weight of the human body.

Although both the P(LLA-co-CL) and ß-TCP scaffolds showed higher osteogenic lineage commitment under the dynamic culture condition, the ß-TCP scaffold was not used for mechanical deformation experiments due to its brittle nature.

Higher calcification was seen when mechanical deformation was applied to the cell-seeded scaffold compared with the dynamic perfusion condition on days 1 and 7. Furthermore, an increase in calcification was also seen on day 7 of the culture under mechanical deformation compared with day 1. This proves that higher calcification can be achieved by mechanical force rather than dynamic or static culture conditions.

The mechanical deformation culture showed an increase in RUNX2 (fourfold) BMP2 (5.5-fold), ALPL (threefold), Col1A1 (fivefold), and SPP1 (twofold) after 1 day, which were significantly upregulated compared with the perfusion culture. When mechanical deformation was applied to the cells for 7 days, the upregulation of OC (twofold), osteonectin (onefold), RUNX2 (3.5-fold), collagen type 1 (2.5-fold), TGF-ß threefold), VEGF (fivefold), and BMP2 (threefold) gene markers was seen compared with the dynamic perfusion condition. Interestingly, there was no difference in SPP1 expression compared with the dynamic condition. Studies have shown that bone-related genes such as OC, collagen, TFG-ß, BMP2, and VEGF play a major role in bone regeneration. The above results suggest that mechanical force significantly impacts the upregulation of bone-related genes to assist with regeneration[55].

5.13 Identifying the type of force for better osteogenic lineage commitment

Because mechanical stimulation of primary stem cells leads to better osteogenic lineage commitment, it is of great interest to identify the type of force that would provide better calcification. The right of amount of force can be determined by varying amplitude and frequency to apply different combinations to the stem cells. This gives us a way to predict the ideal type.

Mechanical compression was induced over 2 days for 1 hour twice a day. The mechanical deformation comprised sinusoidal uniaxial scaffold deformation amplitude (%) and frequency of scaffold deformation (Hz). Combinations covering a range of 1–2% at 1–2 Hz resulted in higher calcification of the TERT-AP1 cell line. The calcification level was significantly increased when the scaffold was deformed at 1 Hz. Increased compression frequency led to comparable readouts as the control, but changes based on amplitude had no effect on calcification. A notable increase of ALPL gene expression was seen when the amplitude was raised to 2%. Similarly, when the same experiment was done on the primary stem cell culture over 21 days under similar conditions, it showed an elevated level of calcification—up to threefold—compared with data produced from the TERT-AP1 cell line. This finding indicates that the kinetics of the calcification process which increase calcium deposition are time dependent.

Supporting the results presented in this thesis, Baumgartner et al. also demonstrated that mechanical deformation applied for 5 days in the presence of an osteogenic medium not only increases mineralization but also leads to better osteogenesis[117]. Petri et al. have reported an increase in ECM under mechanical deformation applied over 14 days[118]. Further, Zhang et al. described an increase in OC and ALPL expression following 28 days of culture in the presence of an osteogenic medium under mechanical deformation[119]. Toa Li et al. also reported increases in ALPL and calcium expression in mouse MSCs cultured under mechanical deformation in an osteogenic medium for 21 days[120].

5.14 Mechanical deformation or shear stress as the main physical driver in early osteogenesis

Despite so many studies, it is not yet clear whether mechanical deformation or shear stress has a greater impact on achieving higher calcification in bone regeneration[45]. Several studies showed that fluid–flow-induced shear stress represents the predominant stimulus for bone remodeling by osteocytes[121]. To individually evaluate the contribution of mechanical deformation and deformation-induced fluid–flow shearing to the strengthened MSC osteogenic lineage commitment, a computational model (Comsol Multiphysics GmbH) was established which could investigate the shear stress regime in the perfusion bioreactor.

A significant upregulation of bone-related genes as well as higher calcification was seen in the dynamic 3D culture condition with mechanical deformation compared with shear stress inside the scaffold due to mechanical deformation. It shows that strong effects of mechanical deformation on early osteogenic differentiation might be associated with situations that require an immediate response. These results show that mechanical stimulation could be a driver in the early phase of wound healing following a fracture, whereas the influence of fluid flow (shear stress) on mature osteocytes is more important in the remodeling phase. Hence, our findings obtained in this thesis suggest that mechanical force strain is the main driver for skeletal precursors to undergo osteogenesis in the earlier stages of osteogenic cell maturation.

5.15 Mechanical stimulation bioreactor influence on *in vivo* studies

Although the mechanical deformation stimulation of MSCs has shown improved osteogensis, insufficient reports are available on the success rate of these implants *in vivo*. Some of the *in vivo* research done on mice over 56 days has indicated that bone implants subjected to mechanical deformation with electromagnetic stimulation have resulted in fast bone formation[122]. Uto et al. showed that a mechanically stimulated bone-cell construct implanted in mice resulted in higher bone mineral density around the implant, assisting with new bone formation[123]. Other studies have shown that developing the osteocyte network through mechanical deformation via dental implants improved the quality of bone in rabbit long bones [124],[125],[126]. These studies show that mechanical stimulation is an integral part of *in vivo* studies, but more studies must be conducted to better understand its role.

5.16 Developing an *in vitro* test system for osteoporosis

After establishing bioreactor technology which enables 3D cell culture in the presence of shear stress and mechanical deformation by mimicking the human body environment, the new bioreactor became an interesting tool for investigating a major bone disease such as osteoporosis.

Osteoblasts enable bone formation, while osteoclasts break the bone tissue, and both are critical to bone remodeling; any failure to perform their work properly leads to osteoporosis. One approach for treating this is to enhance the stimulation of stem cells into osteoblast differentiation using a drug. An alternative method is to reduce the recruitment of osteoclast precursors and their activity and maturation towards osteoclast, which results in controlling the osteoporosis disease[127]. Most of the medication available on the market treats osteoporosis this way. To find a permanent cure, we need to treat stem cells so they can differentiate into osteoblasts, resulting in healthy bone. The bioreactor technology developed in this thesis can be used to study cases when stem cells fail to differentiate into osteoblasts, consequently leading to osteoporosis. Moreover, it may be used to identify drugs that can restrore their osteogonic and regenerative capacity at an individual basis strontium ranelate.

Treatment with the osteoporotic drug resulted in increased expression of collagen type 1 staining compared with the nondrug-treated osteoporotic stem cells. Similarly, a calcification assay showed an increased level of calcium when the osteoporotic stem cells were treated with the drug compared with the nondrug-treated cells. An increase in the expression of genes such as osteonectin, RUNX2, ALPL, and Col1A1 in drug-treated osteoporotic stem cells compared with nondrug-treated cells was also observed.

Even though this test system can predict osteogenic lineage commitment in the organic phase of maintaining healthy bone, we have yet to make a model which can identify unintended effects of medicine on osteoblast, when treated in an osteoporosis patient. Hence, this system will be more efficient as a test system when it becomes possible to identify putatively ineffective medication in a setting of personalized medicine.

5.17 Problems in *in vitro* and *in vivo* studies when testing osteoporosis drugs

In the drug discovery process, most of the *in vitro* studies have been done on 2D cell cultures. But 3D cell cultures are closer to a real-time human environment. In the *in vivo* studies, different models are available for primary and secondary osteoporosis. Two have been commonly used in the recent years—the ovariectomized (OVX) model for postmenopausal osteoporosis, and the orchidectomy (ORX) model for male osteoporosis[127]. Most of the drug discovery process has been done using either of these two models. Even after their development, studies have shown that 90% of the drugs fail in the phase of drug discovery [128]. This is due to the lack of a proper model available in both *in vitro* and *in vivo* models as well as a large gap between preclinical studies and human clinical trials.

The biggest advantage of *in vivo* studies is that we can study absorption, metabolism, and possible side effects of the drugs, which is lacking in the *in vitro* models available in recent years. To overcome this issue, many *in vitro* tests are being developed, with companies such as Flexcell International Corp., Zetos System, Don Whitley Scientific Ltd., ADMET, Inc., TA Instruments Inc., and EBERS Medical Technology researching to find an efficient system. Most of the 3D mechanical stimulation bioreactors available in the market need a large amount of space and money , making it more difficult to do high throughout put screening bioreactor for the drug development. Even though many types of research are going on in this field, studies

have shown no proper alternating or competing technology is available as an osteoporotic test system.

5.18 Bioreactor automation in clinical use

Bioreactor automation can be achieved with a feedback mechanism from the bioreactor culture condition through the sensors. Once the technology is established in hospitals, a bone graft implant can be made using the automated process control under GMP conditions[129]. Automation in the bioreactor system can have multiple advantages, such reducing time, avoiding contamination, and achieving better reproducibility of the bone graft. It can be introduced in hospitals in steps such as cell expansion, medium change, and cell seeding into the scaffolds, and it will help monitor the bone implant in the culture condition through a pressure sensor as well as the pH of the culture condition[130]. This bioreactor can be manufactured for one-time use to ensure it is sterile, which helps prepare the cell-seeded scaffold implants under GMP conditions.

6 Conclusions and Future Perspectives

Tissue-engineered bone grafts are an alternative treatment for patients suffering from critical size bone defects. Achieving a viable cell-seeded bone implant is the biggest challenge, but the bioreactor technology used in this thesis provides an efficient and innovative solution to generate viable cell-loaded bone substitutes. This newly developed bioreactor overcomes the limitations of nutrient supply in a complex 3D scaffold by the perfusion of cell culture media on different scaffold materials using a peristaltic pump, which enables nutrients to reach the cells. This media perfusion causes shear stress that further bolsters stem cell differentiation toward osteogenic lineage, significantly increasing the calcification observed in most of the scaffold materials used in perfusion culture media compared with static culture conditions. This in turn results in the beneficial effect of shear stress on osteogenic lineage commitment.

When mechanical deformation was applied on the cell-loaded P(LLA-co-CL) scaffold, higher osteogenic lineage commitment was achieved compared with the shear stress culture condition. This shows that mechanical deformation may be a key to achieving osteogenic lineage commitment. This thesis further demonstrates that deformation strain is the main driver for skeletal precursors to undergo osteogenesis in the earlier stages of osteogenic cell maturation. The strong effects of mechanical deformation and fluid–flow shear stress yielded better and earlier osteogenic differentiation, which are both very promising for the clinical application of this developed technology. Early osteogenic differentiation caused by mechanical deformation might be associated with situations that require an immediate response. Another advantage of this new bioreactor technology is that early osteogenic lineage commitment was achieved solely by mechanical stimulation without using exogenous growth factors. This offers hope that cell-loaded bone substitutes can be generated in a cost-effective way.

The newly developed bioreactor technology was also used to predict the effectiveness of strontium ranelate for treating osteoporosis. Thus, it can easily be adapted as an *in vitro* osteoporotic drug test system. Moreover, it may also be used to identify individually ineffective medication and avoid ineffective clinical treatment strategies. The current bioreactor can efficiently show the effect of drugs on calcification based on osteogenic differentiation , yet it cannot identify the side effects. Nonetheless, it can reduce the number

of animals used in the drug screening process and be used as an alternative to animal studies in some cases.

7 References

1. Campana, V., et al., *Bone substitutes in orthopaedic surgery: from basic science to clinical practice.* J Mater Sci Mater Med, 2014. **25**(10): p. 2445-61.

2. Telfer, N.R., T.P. Cutler, and R.P. Dawber, *The natural history of 'dystrophic' pili torti.* Br J Dermatol, 1989. **120**(2): p. 323-5.

3. Li, F., A. Wang, and C. Wang, *Analysis of friction between articular cartilage and polyvinyl alcohol hydrogel artificial cartilage.* J Mater Sci Mater Med, 2016. **27**(5): p. 87.

4. Polisetti, N., M.M. Islam, and M. Griffith, *The artificial cornea.* Methods Mol Biol, 2013. **1014**: p. 45-52.

5. Guo, H.F., et al., *A simply prepared small-diameter artificial blood vessel that promotes in situ endothelialization.* Acta Biomater, 2017. **54**: p. 107-116.

6. Maziz, A., et al., *Knitting and weaving artificial muscles.* Sci Adv, 2017. **3**(1): p. e1600327.

7. Calori, G.M., et al., *The use of bone-graft substitutes in large bone defects: any specific needs?* Injury, 2011. **42 Suppl 2**: p. S56-63.

8. Fishman, J.A., M.A. Greenwald, and P.A. Grossi, *Transmission of infection with human allografts: essential considerations in donor screening.* Clin Infect Dis, 2012. **55**(5): p. 720-7.

9. Sundelacruz, S. and D.L. Kaplan, *Stem cell- and scaffold-based tissue engineering approaches to osteochondral regenerative medicine.* Semin Cell Dev Biol, 2009. **20**(6): p. 646-55.

10. Clarke, B., *Normal bone anatomy and physiology.* Clin J Am Soc Nephrol, 2008. **3 Suppl 3**: p. S131-9.

11. Farbod, K., et al., *Interactions between inorganic and organic phases in bone tissue as a source of inspiration for design of novel nanocomposites.* Tissue Eng Part B Rev, 2014. **20**(2): p. 173-88.

12. Green, J., *The physicochemical structure of bone: cellular and noncellular elements.* Miner Electrolyte Metab, 1994. **20**(1-2): p. 7-15.

13. in *Report of the Surgeon General's Workshop on Osteoporosis and Bone Health: December 12 - 13, 2002, Washington, DC*. 2003: Rockville (MD).

14. in *Bone Health and Osteoporosis: A Report of the Surgeon General*. 2004: Rockville (MD).

15. Mohamed, A.M., *An overview of bone cells and their regulating factors of differentiation.* Malays J Med Sci, 2008. **15**(1): p. 4-12.

16. Bellido, T., *Osteocyte-driven bone remodeling.* Calcif Tissue Int, 2014. **94**(1): p. 25-34.

17. Loi, F., et al., *Inflammation, fracture and bone repair.* Bone, 2016. **86**: p. 119-30.

18. Schemitsch, E.H., *Size Matters: Defining Critical in Bone Defect Size!* J Orthop Trauma, 2017. **31 Suppl 5**: p. S20-S22.

19. Wang, X., et al., *Role of mesenchymal stem cells in bone regeneration and fracture repair: a review.* Int Orthop, 2013. **37**(12): p. 2491-8.

20. Marolt, D., M. Knezevic, and G.V. Novakovic, *Bone tissue engineering with human stem cells.* Stem Cell Res Ther, 2010. **1**(2): p. 10.

21. Kolf, C.M., E. Cho, and R.S. Tuan, *Mesenchymal stromal cells. Biology of adult mesenchymal stem cells: regulation of niche, self-renewal and differentiation.* Arthritis Res Ther, 2007. **9**(1): p. 204.

22. Hass, R., et al., *Different populations and sources of human mesenchymal stem cells (MSC): A comparison of adult and neonatal tissue-derived MSC.* Cell Commun Signal, 2011. **9**: p. 12.

23. Alt, E.U., et al., *Aging alters tissue resident mesenchymal stem cell properties.* Stem Cell Res, 2012. **8**(2): p. 215-25.

24. Chen, Q., et al., *Fate decision of mesenchymal stem cells: adipocytes or osteoblasts?* Cell Death Differ, 2016. **23**(7): p. 1128-39.

25. Langenbach, F. and J. Handschel, *Effects of dexamethasone, ascorbic acid and beta-glycerophosphate on the osteogenic differentiation of stem cells in vitro.* Stem Cell Res Ther, 2013. **4**(5): p. 117.

26. Schack, L.M., et al., *The Phosphate Source Influences Gene Expression and Quality of Mineralization during In Vitro Osteogenic Differentiation of Human Mesenchymal Stem Cells.* PLoS One, 2013. **8**(6): p. e65943.

27. Clause, K.C., L.J. Liu, and K. Tobita, *Directed stem cell differentiation: the role of physical forces.* Cell Commun Adhes, 2010. **17**(2): p. 48-54.

28. Charles, J.F. and A.O. Aliprantis, *Osteoclasts: more than 'bone eaters'.* Trends Mol Med, 2014. **20**(8): p. 449-59.

29. Lee, E.J., F.K. Kasper, and A.G. Mikos, *Biomaterials for tissue engineering.* Ann Biomed Eng, 2014. **42**(2): p. 323-37.

30. Zhang, D., et al., *The development of collagen based composite scaffolds for bone regeneration.* Bioact Mater, 2018. **3**(1): p. 129-138.

31. Fu, Q., et al., *Bioactive glass scaffolds for bone tissue engineering: state of the art and future perspectives.* Mater Sci Eng C Mater Biol Appl, 2011. **31**(7): p. 1245-1256.

32. Gerhardt, L.C. and A.R. Boccaccini, *Bioactive Glass and Glass-Ceramic Scaffolds for Bone Tissue Engineering.* Materials (Basel), 2010. **3**(7): p. 3867-3910.

33. Liu, X. and P.X. Ma, *Polymeric scaffolds for bone tissue engineering.* Ann Biomed Eng, 2004. **32**(3): p. 477-86.

34. Turnbull, G., et al., *3D bioactive composite scaffolds for bone tissue engineering.* Bioact Mater, 2018. **3**(3): p. 278-314.

35. Sivaraj, K.K. and R.H. Adams, *Blood vessel formation and function in a bone.* Development, 2016. **143**(15): p. 2706-15.

36. Chen, H.C. and Y.C. Hu, *Bioreactors for tissue engineering.* Biotechnol Lett, 2006. **28**(18): p. 1415-23.

37. Gaspar, D.A., V. Gomide, and F.J. Monteiro, *The role of perfusion bioreactors in bone tissue engineering.* Biomatter, 2012. **2**(4): p. 167-75.

38. Yeatts, A.B. and J.P. Fisher, *Bone tissue engineering bioreactors: dynamic culture and the influence of shear stress.* Bone, 2011. **48**(2): p. 171-81.

39. Botchwey, E.A., et al., *Bone tissue engineering in a rotating bioreactor using a microcarrier matrix system.* J Biomed Mater Res, 2001. **55**(2): p. 242-53.

40. David, B., et al., *A perfusion bioreactor for engineering bone constructs: an in vitro and in vivo study.* Tissue Eng Part C Methods, 2011. **17**(5): p. 505-16.

41. Bhaskar, B., et al., *Design and Assessment of a Dynamic Perfusion Bioreactor for Large Bone Tissue Engineering Scaffolds.* Appl Biochem Biotechnol, 2018. **185**(2): p. 555-563.

42. Wang, N., *Review of Cellular Mechanotransduction.* J Phys D Appl Phys, 2017. **50**(23).

43. McBride, S.H. and M.J. Silva, *Adaptive and Injury Response of Bone to Mechanical Loading.* Bone key Osteovision, 2012. **1**.

44. Hart, N.H., et al., *Mechanical basis of bone strength: influence of bone material, bone structure and muscle action.* J Musculoskelet Neuronal Interact, 2017. **17**(3): p. 114-139.

45. Ramani-Mohan, R.K., et al., *Deformation strain is the main physical driver for skeletal precursors to undergo osteogenesis in earlier stages of osteogenic cell maturation.* J Tissue Eng Regen Med, 2018. **12**(3): p. e1474-e1479.

46. Chu, E.K., et al., *Bronchial epithelial compression regulates epidermal growth factor receptor family ligand expression in an autocrine manner.* Am J Respir Cell Mol Biol, 2005. **32**(5): p. 373-80.

47. Agha, R., et al., *A review of the role of mechanical forces in cutaneous wound healing.* J Surg Res, 2011. **171**(2): p. 700-8.

48. Yourek, G., et al., *Shear stress induces osteogenic differentiation of human mesenchymal stem cells.* Regen Med, 2010. **5**(5): p. 713-24.

49. Du, D., K.S. Furukawa, and T. Ushida, the *3D culture of osteoblast-like cells by unidirectional or oscillatory flow for bone tissue engineering.* Biotechnol Bioeng, 2009. **102**(6): p. 1670-8.

50. Ignatius, A., et al., *Tissue engineering of bone: effects of mechanical strain on osteoblastic cells in type I collagen matrices.* Biomaterials, 2005. **26**(3): p. 311-8.

51. Seefried, L., et al., *A small scale cell culture system to analyze mechanobiology using reporter gene constructs and polyurethane dishes.* Eur Cell Mater, 2010. **20**: p. 344-55.

52. Diaz, M.F., et al., *Biomechanical Forces Promote Immune Regulatory Function of Bone Marrow Mesenchymal Stromal Cells.* Stem Cells, 2017. **35**(5): p. 1259-1272.

53. Wang, J.H. and B.P. Thampatty, *An introductory review of cell mechanobiology.* Biomech Model Mechanobiol, 2006. **5**(1): p. 1-16.

54. MacQueen, L., Y. Sun, and C.A. Simmons, *Mesenchymal stem cell mechanobiology and emerging experimental platforms.* J R Soc Interface, 2013. **10**(84): p. 20130179.

55. Dimitriou, R., E. Tsiridis, and P.V. Giannoudis, *Current concepts of molecular aspects of bone healing.* Injury, 2005. **36**(12): p. 1392-404.

56. Janssen, F.W., et al., *Human tissue-engineered bone produced in clinically relevant amounts using a semi-automated perfusion bioreactor system: a preliminary study.* J Tissue Eng Regen Med, 2010. **4**(1): p. 12-24.

57. Bernhardt, A., et al., *Crosstalk of osteoblast and osteoclast precursors on mineralized collagen--towards an in vitro model for bone remodelling.* J Biomed Mater Res A, 2010. **95**(3): p. 848-56.

58. de Peppo, G.M., et al., *Human embryonic stem cell-derived mesodermal progenitors display substantially increased tissue formation compared to human mesenchymal stem cells under dynamic culture conditions in a packed bed/column bioreactor.* Tissue Eng Part A, 2013. **19**(1-2): p. 175-87.

59. Cheung, J.W., E.E. Rose, and J. Paul Santerre, *Perfused culture of gingival fibroblasts in a degradable/polar/hydrophobic/ionic polyurethane (D-PHI) scaffold leads to enhanced proliferation and metabolic activity.* Acta Biomater, 2013. **9**(6): p. 6867-75.

60. Bernhardt, A., et al., *Optimization of culture conditions for osteogenically-induced mesenchymal stem cells in beta-tricalcium phosphate ceramics with large interconnected channels.* J Tissue Eng Regen Med, 2011. **5**(6): p. 444-53.

61. Bjerre, L., et al., *Flow perfusion culture of human mesenchymal stem cells on silicate-substituted tricalcium phosphate scaffolds.* Biomaterials, 2008. **29**(17): p. 2616-27.

62. Matziolis, D., et al., *Osteogenic differentiation of human bone marrow-derived stem cells by short-term mechanical stimulation.* Open Orthop J, 2011. **5**: p. 1-6.

63. Liu, C., et al., *Influence of perfusion and compression on the proliferation and differentiation of bone mesenchymal stromal cells seeded on polyurethane scaffolds.* Biomaterials, 2012. **33**(4): p. 1052-64.

64. Peters, A.S., et al., *Cyclic mechanical strain induces TGFbeta1-signalling in dermal fibroblasts embedded in a 3D collagen lattice.* Arch Dermatol Res, 2015. **307**(2): p. 191-7.

65. Yang, X., et al., *Mechanical stretch inhibits adipogenesis and stimulates osteogenesis of adipose stem cells.* Cell Prolif, 2012. **45**(2): p. 158-66.

66. Kleinhans, C., et al., *A perfusion bioreactor system efficiently generates cell-loaded bone substitute materials for addressing critical size bone defects.* Biotechnol J, 2015. **10**(11): p. 1727-38.

67. Ramirez-Rodriguez, G.B., et al., *(*) Biomineralized Recombinant Collagen-Based Scaffold Mimicking Native Bone Enhances Mesenchymal Stem Cell Interaction and Differentiation.* Tissue Eng Part A, 2017. **23**(23-24): p. 1423-1435.

68. McGovern, J.A., M. Griffin, and D.W. Hutmacher, *Animal models for bone tissue engineering and modelling disease.* Dis Model Mech, 2018. **11**(4).

69. Viateau, V., et al., *Long-bone critical-size defects treated with tissue-engineered grafts: a study on sheep.* J Orthop Res, 2007. **25**(6): p. 741-9.

70. Kon, E., et al., *Autologous bone marrow stromal cells loaded onto porous hydroxyapatite ceramic accelerate bone repair in critical-size defects of sheep long bones.* J Biomed Mater Res, 2000. **49**(3): p. 328-37.

71. Motamedi, S.R., M. Khojaste, and A. Khojasteh, a *Success rate of implants placed in autogenous bone blocks versus allogenic bone blocks: A systematic literature review.* Ann Maxillofac Surg, 2016. **6**(1): p. 78-90.

72. Stephenson, M. and W. Grayson, *Recent advances in bioreactors for cell-based therapies.* F1000Res, 2018. **7**.

73. Harris, J.S., et al., *A review of mouse critical size defect models in weight-bearing bones.* Bone, 2013. **55**(1): p. 241-7.

74. Pearce, A.I., et al., *Animal models for implant biomaterial research in bone: a review.* Eur Cell Mater, 2007. **13**: p. 1-10.

75. Majidinia, M., A. Sadeghpour, and B. Yousefi, *The roles of signalling pathways in bone repair and regeneration.* J Cell Physiol, 2018. **233**(4): p. 2937-2948.

76. Rychly, J. and B. Nebe, *Interface biology of implants.* Cell Adh Migr, 2009. **3**(4): p. 390-4.

77. Gao, C., et al., *Bone biomaterials and interactions with stem cells.* Bone Res, 2017. **5**: p. 17059.

78. Morishita, T., et al., *Tissue engineering approach to the treatment of bone tumours: three cases of cultured bone grafts derived from patients' mesenchymal stem cells.* Artif Organs, 2006. **30**(2): p. 115-8.

79. Marcacci, M., et al., *Stem cells associated with macroporous bioceramics for long bone repair: 6- to 7-year outcome of a pilot clinical study.* Tissue Eng, 2007. **13(**5): p. 947-55.

80. Garcia-Gareth, E., J. Hua, and G.W. Blunn, *Osseointegration of acellular and cellularized osteoconductive scaffolds: is tissue engineering using mesenchymal stem cells necessary for implant fixation?* J Biomed Mater Res A, 2015. **103**(3): p. 1067-76.

81. Herberts, C.A., M.S. Kwa, and H.P. Hermsen, *Risk factors in the development of stem cell therapy.* J Transl Med, 2011. **9**: p. 29.

82. Parekkadan, B. and J.M. Milwid, *Mesenchymal stem cells as therapeutics.* Annu Rev Biomed Eng, 2010. **12**: p. 87-117.

83. Wakitani, S., et al., *Safety of autologous bone marrow-derived mesenchymal stem cell transplantation for cartilage repair in 41 patients with 45 joints followed for up to 11 years and 5 months.* J Tissue Eng Regen Med, 2011. **5**(2): p. 146-50.

84. Thevenot, P., et al., *Method to analyze three-dimensional cell distribution and infiltration in degradable scaffolds.* Tissue Eng Part C Methods, 2008. **14**(4): p. 319-31.

85. Baker, B.M. and C.S. Chen *Deconstructing the third dimension: how 3D culture microenvironments alter cellular cues.* J Cell Sci, 2012. **125**(Pt 13): p. 3015-24.

86. Chen, J.C. and C.R. Jacobs, *Mechanically induced osteogenic lineage commitment of stem cells.* Stem Cell Res Ther, 2013. **4**(5): p. 107.

87. Loh, Q.L. and C. Choong, *Three-dimensional scaffolds for tissue engineering applications: role of porosity and pore size.* Tissue Eng Part B Rev, 2013. **19**(6): p. 485-502.

88. Bruzauskaite, I., et al., *Scaffolds and cells for tissue regeneration: different scaffold pore sizes-different cell effects.* Cytotechnology, 2016. **68**(3): p. 355-69.

89. El Haj, A.J. and S.H. Cartmell, *Bioreactors for bone tissue engineering.* Proc Inst Mech Eng H, 2010. **224**(12): p. 1523-32.

90. Carpentier, B., P. Layrolle, and C. Legallais, *Bioreactors for bone tissue engineering.* Int J Artif Organs, 2011. **34**(3): p. 259-70.

91. Filipowska, J., G.C. Reilly, and A.M. Osyczka, *A single short session of media perfusion induces osteogenesis in hBMSCs cultured in porous scaffolds, dependent on cell differentiation stage.* Biotechnol Bioeng, 2016. **113**(8): p. 1814-24.

92. Robling, A.G. and C.H. Turner, *Mechanical signalling for bone modelling and remodelling.* Crit Rev Eukaryot Gene Expr, 2009. **19**(4): p. 319-38.

93. Frohlich, M., et al., *Tissue-engineered bone grafts: biological requirements, tissue culture and clinical relevance.* Curr Stem Cell Res Ther, 2008. **3**(4): p. 254-64.

94. Qin, Y., J. Guan, and C. Zhang, *Mesenchymal stem cells: mechanisms and role in bone regeneration.* Postgrad Med J, 2014. **90**(1069): p. 643-7.

95. Tanaka, Y., S. Nakayama, and Y. Okada, *Osteoblasts and osteoclasts in bone remodelling and inflammation.* Curr Drug Targets Inflamm Allergy, 2005. **4**(3): p. 325-8.

96. Ng, R., J.S. Gurm, and S.T. Yang, *Centrifugal seeding of mammalian cells in nonwoven fibrous matrices.* Biotechnol Prog, 2010. **26**(1): p. 239-45.

97. Stiehler, M., et al., *Effect of dynamic 3-D culture on proliferation, distribution, and osteogenic differentiation of human mesenchymal stem cells.* J Biomed Mater Res A, 2009. **89**(1): p. 96-107.

98. Jones, G. and S.H. Cartmell, *Optimization of cell seeding efficiencies on a three-dimensional gelatin scaffold for bone tissue engineering.* J Appl Biomater Biomech, 2006. **4**(3): p. 172-80.

99. Alvarez-Barreto, J.F. and V.I. Sikavitsas, *Improved mesenchymal stem cell seeding on RGD-modified poly(L-lactic acid) scaffolds using flow perfusion.* Macromol Biosci, 2007. **7**(5): p. 579-88.

100. Cartmell, S.H., et al., *Effects of medium perfusion rate on cell-seeded three-dimensional bone constructs in vitro.* Tissue Eng, 2003. **9**(6): p. 1197-203.

101. Idris, S.B., et al., *Polyester copolymer scaffolds enhance expression of bone markers in osteoblast-like cells.* J Biomed Mater Res A, 2010. **94**(2): p. 631-9.

102. Alepee, N., et al., *State-of-the-art of 3D cultures (organs-on-a-chip) in safety testing and pathophysiology.* ALTEX, 2014. **31**(4): p. 441-77.

103. Mala, J.G. and C. Rose, *Interactions of heat shock protein 47 with collagen and the stress response: an unconventional chaperone model?* Life Sci, 2010. **87**(19-22): p. 579-86.

104. Li, S., et al., *Fluid shear stress induces the phosphorylation of small heat shock proteins in vascular endothelial cells.* Am J Physiol, 1996. **271**(3 Pt 1): p. C994-1000.

105. Feng, X., *Chemical and Biochemical Basis of Cell-Bone Matrix Interaction in Health and Disease.* Curr Chem Biol, 2009. **3**(2): p. 189-196.

106. Fassbender, M., et al., *Stimulation of bone healing by sustained bone morphogenetic protein 2 (BMP-2) delivery.* Int J Mol Sci, 2014. **15**(5): p. 8539-52.

107. Chen, C.Y., et al., *3D porous calcium-alginate scaffolds cell culture system improved human osteoblast cell clusters for cell therapy.* Theranostics, 2015. **5**(6): p. 643-55.

108. Wu, W., et al., *Osteogenic performance of donor-matched human adipose and bone marrow mesenchymal cells under dynamic culture.* Tissue Eng Part A, 2015. **21**(9-10): p. 1621-32.

109. Silva, A.R., et al., *Synergistic effect between bioactive glass foam and a perfusion bioreactor on osteogenic differentiation of human adipose stem cells.* J Biomed Mater Res A, 2014. **102**(3): p. 818-27.

110. Katayama, A., et al., *Radial-flow bioreactor enables the uniform proliferation of human mesenchymal stem cells throughout a three-dimensional scaffold.* Tissue Eng Part C Methods, 2013. **19**(2): p. 109-16.

111. Kim, J. and T. Ma, *Bioreactor strategy in bone tissue engineering: pre-culture and osteogenic differentiation under two flow configurations.* Tissue Eng Part A, 2012. **18**(21-22): p. 2354-64.

112. Gomes, M.E., et al., *Effect of flow perfusion on the osteogenic differentiation of bone marrow stromal cells cultured on starch-based three-dimensional scaffolds.* J Biomed Mater Res A, 2003. **67**(1): p. 87-95.

113. Yeatts, A.B., et al., *In vivo bone regeneration using tubular perfusion system bioreactor cultured nanofibrous scaffolds.* Tissue Eng Part A, 2014. **20**(1-2): p. 139-46.

114. Wang, D., et al., *Construction of tissue-engineered bone using a bioreactor and platelet-rich plasma.* Exp Ther Med, 2014. **8**(2): p. 413-418.

115. Gardel, L., et al., *Assessing the repair of critical size bone defects performed in a goat tibia model using tissue-engineered constructs cultured in a bidirectional flow perfusion bioreactor.* J Biomater Appl, 2014. **29**(2): p. 172-185.

116. Pisanti, P., et al., *Tubular perfusion system culture of human mesenchymal stem cells on poly-L-lactic acid scaffolds produced using a supercritical carbon dioxide-assisted process.* J Biomed Mater Res A, 2012. **100**(10): p. 2563-72.

117. Baumgartner, W., et al., *Tissue mechanics of piled critical size biomimetic and biominerizable nanocomposites: Formation of bioreactor-induced stem cell gradients under perfusion and compression.* J Mech Behav Biomed Mater, 2015. **47**: p. 124-134.

118. Petri, M., et al., *Effects of perfusion and cyclic compression on in vitro tissue engineered meniscus implants.* Knee Surg Sports Traumatol Arthrosc, 2012. **20**(2): p. 223-31.

119. Zhang, Z.Y., et al., *A biaxial rotating bioreactor for the culture of fetal mesenchymal stem cells for bone tissue engineering.* Biomaterials, 2009. **30**(14): p. 2694-704.

120. Li, S.T., et al., *A novel axial-stress bioreactor system combined with a substance exchanger for tissue engineering of 3D constructs.* Tissue Eng Part C Methods, 2014. **20**(3): p. 205-14.

121. Rosa, N., et al., *From mechanical stimulus to bone formation: A review.* Med Eng Phys, 2015. **37**(8): p. 719-28.

122. Kang, K.S., et al., *Combined effect of three types of biophysical stimuli for bone regeneration.* Tissue Eng Part A, 2014. **20**(11-12): p. 1767-77.

123. Uto, Y., et al., *Effects of mechanical repetitive load on bone quality around implants in rat maxillae.* PLoS One, 2017. **12**(12): p. e0189893.

124. Kuroshima, S., et al., *Optimally oriented grooves on dental implants improve bone quality around implants under repetitive mechanical loading.* Acta Biomater, 2017. **48**: p. 433-444.

125. Sasaki, M., et al., *Ultrastructural alterations of osteocyte morphology via loaded implants in rabbit tibiae.* J Biomech, 2015. **48**(15): p. 4130-41.

126. Kuroshima, S., et al., *Structural and Qualitative Bone Remodeling Around Repetitive Loaded Implants in Rabbits.* Clin Implant Dent Relat Res, 2015. **17 Suppl 2**: p. e699-710.

127. Rissanen, J.P. and J.M. Halleen, *Models and screening assays for drug discovery in osteoporosis.* Expert Opin Drug Discov, 2010. **5**(12): p. 1163-74.

128. Hartung, T., *Look back in anger - what clinical studies tell us about preclinical work.* ALTEX, 2013. **30**(3): p. 275-91.

129. Russell, A.L., R.C. Lefavor, and A.C. Zubair, *Characterization and cost-benefit analysis of automated bioreactor-expanded mesenchymal stem cells for clinical applications.* Transfusion, 2018. **58**(10): p. 2374-2382.

130. Ravichandran, A., Y. Liu, and S.H. Teoh, *Review: bioreactor design towards generation of relevant engineered tissues: focus on clinical translation.* J Tissue Eng Regen Med, 2018. **12**(1): p. e7-e22.

Publication List

Deformation strain is the main physical driver for skeletal precursors to undergo osteogenesis in earlier stages of osteogenic cell maturation **Ramani-Mohan RK**, Schwedhelm I, Finne-Wistrand A, Krug M, Schwarz T, Jakob F, Walles H, Hansmann J. 2017 J Tissue Eng Regen Med. 2017;1–6

A perfusion bioreactor system efficiently generates cell-loaded bone substitute materials for addressing critical size bone defects. Kleinhans C*, **Mohan RR*,** Vacun G, Schwarz T, Haller B, Sun Y, Kahlig A, Kluger P, Finne-Wistrand A, Walles H, Hansmann J 2015 Biotechnology Journal, 10(11), 1727–1738 2015 ***** equally contributed first author